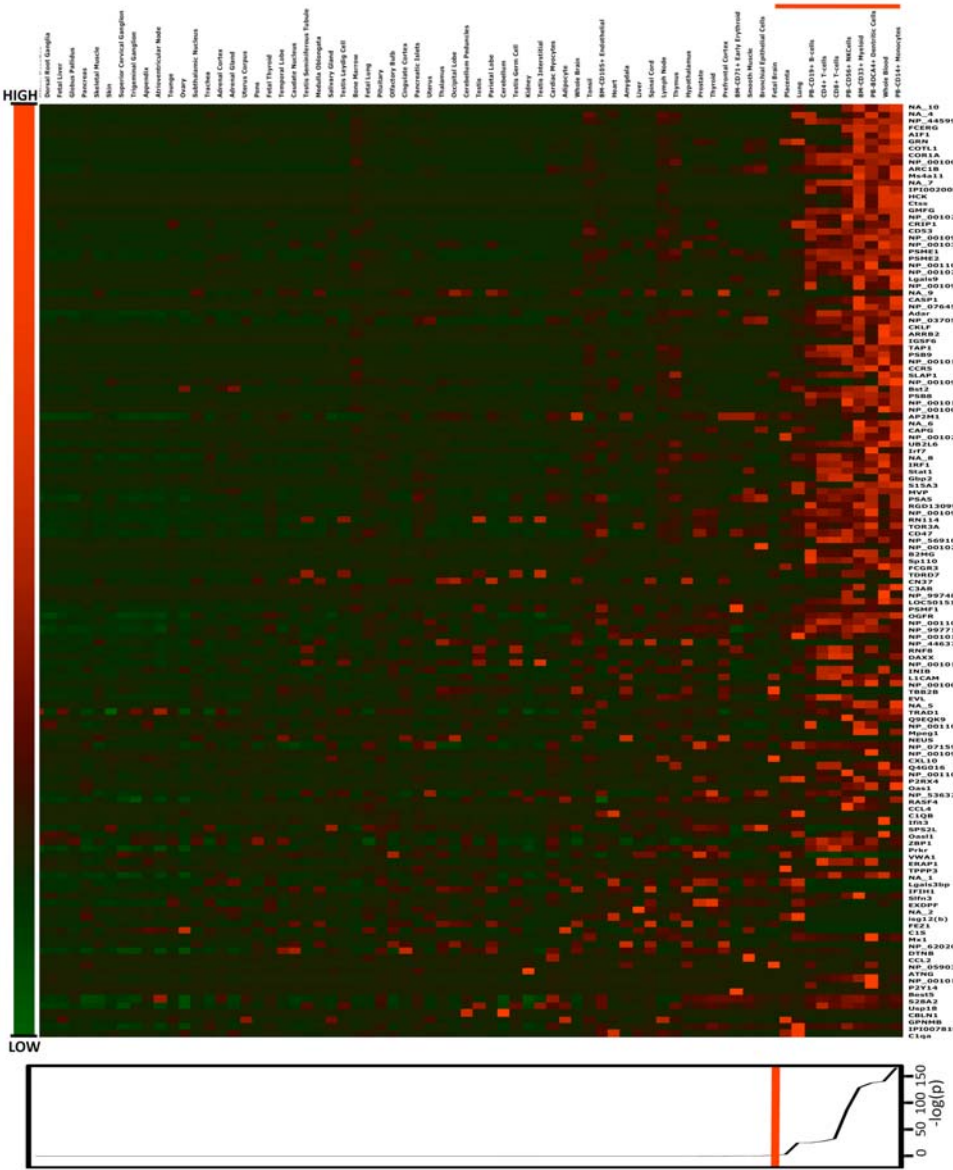
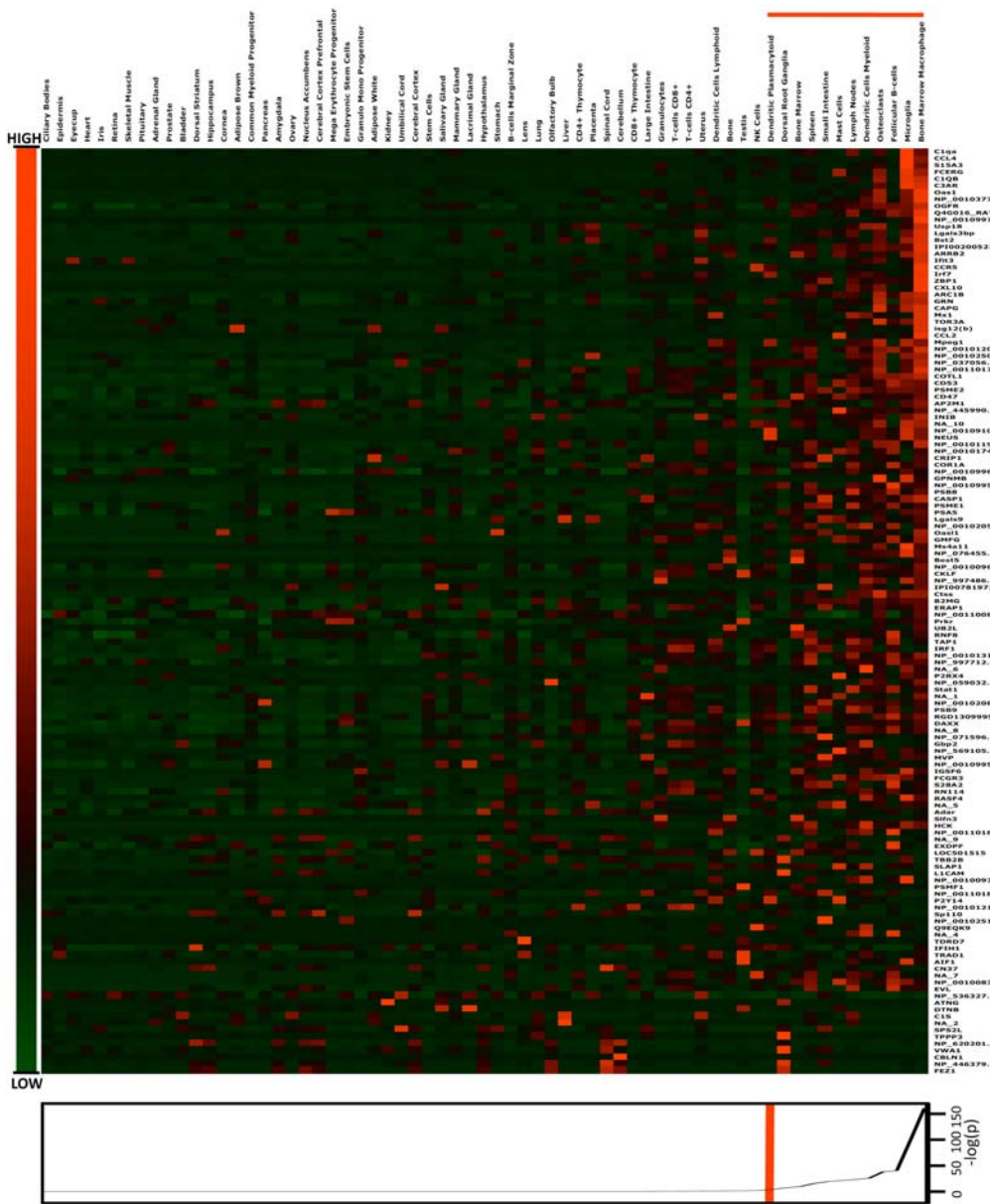


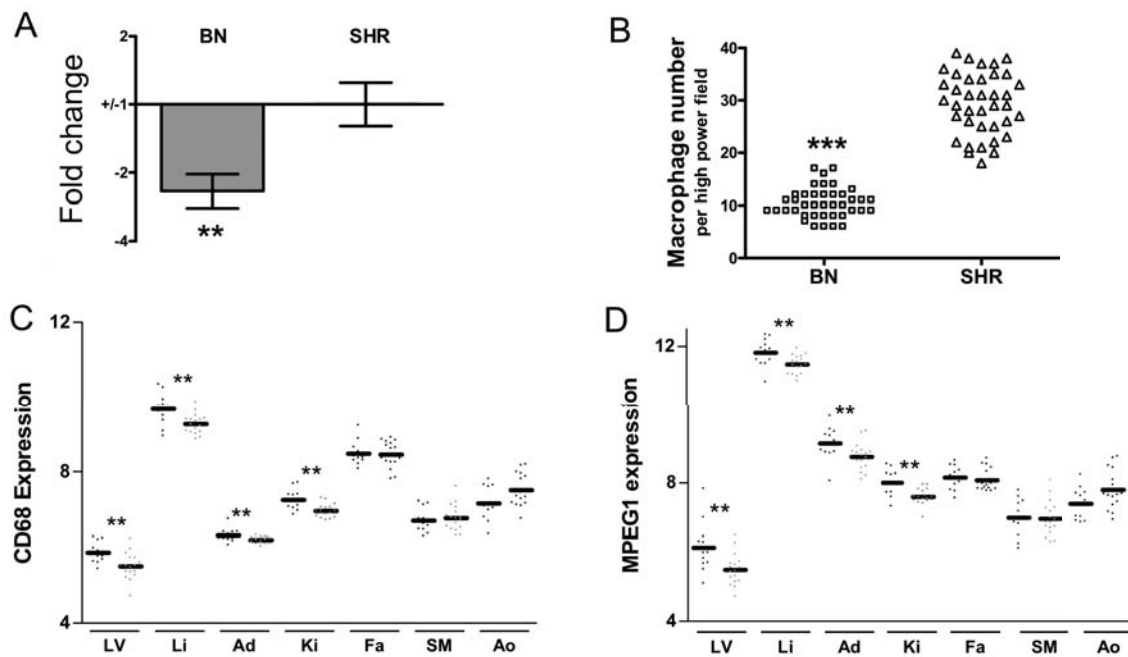
Supplementary Figure 1: Schematic overview of the study design and data analysis pipeline.



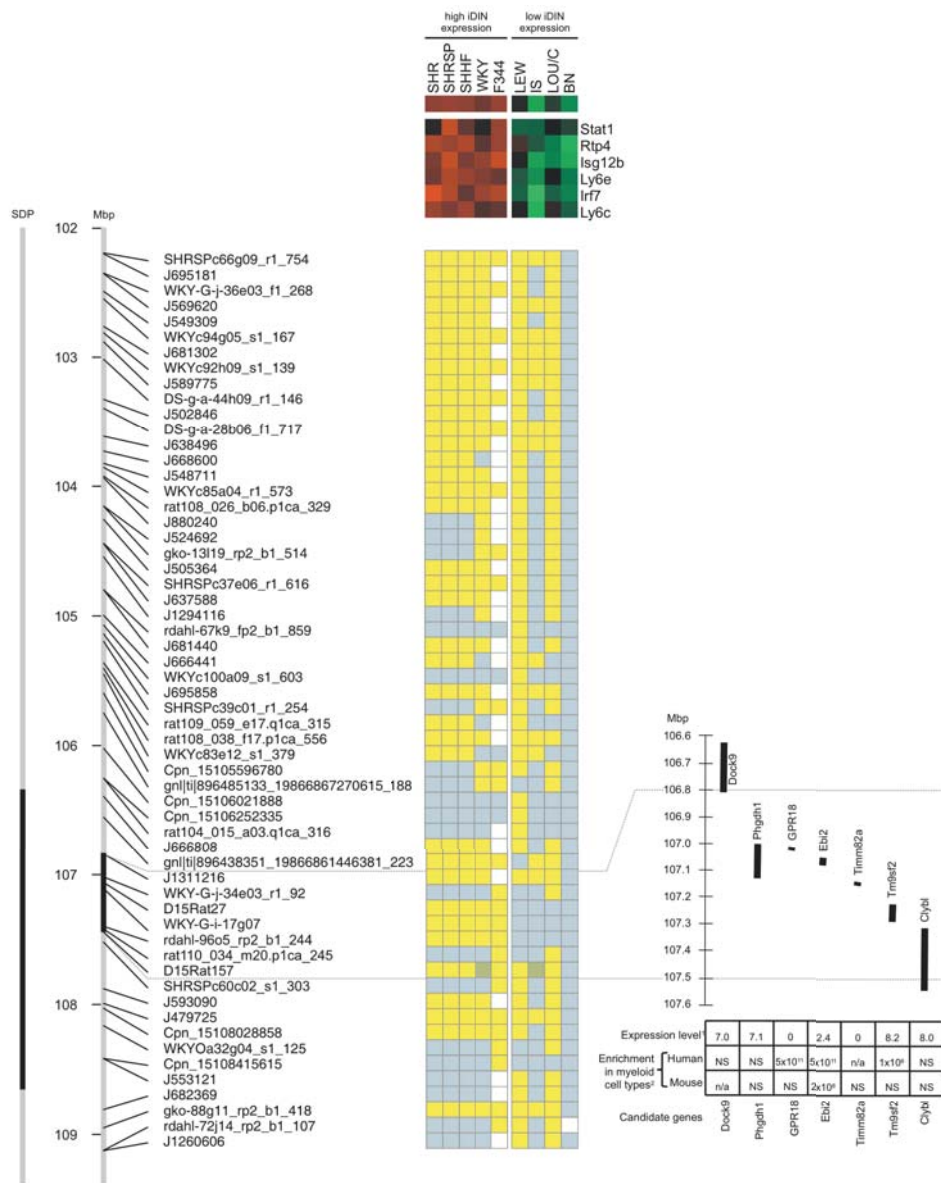
Supplementary Figure 2: Heat map representing the gene expression of human (a) and mouse (b) (see next page) orthologues of the iDIN across cell and tissue types and the distribution of combined *P*-values illustrated at the bottom. Genes are given to the right of the heat maps and cell and tissues, ordered by combined *P*-values, are given at the top of the graph. Red indicates an increase in gene expression whereas green indicates a decrease in gene expression. The red lines both above the cell types indicates the cell an tissue types where there is significant enrichment of the iDIN gene expression. The red bar on the distribution of combined *P*-values indicates the Bonferroni threshold used to correct for multiple testing.



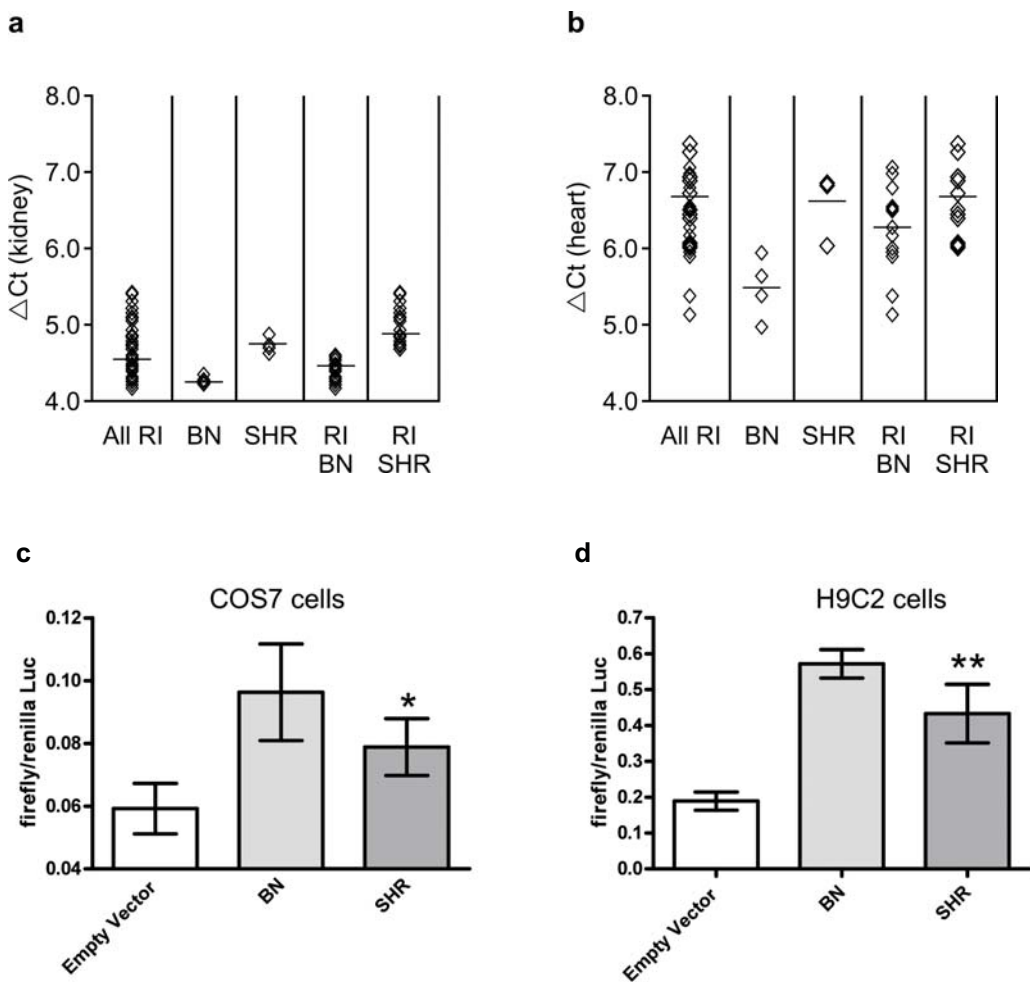
Supplementary Figure 2: b) Heat map representing the gene expression mouse orthologues of the iDIN across cell and tissue types.



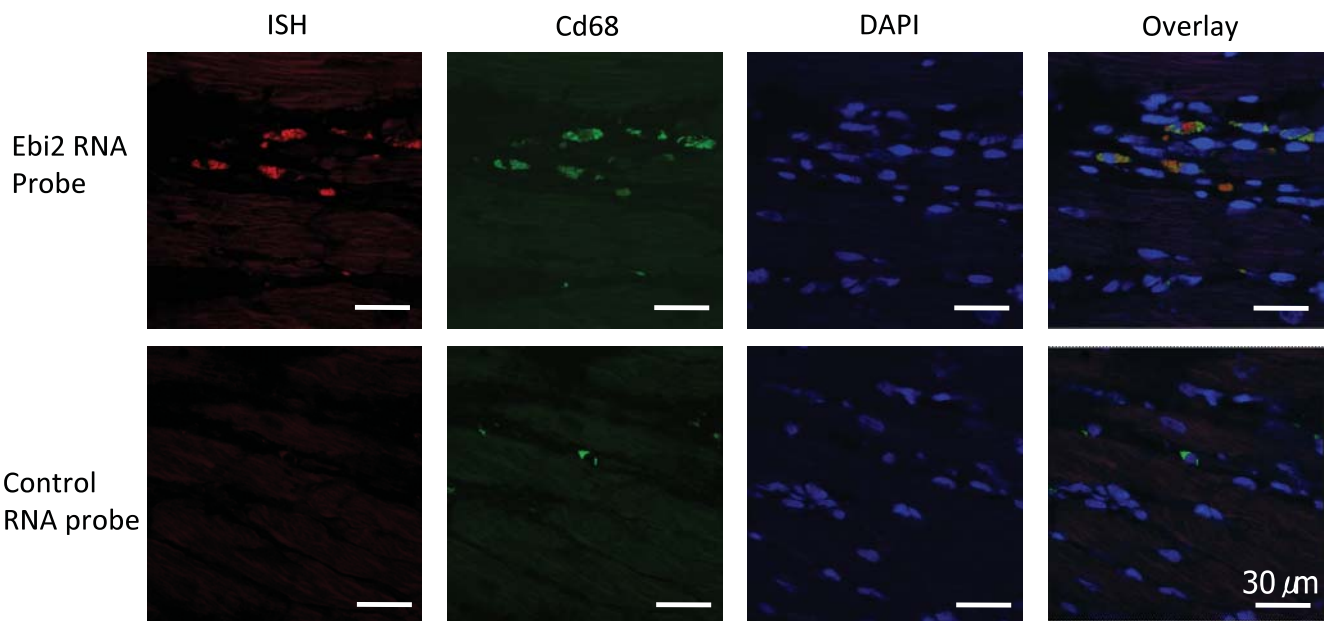
Supplementary Figure 3: Genotype dependent effects on macrophage numbers in SHR and BN tissues. **(a)** Quantification of RT-PCR analysis of macrophage-specific *Cd68* expression in BN and SHR heart (**, $P = 0.01$). **(b)** Quantification of the number of *Cd68⁺* macrophages in BN and SHR heart sections in 20 high power fields (***, $P = 2 \times 10^{-22}$) (see Supplementary Information). **(c)** and **(d)** Microarray-derived *Cd68* **(c)** and Macrophage-expressed gene 1 protein (*Mpeg1*, **d**) expression levels (Log_2) across all tissues (left ventricle (LV), liver (Li), adrenal (Ad), kidney (Ki), fat (Fa), skeletal muscle (SM) and aorta (Ao) in the BXH/HXB RI strain panel stratified by SHR (black dots) or BN (grey dots) genotype at SNP (J666808) on chromosome 15, mean expression levels are depicted as solid bars (**, $P < 0.01$).



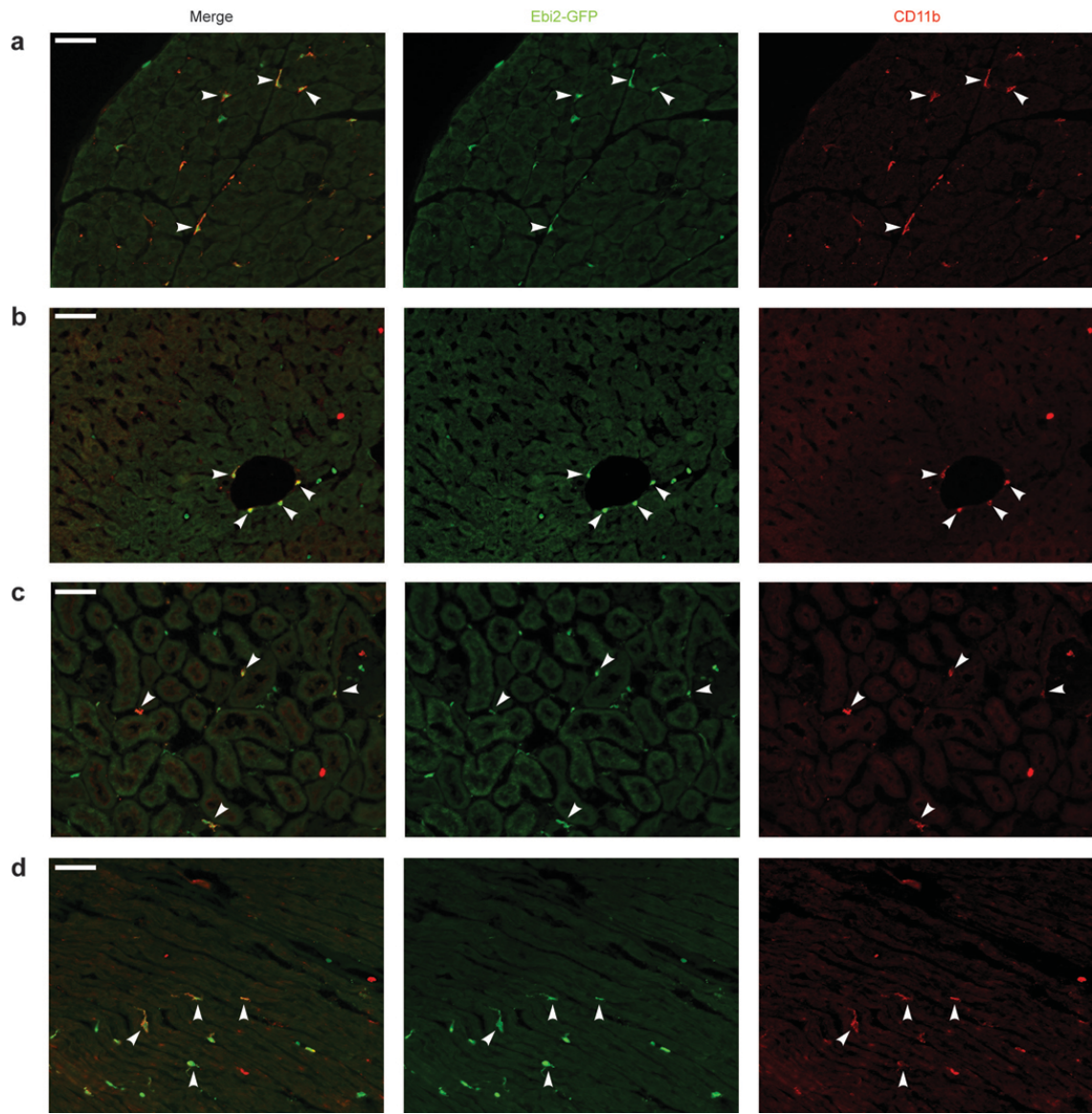
Supplementary Figure 4: Fine mapping of the candidate region controlling iDIN in the rat. Sequence map of the chromosome 15 locus associated with the iDIN expression. The black bar denotes the mapping of the locus to a specific strain distribution pattern in the recombinant inbred strains. Low and high iDIN expression denote additional rat strains with low and high expression of key genes of the iDIN (quantitative RT-PCR for *Stat1*, *Rtp4*, *Isg12b*, *Ly6e*, *Irf7*, *Ly6c*). Colored boxes indicate classification of alleles: blue = BN or identical to BN; yellow = SHR or identical to SHR; green = WKY or identical to WKY, and white for missing data. The dotted lines correspond to the markers delimiting the 0.7 Mb region of haplotype similarity within the locus that controls iDIN (for delimitation of the haplotype border we used, as a conservative estimate, the second consecutive marker outside the shared region, respectively). Right panel, genomic locations of the genes encoded within the shared segment that is indicative for low and high expression of iDIN genes. Bottom panel, RNA-Seq-derived gene expression in the heart (log₂ scale) and the significance of enrichment in myeloid-derived cell types is reported for each gene in the table.



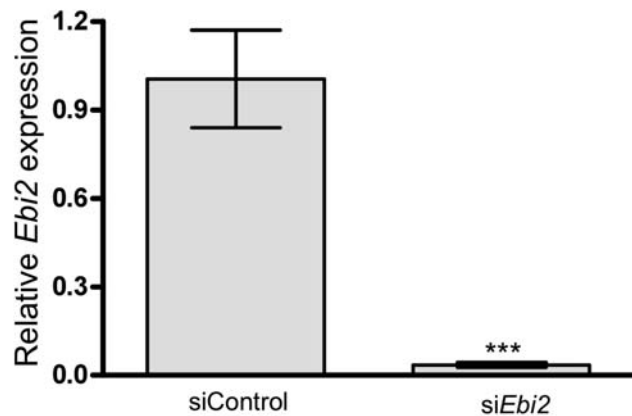
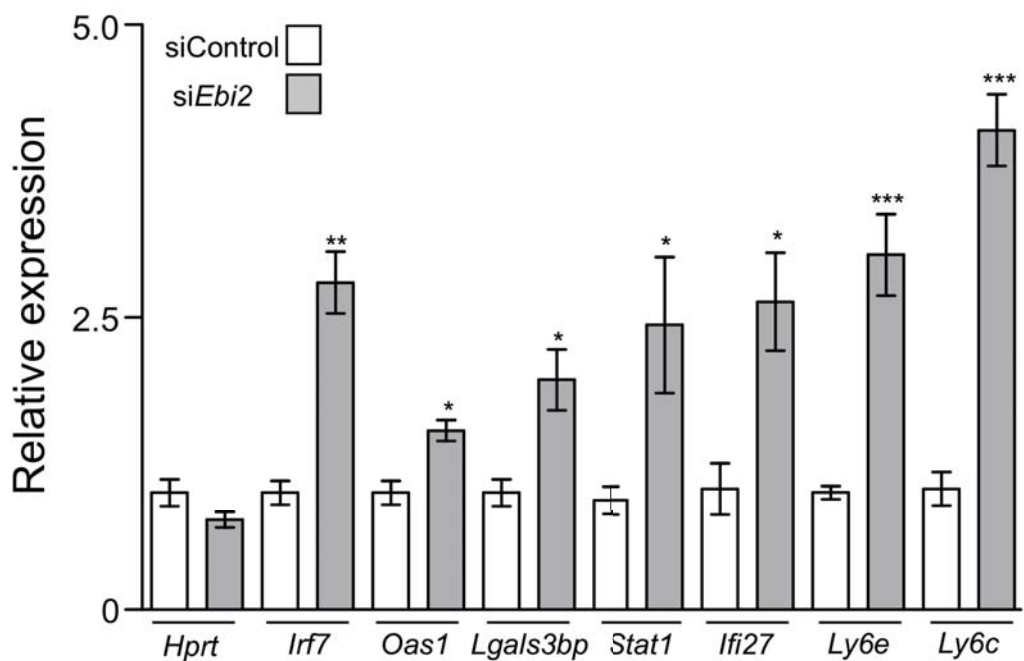
Supplementary Figure 5. (a, b) QPCR analysis of *Ebi2* expression in kidney and heart of parental and RI strains. Expression of *Ebi2* was measured in the parental strains SHR and BN and 29 RI strains using qPCR. *Ebi2* was differentially expressed in the parental strains and shows allele dependent expression in the RI strains with respect to the SNP J666808 in both tissues. **(c, d)** Effect of the 5'UTR *Ebi2* SNP between BN and SHR on protein expression. To determine the functional effects of this on protein expression the 5'UTR of BN or SHR were cloned upstream of Firefly luciferase (Luc) in the pGL3 vector. Effects on Luc protein expression were examined in two cell lines, a rat cell line (H9C2) and a human cell line (COS7) and normalised for transfection efficiency using Renilla Luc. There was a significant decrease in Luc translation by the SHR allele as compared to the BN allele. Data are shown as means and SDs. *, $P = 0.023$; **, $P = 0.009$.



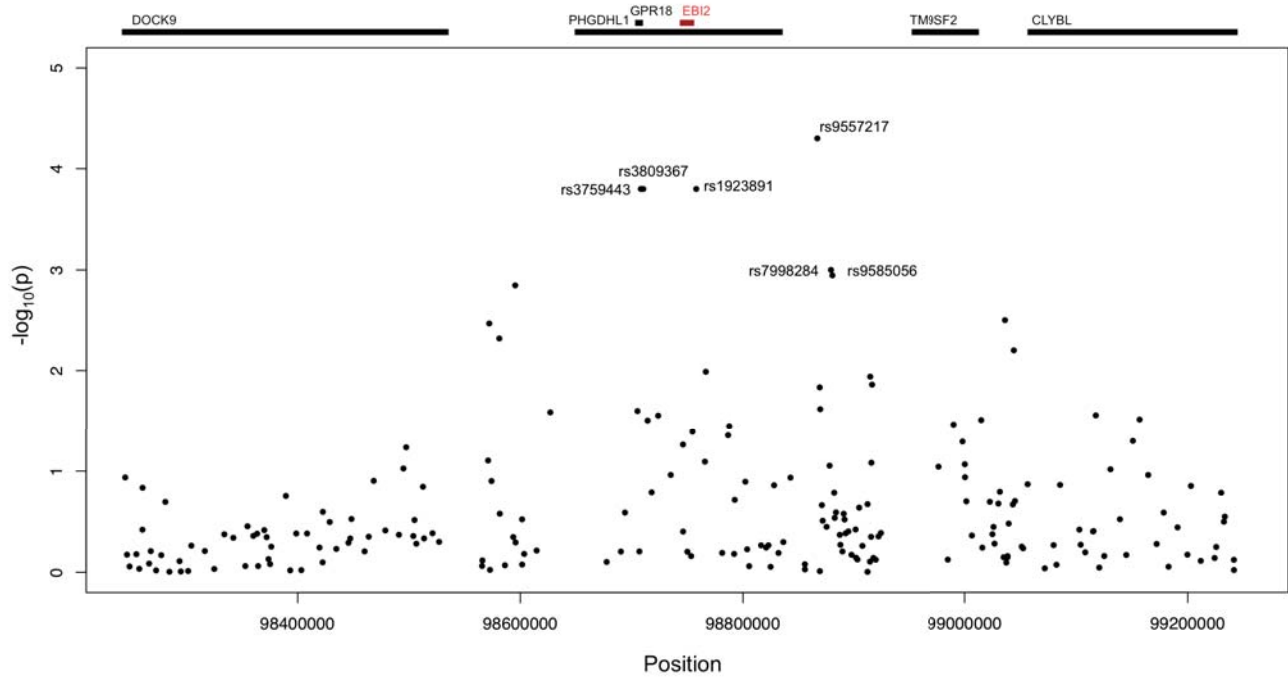
Supplementary Figure 6: Localisation of *Ebi2* gene expression to Cd68^{+ve} macrophages in the rat. Sections from SHR heart were probed with locked nucleic acid oligonucleotide against *Ebi2* RNA (top row) or control oligonucleotide (bottom row) by in situ hybridization. Bound oligonucleotides were detected with anti-DIG antibodies (first column, red). Sections were counterstained with anti-Cd68 (second column, green) and nuclei were visualized with DAPI (third column, blue). The combined images are represented as an overlay (see Supplementary Information).



Supplementary Figure 7: Ebi2-expressing CD11b⁺ myeloid cells in adult Ebi2^{GFP/+} mice across multiple tissues. Fluorescent microscopy of (a) pancreas, (b) liver, (c) kidney, and (d) heart tissue from Ebi2^{GFP/+} mice that were stained with antibodies to GFP (green) and CD11b (red). White arrowheads highlight GFP and CD11b double-positive cells. Scale bar = 50μm.

a**b**

Supplementary Figure 8: Effect of siRNA-mediated knockdown of *Ebi2* on expression of *Irf7* and iDIN genes in rat bone marrow-derived macrophages. **a**, as compared to control siRNA (siControl), siRNA against *Ebi2* (si*Ebi2*) significantly downregulated (97% inhibition) *Ebi2* mRNA expression. **b**, While si*Ebi2* had no effect on control gene expression (*Hprt*) there was a significantly increase in expression of *Irf7* and of iDIN genes *Oas1*, *Lgals3bp*, *Stat1*, *Ifi27*, *Ly6e* and *Ly6c*. Data, normalized to β -actin levels ($\Delta\Delta Ct$; see Supplementary Information), are shown as means relative to control \pm SEMs. *, $P < 0.05$; ** $P < 0.01$; *** $P < 0.005$. The experiment was repeated with similar results.



Supplementary Figure 9: Results of MANOVA analysis for *IRF7* and the *IRF7*-target genes in the Cardiogenics cohort. For all SNPs within the chromosome 13q32 locus, we report the nominal $-\log_{10} P$ -value (y-axes) from the MANOVA test. Significant association (FDR < 5%) between SNPs and network genes that are also confirmed by the non-parametric robust MANOVA ($n=6$) are indicated in the graph (Supplementary Information). Similar analyses in the Gutenberg Heart Study (GHS) cohort did not detect an association of *IRF7* or *IRF7*-target genes with SNPs at this locus (data not shown).

Supplementary information

Rat expression data

Expression data for eQTL analysis has been generated for seven tissues: adrenal, aorta, fat, kidney, left ventricle, liver and skeletal muscle using Affymetrix RAE230a and RAE230_2.0 arrays. For each of the SHR and BN parental strains and the 29 RI strains 4-5 biological replicates were profiled. Altogether 907 expression arrays were analyzed. Data was normalized using the RMA algorithm¹ with quantile normalization and log2 transformation together for each set of microarrays profiled in each tissue. For each transcript and within the replicates of one strain, we removed outliers from the expression data using the Nalimov outlier test, as previously described^{2,3}.

Expression QTL mapping in the rat

We have used the genetic map of the BXH/HXB RI strains² generated in a previous large scale effort by the STAR consortium⁴. This map was derived from around 13,000 polymorphic SNP markers leading to ~1,400 unique strain distribution patterns (SDP) for the genetic analysis. The average strain expression values were used for mapping using QTL reaper software⁵. This software implements a marker regression with permutation to calculate genome-wide corrected *P*-values (P_{GW}) for each transcript. Here we used one million permutations to assess genome-wide significance of the eQTLs.

Genome-wide analysis of TF – target eQTLs

We have analyzed eQTL data in conjunction with transcription factor binding site (TFBS) predictions following the hypothesis that genetic changes of gene expression of TFs will impact on the expression of their direct targets. The first prerequisite is to find TFs linked to a genetic variation, and second, to score the differential expression of the TF together with its predicted targets. From the eQTL data we have identified a total of 147 transcription factors with an eQTL in at least one tissue and a known TFBS with a model in TRANSFAC⁶ at a genome-wide corrected $P < 0.1$ using QTL-reaper⁴ (see eQTL mapping). In order to quantify the effect of this dysregulation of the TF on its targets, we

searched for *trans*-eQTLs co-occurring at the peak markers of the TF eQTLs. For each TF, we retrieved a list of 1,000 top-ranked transcripts according to their Likelihood Ratio Statistics (LRS) score at the TF eQTL peak marker and subjected this ranked list to a TFBS enrichment analysis using PASTAA⁷. PASTAA compares this LRS-determined ranking to a ranking based on predicted TF binding affinities to the 200 bp proximal promoter determined by a biophysical model⁷. Promoter sequences were extracted from ENSEMBL and TSS annotation provided by P. Carnici (unpublished). The comparison is performed using an iterated hypergeometric test for the overlap of the 'top ranked' genes when varying the thresholds on both lists. This procedure circumvents the recurring problem of setting more or less arbitrary thresholds on eQTL *P*-values or TFBS predictions. In addition to quantifying the overall enrichment this procedure also determines the thresholds used to define eQTLs and TF targets and moreover the set of genes satisfying both criteria which is used to define the differentially expressed targets of the TF. The statistical significance of this procedure is assessed using a null distribution generated from 1×10^6 permuted gene lists.

Quantitative chromatin immunoprecipitation (ChIP)

For quantitative ChIP, chromatin was prepared from 100 mg tissue (left ventricle of the heart and liver) using EpiQuik Tissue ChIP Kit (Epigentek, NY, USA) according to the manufacturer's instructions and then fragmented to a size range of 300-700 bases by sonication. Chromatin immunoprecipitation was performed essentially as described previously⁸. Rabbit antibodies against Irf7 (Invitrogen, Germany) or pre-immune IgG (Santa Cruz Biotechnology, CA, USA) were bound to protein A-coupled Dynabeads (Invitrogen, Germany) prior to incubation with chromatin. Each immunoprecipitated DNA sample was subjected to Taqman quantitative PCR analysis. Primer and probe sequences are listed in Supplementary Table 10.

Co-expression network analysis in the rat

In order to gain insight into potential upstream regulators of the *Irf7* network we have used a co-expression network derived from gene expression profiles across 7 tissues and 30 strains. For this analysis we removed tissue mean expression values for each

gene because we were only interested in the genetic variability across strains. Assuming independence of expression values between tissues within the same strain we have used all 203 samples for pairs of transcripts where both transcripts were measured in all tissues. For pairs of transcripts where at least one transcript was present only on the Affymetrix array RAE230 2.0 miroarrays we used the available 116 samples to compute pair-wise Pearson correlation coefficients. The network is formally defined by the tuple (V, E) with V being the set of nodes or vertices and E the set of edges. Here V corresponds to the set of all transcripts profiled on the Affymetrix RAE230a gene array. Since we are interested in the network neighborhood of the predicted *Irf7* targets we define the set I (subset of V) of predicted targets. The set of Edges E is defined as all tuples of transcripts where one is a predicted target (element of I) and the other is from the rest of nodes ($V \setminus I$) with significant Pearson correlation coefficients. We used a false discovery rate (FDR) approach to determine significance of Pearson correlation coefficients⁹. This approach estimates the FDR using a mixture model on the correlation coefficients with an empirical parametric null-distribution and a non-parametric alternative distribution. For the estimation of the null distribution we have used 99% of the data. We considered the correlation significant with $\text{FDR} < 0.001$. Finally, we have removed unconnected nodes leading to the final set of nodes V' of the expanded *Irf7* network. For the visualization we then re-estimated the FDR using the same approach described above using the complete correlation matrix for the set V' . All genes in rat *Irf7*-driven inflammatory network (iDIN) are reported in Supplementary Table 2.

Gutenberg Heart Study sample and expression analysis

The Gutenberg Heart Study (GHS) included 1,490 participants successively enrolled into a community-based, prospective, observational single-center study in the Rhein-Main region in western mid-Germany. All subjects gave written informed consent. Ethical approval was given by the local ethics committee and by the local and federal data safety commissioners. Separation of monocytes was conducted within 60 min after blood collection. 8 mL blood was collected using the Vacutainer CPT Cell Preparation Tube System (BD, Heidelberg, Germany) and 400 μL RosetteSep Monocyte Enrichment Cocktail (StemCell Technologies, Vancouver, Canada) was added immediately after

blood collection. This cocktail contains antibodies directed against cell surface antigens on human hematopoietic cells (CD2, CD3, CD8, CD19, CD56, CD66b) and glycophorin A on red blood cells. Total RNA was extracted the same day using Trizol extraction and purification by silica-based columns and 200 ng of total RNA was reverse transcribed, amplified and biotinylated using the Illumina TotalPrep-96 RNA Amplification Kit (Ambion/Applied Biosystems, Darmstadt, Germany). cDNA and cRNA purification were performed automatically using the MagMax Express96 magnetic particle processor (Applied Biosystems, Darmstadt, Germany) and cRNA was controlled on an Agilent Bioanalyzer 2100 (Agilent Technologies, Boeblingen, Germany). Gene expression profiling was performed using the Illumina HT-12 v3 BeadChip. BeadChips were scanned using the Illumina Bead Array Reader and pre-processing of data was performed with Beadstudio. Out of the 48,803 probes present on the HT-12 BeadChips, 27,029 were annotated in Ensembl that matched to 17,156 distinct Ensembl genes. After filtering transcripts undetected in monocytes and those exhibiting low intra-individual variation, 10,742 transcripts were analyzed. Genotyping was performed using the Affymetrix Genome-Wide Human SNP Array 6.0 and the Genome-Wide Human SNP NspI/Styl 5.0 Assay kit. Genotypes were called using the Affymetrix Birdseed-V2 calling algorithm and quality control was performed using GenABEL (<http://mga.bionet.nsc.ru/nlru/GenABEL/>).

TF – target analysis in humans in the Gutenberg Heart Study

In the human monocyte expression data, we were interested in the TF – target relationships without a special focus on the genetic regulation. Therefore we ranked all potential TF targets of *Irf7* according to their co-expression with the TF, as measured by the absolute Pearson correlation coefficient. Analogously to the rat TFBS enrichment analysis we obtained sequences 200 bp upstream of the transcription start site (TSS) as annotated in the ENSEMBL database and ranked them according to predicted TF affinities. Subsequently we quantified the enrichment of predicted TFBS in the top 1,000 co-expressed genes using PASTAA⁷. Subsequent network expansion was performed using the same procedure as in the rat. All genes within human iDIN are reported in Supplementary Table 5.

Overlap between human and rat iDIN

In order to compare the genes in the rat and human iDIN we used ENSEMBL to derive orthologous genes between rat and human. Of all genes represented on the rat and human expression arrays we were able to identify a common set of 9,909 human genes that had a rat orthologue and were represented on both expression arrays. We defined this as the “orthologue expression set”. The human iDIN in the GHS contained 495 Ensembl genes (Supplementary Table 5) of the orthologue expression set. Out of the Ensembl 305 rat iDIN genes (Supplementary Table 2), 252 Ensembl genes were contained in the orthologue expression set. The overlap between the two sets was 51 Ensembl genes ($P = 9.1 \times 10^{-20}$), which we report in the table below.

Ensembl genes that were in common between the rat and human iDIN

Ensembl ID	Gene Symbol	Gene Name	Chr*	Gene Start-End (Mbp)
ENSG00000187608	<i>ISG15</i>	ISG15 ubiquitin-like modifier	1	0.948803-0.94992
ENSG00000137965	<i>IFI44</i>	interferon-induced protein 44	1	79.115481-79.129763
ENSG00000162645	<i>GBP2</i>	guanylate binding protein 2, interferon-inducible	1	89.571815-89.616139
ENSG00000162654	<i>GBP4</i>	guanylate binding protein 4	1	89.646831-89.664615
ENSG00000143119	<i>CD53</i>	CD53 molecule	1	111.415722-111.442558
ENSG00000155363	<i>MOV10</i>	Mov10, Moloney leukemia virus 10, homolog (mouse)	1	113.215763-113.243368
ENSG00000160710	<i>ADAR</i>	adenosine deaminase, RNA-specific	1	154.554537-154.600475
ENSG00000163565	<i>IFI16</i>	interferon, gamma-inducible protein 16	1	158.969758-159.024945
ENSG00000186517	<i>ARHGAP30</i>	Rho GTPase activating protein 30	1	161.016732-161.03976
ENSG00000158869	<i>FCER1G</i>	Fc fragment of IgE, high affinity I, receptor for; gamma polypeptide	1	161.185024-161.190489
ENSG00000186283	<i>TOR3A</i>	torsin family 3, member A	1	179.050512-179.067158
ENSG00000162772	<i>ATF3</i>	activating transcription factor 3	1	212.738676-212.794119
ENSG00000134326	<i>CMPK2</i>	cytidine monophosphate (UMP-CMP) kinase 2, mitochondrial	2	6.980701-7.006766
ENSG00000134321	<i>RSAD2</i>	radical S-adenosyl methionine domain containing 2	2	7.005937-7.03837
ENSG00000115415	<i>STAT1</i>	signal transducer and activator of transcription 1	2	191.829084-191.885686
ENSG00000196141	<i>SPATS2L</i>	spermatogenesis associated, serine- rich 2-like	2	201.170604-201.343253
ENSG00000135899	<i>SP110</i>	SP110 nuclear body protein	2	231.032009-231.090444
ENSG00000079263	<i>SP140</i>	SP140 nuclear body protein	2	231.090445-231.265029
ENSG00000138496	<i>PARP9</i>	poly (ADP-ribose) polymerase family, member 9	3	122.246806-122.283424

ENSG00000136514	<i>RTP4</i>	receptor (chemosensory) transporter protein 4	3	187.08612-187.089864
ENSG00000169245	<i>CXCL10</i>	chemokine (C-X-C motif) ligand 10	4	76.942273-76.94465
ENSG00000145287	<i>PLAC8</i>	Placenta-specific 8	4	84.011201-84.035911
ENSG00000138642	<i>HERC6</i>	hect domain and RLD 6	4	89.299891-89.364248
ENSG00000137628	<i>DDX60</i>	DEAD (Asp-Glu-Ala-Asp) box polypeptide 60	4	169.137443-169.239958
ENSG00000043462	<i>LCP2</i>	lymphocyte cytosolic protein 2	5	169.675089-169.724822
ENSG00000160932	<i>LY6E</i>	lymphocyte antigen 6 complex, locus E	8	144.099902-144.103825
ENSG00000178685	<i>PARP10</i>	poly (ADP-ribose) polymerase family, member 10	8	145.051321-145.060635
ENSG00000119922	<i>IFIT2</i>	interferon-induced protein with tetratricopeptide repeats 2	10	91.061712-91.069033
ENSG00000119917	<i>IFIT3</i>	interferon-induced protein with tetratricopeptide repeats 3	10	91.087651-91.100728
ENSG00000185507	<i>IRF7</i>	interferon regulatory factor 7	11	0.612555-0.615999
ENSG00000132256	<i>TRIM5</i>	tripartite motif-containing 5	11	5.684787-5.959849
ENSG00000156587	<i>UBE2L6</i>	ubiquitin-conjugating enzyme E2L 6	11	57.319129-57.335453
ENSG00000149131	<i>SERPING1</i>	serpin peptidase inhibitor, clade G (C1 inhibitor), member 1	11	57.36486-57.382326
ENSG00000110077	<i>MS4A6A</i>	membrane-spanning 4-domains, subfamily A, member 6A	11	59.939081-59.950674
ENSG00000168062	<i>BATF2</i>	basic leucine zipper transcription factor, ATF-like 2	11	64.755416-64.764517
ENSG00000123338	<i>NCKAP1L</i>	NCK-associated protein 1-like	12	54.891495-54.936898
ENSG00000135148	<i>TRAFD1</i>	TRAF-type zinc finger domain containing 1	12	112.563349-112.591407
ENSG00000089127	<i>OAS1</i>	2',5'-oligoadenylate synthetase 1	12	113.344739-113.369794
ENSG00000135114	<i>OASL</i>	2'-5'-oligoadenylate synthetase-like	12	121.458121-121.477045
ENSG00000100911	<i>PSME2</i>	proteasome (prosome, macropain) activator subunit 2	14	24.612571-24.61643
ENSG00000165949	<i>IFI27</i>	interferon, alpha-inducible protein 27	14	94.577079-94.583033
ENSG00000140105	<i>WARS</i>	tryptophanyl-tRNA synthetase	14	100.800125-100.84268
ENSG00000172183	<i>ISG20</i>	interferon stimulated exonuclease gene 20kDa	15	89.181974-89.199714
ENSG00000168961	<i>LGALS9</i>	lectin, galactoside-binding, soluble, 9	17	25.956824-25.976586
ENSG00000108691	<i>CCL2</i>	chemokine (C-C motif) ligand 2	17	32.582313-32.584222
ENSG00000108771	<i>DHX58</i>	DEXH (Asp-Glu-X-His) box polypeptide 58	17	40.253422-40.264751
ENSG00000068079	<i>IFI35</i>	interferon-induced protein 35	17	41.158769-41.166475
ENSG00000108679	<i>LGALS3BP</i>	lectin, galactoside-binding, soluble, 3 binding protein	17	76.967337-76.976061
ENSG00000180843	AC124319.2	Protein ALO17 (ALK lymphoma oligomerization partner on chromosome 17)	17	78.234667-78.310304

ENSG00000130589	<i>RP4-697K14.2</i>	Peroxisomal proliferator-activated receptor A-interacting complex	20	62.189439-62.205592
ENSG00000157601	<i>MX1</i>	myxovirus (influenza virus) resistance 1, interferon-inducible protein p78 (mouse)	21	42.792231-42.831141

*Table is sorted according to chromosome number (Chr) and genomic location of each gene

Combined In situ hybridisation and immunohistochemistry

Immunofluorescent *in situ* hybridization was performed using 10 µm thick SHR heart cryosections. Sections were fixed in 4% (w/v) paraformaldehyde, incubated with 1 µg/ml proteinase K (Sigma) and re-fixed in 4% (w/v) paraformaldehyde. Sections were pre-hybridised in hybridisation buffer (50% formamide, 5X SSC buffer, 250 µg/ml yeast RNA, 1× Denhardt's solution in DEPC treated water), incubated with 2 µM *Ebi2*-specific locked nucleic acid probe (5' AAAGAACGCTATGCCCA 3') or scrambled probe (5' GTGTAAACACGTCTATGCCCA 3') 5' labelled with digoxigenin (DIG) (Exiquon, Denmark) in hybridisation buffer for 18 h. Sections were washed twice in buffer (50% (v/v) formamide, 5X SSC buffer in DEPC-treated water), incubated in blocking buffer (10% (v/v) sheep serum), and hybridised with sheep anti-DIG fAb fragments labelled TRITC diluted in 10% (v/v) sheep serum (Roche Diagnostics). Sections were washed in PBS and incubated with 10% rabbit serum and hybridised overnight at room temperature with anti-Cd68-ALEXA488 antibody (MCA341A488, AbD Serotec, Oxford UK) at 1µg/ml in 10% rabbit serum in PBS. Nuclei were stained with DAPI. Sections were imaged using Leica SP1 confocal microscope.

Quantitative PCR analysis

cDNA were synthesized from DNase I (Invitrogen) treated total RNA samples using iScript™ cDNA Synthesis Kit (Bio-Rad) following manufacturer's protocol. QPCR was performed using SYBR® Green JumpStart Taq Ready Mix (Sigma) or Taqman probes (ABI) following manufacturer's protocol. PCR conditions: 94 °C for 2 minutes (SYBR® Green) or 10 minutes (TaqMan) followed by 40 cycles of 94 °C for 15 seconds, 60 °C for 1 minute and 72 °C for 1 minute, with data collection at end of each cycle.

Primers: *Phgdhl1* F: CTGGATTATCTCCGGCATGT, *Phgdhl1* R: GGTGGGTTCTGAAGATGAGAAG, *Clybl* F: GCCTGGGAATGACGAAAAGA, *Clybl* R: GCAGTCCAGCACAGCACAAT, *Gpr18* F: GCCGAAATACGCCAAGGA, *Gpr18* R:

CATTATCCAGACCCCCACAC, *Tm9sf2* F: AGAGGAGGCCATAATACTGACGAT,
Tm9sf2 R: TCCACCTACCGAGTCTAGAAAACC, *Cd68* F:
CTGTTGCGGAAATACAAGCA, *Cd68* R: GGCAGCAAGAGAGATTGGTC, *Irf7* F:
GTGTGCCCTGGAAGCATTTC, *Irf7* R: AGCCCAGGCCTTGAAGATCT, *Ly6c* F:
CTGGCCCTACTGTGTGCAGAA, *Ly6c* R: TGTCGGTCTTACAGAGGCCCTCA, *Ly6e* F:
5' GGCTTCGGGAATGTCAACCT, *Ly6e* R: GCAGTGGGATACTAGCACGAAGTC,
Stat1 F: 5' GAACGTGCTCTGCTCAAGGA, *Stat1* R: GTCGGGTTCACCTCCATTTG,
Ifi27 F: 5' GCTTCACTGGGTCAAGCATT, *Ifi27* R: TCCTATGGCTGCCCAACA,
Oas1a F: GCCCAACCAAGCTTAAGAGTC, *Oas1a* R: GTTCCAAGATTGTCCCGAAG,
Lgals3bp F: ACAGTGTGCGACAAACCTCTG, *Lgals3bp* R:
GACTCGTCCCTGTGCATTC; *Ebi2* TaqMan Probe (Rn01468255_m1), *Dock9* TaqMan
Probe (Rn01468134_m1). Data were analyzed using ΔCt or $\Delta\Delta Ct$ techniques¹⁰ as
detailed in the text.

RNA-Sequencing

RNA-Sequencing was performed upon pooled, poly(A) enriched RNA from left ventricle (LV) tissue from four BN rats aged 6-8 weeks (Charles River). Total RNA was extracted from frozen tissue using TRIzol & RNeasy columns (Qiagen). RNA was enriched for poly(A) transcripts using an oligo-dT pull down with Poly(A) Purist kit (Ambion). Equal amounts of poly(A) RNA from BN biological replicates were pooled and whole transcriptome libraries prepared with Whole Transcriptome Analysis Kit (Ambion). Sequencing beads were prepared using standard protocols from Applied Biosystems. One flow was sequenced using the Applied Biosystems SOLiD V2 system, at 40 bases per bead. Reads were aligned to the rat reference genome (RGSC 3.4 assembly) using the Whole Transcriptome pipeline (<http://solidsoftwaretools.com>, Applied Biosystems). A total of 150 million reads were generated (6Gb), of which 50% mapped to the reference BN genome, 35% to unique positions. Reads mapping to genes within the locus controlling the rat iDIN were quantified at the exonic and whole transcript level.

Characterization of *Ebi2* expressing cells in *Ebi2*^{GFP/+} mouse

Tissues were isolated from adult *Ebi2*^{GFP/+} mice that were 7 generations backcrossed to C57BL/6J¹¹. Each organ was cut into small pieces (approx. 0.5 cm diameter), fixed in 4%

PFA for 2 hours, washed in PBS for 10 minutes 4-6 times, and then dehydrated overnight in 30% sucrose in PBS. The tissue was then flash-frozen in OCT in a dry ice/ethanol bath. Antibodies were diluted in 0.3% Triton-X100, 0.2% BSA, and 0.1% sodium azide to stain 7um sections. Tissues were stained with anti-CD11b-PE (clone M1/70, Invitrogen), anti-CD16/32-Alex Fluor 647 (clone 2.4G2, UCSF Hybridoma and Monoclonal Antibody Core), rabbit anti-GFP (Invitrogen) and anti-rabbit-FITC (Caltag). All images were collected on a Zeiss AxioObserver Z1 microscope and processed using Adobe PhotoShop CS2. Images are representative of 1-2 mice.

Luciferase assay

COS7 cells (2×10^5) were plated in a 24-well plates and transfected with (0.2 μ g) empty pGL3 promoter (Promega), pGL3promoter with the BN 5'UTR upstream of Firefly luciferase (BN-pGL3) or pGL3promoter with the SHR 5'UTR upstream of Firefly luciferase (SHR-pGL3). All cells were also co-transfected with pRL-SV40 (Promega) using (2 μ l) Lipofectamine 2000 (Invitrogen). 24h post-transfection, cells were washed with PBS and then lysed in 100 μ l 1x passive lysis buffer (Promega) on a rocking platform for 30min at room temperature. 50 μ l/well lysate (in duplicate) was transferred to a white opaque plate, followed by addition of dual-glo reagent (50 μ l/well; Promega). After 15m, the plate was read on a GloMax®-96 microplate Luminometer (Promega). For Renilla luminescence, 50 μ l/well freshly prepared stop-glo reagent (Promega) was added. After 15m, the plate was read on a GloMax®-96 microplate Luminometer (Promega). Data was determined as Firefly luminescence/Renilla Luminescence.

BN and SHR 5'UTRs with the 5'UTR SNP underlined and in bold:

BN 5'UTR upstream of Firefly luciferase in the BN-pGL3promoter:

GAAAAAGGCACCACCAAAAGGACGCCTGCTCAGTCGCTCTAAAGCAACATGCC
CAGTTCAGCTGACTCCAGTCTGGGCAAACACAGACGGCCACCTGGAGGGCTCTAG
CCACCCTCTGATAACTCTGACCACTGCGGATACAGAAA

BN 5'UTR upstream of Firefly luciferase in the SHR-pGL3promoter:

GAAAAAGGCACCACCAAAAGGACGCCTGCTCAGTCGCTCTAAAGCAACATGCC
CAGTTCAGCTGACTCCAGTCTGGGCAAACACGGACGGCCACCTGGAGGGCTCTAG
CCACCCTCTGATAACTCTGACCACTGCGGATACAGAAA

Bone marrow-derived macrophage (BMDM) culture and *Ebi2* silencing by siRNA

BMDM were cultured as previously described¹². Briefly, femurs from adult BN rats were isolated and flushed with Hank's buffer (Gibco). Total bone marrow-derived cells were plated and cultured for 5 days in DMEM (Gibco) supplemented with 25% L929 conditioned media, 25% fetal bovine serum (Gibco), penicillin (100U/ml, Invitrogen) and streptomycin (100µg/ml, Invitrogen). Adherent BMDM were seeded in six-well plates (10^6 cells per well) and treated with DMEM on the day before siRNA transfection. Cells were transfected with ON-TARGETplus SMARTpool siRNA (100nmol/L), which consists four individual siRNAs targeting rat *Ebi2* (Dharmacon, Thermo Scientific). For control, cells were transfected with ON-TARGETplus Non-Targeting siRNA (Dharmacon, Thermo Scientific). Cells were harvested 48 hours after transfection. Total RNA samples were prepared using RNeasy spin columns (QIAGEN).

T1D sample selection and genotyping

Analysis of SNPs across the region was described elsewhere¹³. SNP rs9585056 was genotyped using TaqMan (Applied Biosystems) on a subset of samples used in a genomewide scan for T1D^{13,14}, additional case-control samples, and a set of samples from 3,733 families with T1D affected offspring. All samples have been described previously^{14,15}. Briefly, all subjects were of White European ancestry, and samples were excluded if they showed evidence of non-European ancestry, or of being duplicates or closely related to another sample in the study. All Taqman genotyping data were scored twice to minimize error; the second operator was unaware of case-control status and family structure.

Association testing of rs9585056 with T1D

We used logistic regression to test for association in case control samples, stratifying by broad UK region to control for population structure. Family data were analysed by transmission disequilibrium test, splitting multiplex families into parent offspring trios and using a pseudo-case control framework to estimate allelic effects. A score statistic was also generated, and a score test for association in case-controls and families combined conducted by summing the scores and variances according to the method proposed by Mantel¹⁶.

Cross species cell type enrichment analysis

Cell type enrichment analysis was performed on the mouse and human homologues of the genes of the rat iDIN network. Gene expression profiles for both mouse and human were downloaded from Novartis BioGPS (<http://biogps.gnf.org/downloads>) listed under Gene Expression Omnibus (GEO) code GSE1133¹⁷ and GSE10246¹⁸; disease cell types were removed from both datasets prior to analysis. There were 135 genes in the rat iDIN for which there were both mouse and human orthologues and 71 human and 65 mouse cell types, respectively. We tested each gene for extreme expression in a given cell type, compared to its average expression across all cell types and tissues, using the *Z*-test in separately in both species. Combined *P*-values were calculated across genes using Fisher's combined probability test where the logged *P*-values calculated across cell types were summed and multiplied by negative two, following equation^{19,20}.

$$X^2 = -2 \sum_{i=1}^k \ln(p_i).$$

The test statistic follows a χ^2 distribution with $2n$ degrees of freedom, with n being the number of tests performed. A Bonferroni correction was then applied to the combined *p*-values to correct for multiple testing.

Bayesian mapping of regulatory ‘hot-spots’ for the rat network

Genotypes imputation

Missing genotype values (accounting for 1.2% of the total number of SNPs) were imputed using fastPHASE 1.2²¹, using 29 RI strains and using 10 replicated analyses with different random starts. We also performed the analysis without specifying the number of groups: in this case fastPHASE correctly identified the two strains in the population. To exclude SNPs in perfect linkage disequilibrium, we removed redundant SNPs with $r^2 = 1$. This delineated a set of 1,304 informative SNPs across the rat genome.

Sparse Bayesian Regression (SBR)

Association between expression levels of the network genes and all informative SNPs was carried out using Bayesian multiple linear regression. Since the number of SNPs highly supersedes the number of observations, a sparse detection of the combination of SNPs that explain variation in gene expression was imposed. For each transcript, *a priori* the expected number of distinct genetic control points was set between 0 and 4. To prevent the search algorithm to be stuck in local modes of the model space, a new sampling algorithm, Sparse Bayesian Regression (SBR)^{22,23} has been designed: it combines ideas from Genetic Algorithms and Markov Chain Monte Carlo²⁴ with different tempered chains run in parallel each of which able to explore different regions of the model space.

For each tissue $t = 1, \dots, T$ and for each gene g , $g = 1, \dots, G_t$, we regressed the $n \times 1$ gene expression level y_{tg} on the $n \times p$ set X of non-redundant SNPs. For each gene g , we recorded the models γ_{tg} visited during the search and we ranked them according to their posterior model probability $p(\gamma_{tg} | y_{tg})$, where the binary latent vector γ_{tg} , $\gamma_{tg} = (\gamma_{tg1}, \dots, \gamma_{tgc}, \dots, \gamma_{tgp})^T$ with $\gamma_{tgc} = \{0,1\}$, $c = 1, \dots, p$, indicates the subset of SNPs that predict y_{tg} . The best model visited, γ_{tg}^B , represents the best combination of SNPs that explains the variability in the gene expression level for a particular transcript. We also calculate, in a post-processing analysis, the marginal posterior probability of inclusion $p_{tgc} = p(\gamma_{tgc} | \gamma_{tg \setminus c})$, where $\gamma_{tg \setminus c}$ indicates all the SNPs, but the c th. The marginal posterior probability of inclusion measures the strength of association between the c th SNP and the g th gene in the t th tissue conditionally on all the other SNPs. The SBR algorithm was run for 50,000 sweeps, with 10,000 as burn-in, running in parallel three chains each of which with a different temperature. The different temperatures have the effect of flattening the posterior distribution (likelihood \times prior). This ensures that it is not trapped in any local mode and that the algorithm mixes efficiently, since every chain constantly tries to transmit information about its state to the others²⁵. Convergence of the Markov Chain Monte Carlo have been evaluated looking at the trace of γ_{tg} and counting

the number of times the algorithm visits the same top model, ranked by the posterior model probability, in the two halves of the sweeps.

False Discovery Rate calculation

We derived a procedure to declare a significant association between each SNP j and all the network genes G_t for a given FDR level. In each tissue t , we consider all the $G_t \times p$ marginal posterior probabilities p_{tgi} assuming exchangeability among the genes. Then we estimated the null and the alternative distribution by fitting a mixture of beta distributions with unknown number of components on the $G_t \times p$ set of marginal posterior probabilities²⁶. The Expectation Maximization (EM) algorithm²⁷ was used to fit the beta mixture on the set of $G_t \times p$ marginal posterior probabilities p_{tgi} . We repeated the analyses with 2, 3, 4 and 5-components mixture, respectively, assuming that the alternative distribution is represented by the right outermost component. Finally the best fit was judged using Bayesian Information Criterion (BIC)²⁸ with the 2-components mixture able to better conformed to the data in all tissues. A by-product of the EM algorithm is $p(z_{tgi} = 1)$ which represents, for the 2-component mixture, the posterior probability that p_{tgi} belongs to the alternative distribution, whereas z_{tgi} indicates the latent allocation variable for p_{tgi} . For a fixed level of the FDR, the classification probability $p(z_{tgi} = 1)$ can be used to calculate the cut-off c_t above which the association between the gene g and the SNP j is called significant with strength p_{tgi} . Following Lewin and Richardson²⁹, the optimal cut-off c_t is obtained such that the estimated FDR is not greater than the desired one. Once c_t is derived, all p_{tgi} for which $p(z_{tgi} = 1) > c_t$, $g = 1, \dots, G_t$, $j = 1, \dots, p$, are classified as belonging to the alternative distribution and all the corresponding gene-SNP associations are called significant. To call significant associations between the genes in tissues t and the SNPs we fixed the FDR level at 1%.

Identification of regulatory hot-spots

For each tissue t , it is possible to count the number of control points between the j th SNP, $j = 1, \dots, p$, and all the network genes at a given FDR level. Similarly to Schadt et

al³⁰, we ranked the SNPs according to the number of associated network genes focusing on the top 10 regulatory ‘hot-spots’. In addition, we also measured a rescaled average strength of association m_{tj} , (and $\alpha\%$ percentiles, $q_{tj}(\alpha)$) between each of the 10 putative regulatory hot-spot and the network genes as

$$m_{tj} = f_t \frac{1}{|\mathcal{G}_j|} \sum_{g \in \mathcal{G}_j} p_{tgj},$$

where $j \in \mathcal{J}$, with \mathcal{J} the set 10 putative master regulators, $|\mathcal{G}_j|$ indicates the number of associated genes for SNP j th and p_{tgj} is marginal posterior probability of inclusion at a fixed FDR level. Finally, f_t , $f_t = \frac{|\mathcal{G}_j|}{\max_{j \in \mathcal{J}} |\mathcal{G}_j|}$ is a rescaling factor that equalizes means

(and percentiles) such as all the putative master regulators, in the \mathcal{J} set, control the same number of network genes. To compare the strength of the association between each putative master regulator and the network genes, we used the Bayes Factor³¹. Given p_{tgj} at a fixed FDR level, the Bayes Factor is defined as the ratio of posterior odds on prior odds

$$BF(\gamma_{tgj} = 1; \gamma_{tgj} = 0) = \frac{p_{tgj}/(1 - p_{tgj})}{E(p_{\gamma_{tgj}})/\left(1 - \frac{E(p_{\gamma_{tgj}})}{p}\right)},$$

where $E(p_{\gamma_{tgj}})$ is the expected number of control points in the t th tissue for the g th gene (fixing $E(p_{\gamma_{tgj}}) = 2$ with $p = 1,304$, the prior probability for the j th SNP associated with the g th gene is 0.0015). Finally, following Servin and Stephens³², we define the rescaled average Bayes Factor over the set \mathcal{G}_j for $j \in \mathcal{J}$ as

$$m_{tj}^{BF} = \frac{1}{\max_{j \in \mathcal{J}} |\mathcal{G}_j|} \sum_{g \in \mathcal{G}_j} BF(\gamma_{tgj} = 1; \gamma_{tgj} = 0).$$

In Fig. 2, for each of the ten putative master regulators, the rescaled Bayes Factors are indicated as circles. Values of the Bayes Factor less than one, do not support genetic control. Poor, substantial, strong and decisive evidence for common genetic regulation

by the same SNP is declared if the Bayes Factor is between 1 and 3.2, 3.2 and 10, 10 and 100 and greater than 100, respectively³¹.

Cardiogenics sample and expression analysis

The Cardiogenics study included 758 individuals, including 363 patients with coronary artery disease (CAD) or myocardial infarction (MI) and 395 healthy individuals of European descent recruited in five centers within the Cardiogenics consortium (<http://www.cardiogenics.eu>). Healthy individuals were recruited in Cambridge (UK). CAD/MI patients (n=459) were recruited in Leicester (n=161), Lübeck (n=102), Regensburg (n=122) and Paris (n=74). The study was approved by the Institutional Ethical Committee of each participating center. Blood samples (30ml) from fasting subjects were collected into EDTA and monocytes were isolated with CD14 micro beads using AutoMacs/AutoMacs Pro (Miltenyi) according to the manufacturer's instructions. Monocyte purity was measured as the percentage of CD14^{+ve} cells analyzed by flow cytometry. Isolated monocytes were lysed in Trizol and RNA was extracted in chloroform and ethanol, washed in RNeasy columns (Qiagen) and incubated with DNase 1 before extracting in RNase-free water. RNA was quantified by the Nanodrop® method. Genomic DNA was extracted from peripheral blood monocytes by standard procedures (Qiagen) and sent to the Sanger Institute for genotyping.

Gene expression profiling was performed using the Illumina's Human Ref-8 Sentrix Bead Chip arrays (Illumina Inc., San Diego, CA) containing 24,516 probes corresponding to 18,311 distinct genes and 21,793 Ref Seq annotated transcripts. mRNA was amplified and labelled using the Illumina Total Prep RNA Amplification Kit (Ambion, Inc., Austin, TX). After hybridization, Array images were scanned using the Illumina BeadArray Reader and probe intensities were extracted using the Gene expression module (version 3.3.8) of the Illumina's Bead Studio software (version 3.1.30). Raw intensities were processed in R statistical environment using the Lumi and beadarray packages. All array outliers were excluded and only arrays with high concordance in terms of gene expression measures (pairwise Spearman correlation coefficients within each cell type >0.85) were included in the analyses. After data quality control, 849 monocyte RNA samples were available for statistical analyses. Whole-genome genotyping was carried out using two arrays, the Sentrix Human Custom 1.2M array (1,115,839 SNPs and

80,128 CNVs) and the Human 610 Quad Custom array (594,398 SNP s and 66,049 CNVs) (Illumina). After filtering, which was based on sample call rate, ancestry, duplications and genetic relatedness; 758 were used for further analyses. Subsequent filtering removed SNPs if they had (i) a per-SNP call rate lower than 95% in cases or controls on the two arrays, and/or (ii) a minor allele frequency (MAF) of 1% in cases or in controls and/or (iii) a MAF in controls generated using the Illumina 1.2 M or in those generated on the 670k array and/or (iv) a significant deviation from Hardy-Weinberg equilibrium in the controls ($P < 10^{-5}$). Furthermore, all SNPs on the Y and mitochondrial chromosomes as well as CNV markers were excluded from statistical analysis. After per-SNP data quality control, 522,603 SNPs represented on the two arrays and that passed the quality control, were used for further analyses.

Co-expression network analysis

To build the co-expression network centred on *IRF7*, we correlated expression profiles of all genes that were analyzed for the Gutenberg Heart Study (GHS) versus the predicted *IRF7* targets. Correlation coefficients were computed after stratification for the centre and we estimated the FDR using the Strimmer approach^{9,33}. In keeping with the analysis in the GHS study, we applied a threshold of $\text{FDR} < 0.001$ to identify the significant set of adjacent genes (i.e., co-regulated genes). This threshold corresponded to an absolute correlation of at least 0.53. We have identified a set of 791 genes that are co-expressed with the core set of predicted *IRF7* targets. The overlap with the GHS expression network comprises 186 genes ($P = 8.32 \times 10^{-23}$) and Gene Ontology (GO) enrichment analysis showed the strongest enrichment for immune response ($P = 1.31 \times 10^{-11}$) and response to virus ($P = 4.68 \times 10^{-11}$) categories, respectively.

Association of genetic variation and *EBI2* expression

Association between SNPs at the chromosome 13 locus and *EBI2* mRNA abundance was assessed by linear regression. The subset of SNPs sufficient to explain *EBI2*-gene-expression variation at the locus was determined by using the lasso shrinkage and selection method for linear regression³⁴.

Association of human iDIN with the chromosome 13 locus

We carried out multivariate analysis of variance (MANOVA)³⁵ to determine whether the chromosome 13q32 locus is associated with monocyte expression of *IRF7* and all predicted *IRF7* targets in the GHS and Cardiogenics cohorts. For each SNP at the chromosome 13q32 locus, one-way MANOVA analysis was performed to test the hypothesis that the mean expression levels of *IRF7*-target genes are the same in all genotypes categories. Among the different statistics that can be used to evaluate the MANOVA hypothesis, we employed the Pillai's trace, which is more robust to violations of normality and homogeneity of dispersion³⁶. Significant associations between network genes and SNPs at the locus were assessed using Storey's FDR at the 5% level³⁷.

We also verified the validity of the two most important assumptions of MANOVA analysis, namely, multivariate normality and, conditionally to each SNP, the homogeneity of variance-covariances matrices. We performed multivariate Box-Cox transformation to protect against deviations from the normality assumption, while the homogeneity of variance-covariances matrices among groups was assessed using Box's M statistics³⁸. To ensure that the MANOVA results presented in the manuscript are not affected by these factors, we repeated all analyses using the rank-based Wilks' lambda MANOVA³⁹, which is robust to violations of both conditions. The results of the rank-based MANOVA analysis supported the original MANOVA findings in the Cardiogenics cohort for six out of seven SNPs in the region (see Table below). Similar analyses in the GHS cohort did not detect a significant association of *IRF7* or *IRF7* target genes with SNPs at this locus (data not shown).

Significant MANOVA results at the chromosome 13q32 locus in the Cardiogenics cohort

SNPs	MANOVA	Rank-based MANOVA
rs7991143	$P = 1.4 \times 10^{-3}$	$P = 0.06$
rs3759443	$P = 1.6 \times 10^{-4}$	$P = 0.04$
rs3809367	$P = 1.6 \times 10^{-4}$	$P = 0.04$
rs1923891	$P = 1.6 \times 10^{-4}$	$P = 0.04$
rs9557217	$P = 5.0 \times 10^{-5}$	$P = 3 \times 10^{-4}$
rs7998284	$P = 1.0 \times 10^{-3}$	$P = 0.01$
rs9585056	$P = 1.1 \times 10^{-3}$	$P = 5.0 \times 10^{-3}$

Association of iDIN genes with T1D

To examine whether genes in the network were generally associated with T1D, we divided SNPs genotyped in T1D genome-wide association (GWA) scans into two:

A: those within 1Mb of any gene in the network, and

B: those within 1Mb of any ENSEMBL gene not in network, excluding any in *A*

We used a Wilcoxon rank test to examine whether the distribution of association statistics varied between sets *A* and *B*, on the basis of their one degree of freedom χ^2 test statistics. Note that this approach tests the null hypothesis that the pattern of association is the same in the two datasets, rather than a null that no SNPs in *A* are associated with T1D⁴⁰. We chose to use a nonparametric approach due to the extreme right skew displayed by test statistics for T1D; χ^2 values above 300 are seen for SNPs in the strongly associated HLA region. The more commonly used gene set enrichment analysis is based around the Kolmogorov-Smirnov test, which is underpowered for detecting differences in distributions⁴¹. To avoid potential confounding by allele frequency, we applied inverse probability weighting to the ranks used in the Wilcoxon according to a propensity score measuring the chance of a SNP appearing in the “inside” network group, given minor allele frequency^{42,43}. The propensity score was calculated by binning minor allele frequencies into bins of width 0.05 and taking the ratio of the number of SNPs in *A+B* and the number in *A*.

Correlation between SNPs is substantial in GWA data. While the Wilcoxon test has the helpful property that the mean under the null is unaffected by correlation, correlation does lead to inflation of the standard deviation of the test statistic which we estimated by 200 permutations of the case control labels. Finally, because the GWA datasets were generated on different chips (Affymetrix and Illumina) we used a stratified Wilcoxon⁴⁴ to avoid confounding by chip.

Because we have both human- and rat-derived networks, and because HLA shows extreme association with T1D, we performed four tests:

1. genes in either rat or human networks
2. genes in both rat and human networks, restricting set *B* to genes with a rat orthologue
3. genes in both rat and human networks, excluding SNPs from *A* or *B* within a wide window around human MHC (chr6:29000000..34600000)

4. genes in both rat and human networks, restricting set B to genes in the rat orthologue database and excluding SNPs from A or B within a wide window around human MHC (chr6:29000000..34600000)

Since many immune and viral response genes have been associated to T1D previously, we tested our sets against different background sets of genes: the whole genome and genes annotated to the GO term “immune response”.

References

- 1 Irizarry, R. A. et al. Summaries of Affymetrix GeneChip probe level data. *Nucleic Acids Res* 31, e15, (2003).
- 2 Hubner, N. et al. Integrated transcriptional profiling and linkage analysis for identification of genes underlying disease. *Nat Genet* 37, 243-253, (2005).
- 3 Petretto, E. et al. Integrated genomic approaches implicate osteoglycin (Ogn) in the regulation of left ventricular mass. *Nat Genet* 40, 546-552, (2008).
- 4 Saar, K. et al. SNP and haplotype mapping for genetic analysis in the rat. *Nat Genet* 40, 560-566, (2008).
- 5 Wang, J., Williams, R. W. & Manly, K. F. WebQTL: web-based complex trait analysis. *Neuroinformatics* 1, 299-308, (2003).
- 6 Matys, V. et al. TRANSFAC and its module TRANSCompel: transcriptional gene regulation in eukaryotes. *Nucleic Acids Res* 34, D108-110, (2006).
- 7 Roider, H. G., Manke, T., O'Keeffe, S., Vingron, M. & Haas, S. A. PASTAA: identifying transcription factors associated with sets of co-regulated genes. *Bioinformatics* 25, 435-442, (2009).
- 8 De Santa, F. et al. Jmjd3 contributes to the control of gene expression in LPS-activated macrophages. *EMBO J* 28, 3341-3352, (2009).
- 9 Strimmer, K. A unified approach to false discovery rate estimation. *BMC Bioinformatics* 9, 303, (2008).
- 10 Bustin, S. A. Absolute quantification of mRNA using real-time reverse transcription polymerase chain reaction assays. *J Mol Endocrinol* 25, 169-193, (2000).
- 11 Pereira, J. P., Kelly, L. M., Xu, Y. & Cyster, J. G. EBI2 mediates B cell segregation between the outer and centre follicle. *Nature* 460, 1122-1126, (2009).
- 12 Behmoaras, J. et al. Jund is a determinant of macrophage activation and is associated with glomerulonephritis susceptibility. *Nat Genet* 40, 553-559, (2008).
- 13 Barrett, J. C. et al. Genome-wide association study and meta-analysis find that over 40 loci affect risk of type 1 diabetes. *Nat Genet*, (2009).
- 14 Genome-wide association study of 14,000 cases of seven common diseases and 3,000 shared controls. *Nature* 447, 661-678, (2007).
- 15 Wallace, C. et al. The imprinted DLK1-MEG3 gene region on chromosome 14q32.2 alters susceptibility to type 1 diabetes. *Nat Genet*, (2009).
- 16 Mantel, N. Chi-square tests with one degree of freedom: Extensions of the Mantel-Haenszel procedure. *J Am Stat Assoc* 690-700, (1963).
- 17 Su, A. I. et al. A gene atlas of the mouse and human protein-encoding transcriptomes. *Proc Natl Acad Sci U S A* 101, 6062-6067, (2004).
- 18 Lattin, J. E. et al. Expression analysis of G Protein-Coupled Receptors in mouse macrophages. *Immunome Res* 4, 5, (2008).
- 19 Fisher, R. A. Statistical Methods for Research Workers. (Oliver and Boyd, Edinburgh, 1932).
- 20 Hess, A. & Iyer, H. Fisher's combined p-value for detecting differentially expressed genes using Affymetrix expression arrays. *BMC Genomics* 8, 96, (2007).
- 21 Scheet, P. & Stephens, M. A fast and flexible statistical model for large-scale population genotype data: applications to inferring missing genotypes and haplotypic phase. *Am J Hum Genet* 78, 629-644, (2006).

- 22 Petretto, E. et al. New insights into the genetic control of gene expression using a
23 Bayesian multi-tissue approach. PLoS Computational Biology 6, (2010).
- 24 Bottolo, L. & Richardson, S. Evolutionary Stochastic Search for Bayesian model
25 exploration. *To appear in Bayesian Analysis*, (2010).
- 26 Liang, F. & Wong, W. H. Evolutionary Monte Carlo: application to Cp model
27 sampling and change point problem. Stat. Sinica 10, 317-342, (2000).
- 28 Iba, Y. Extended Ensemble Monte Carlo. Int. J. Mod. Phys., C 12, 623-656,
29 (2001).
- 30 Efron, B. Microarrays, empirical Bayes and the two-groups model. Stat. Science
31 23, 1-22, (2008).
- 32 McLachlan, G. & Peel, D. Finite mixture models. (2000).
- 33 Allison, D. B. et al. A mixture model approach for the analysis of microarray gene
34 expression data. Computational Statistics & Data Analysis 39, 1-20, (2002).
- 35 Lewin A. and Richardson, S. in Handbook of Statistical Genetics, 3rd edition (ed
36 Martin Bishop and Chris Cannings David Balding) (Chichester: Wiley, 2007).
- 37 Schadt, E. E. et al. Genetics of gene expression surveyed in maize, mouse and
38 man. Nature 422, 297-302, (2003).
- 39 Kass, R. E. & Raftery, A. E. Bayes Factors. Journal of the American Statistical
40 Association 90, 773-795, (1995).
- 41 Servin, B. & Stephens, M. Imputation-based analysis of association studies:
42 candidate regions and quantitative traits. PLoS Genet 3, e114, (2007).
- 43 Strimmer, K. fdrtool: a versatile R package for estimating local and tail area-
44 based false discovery rates. Bioinformatics 24, 1461-1462, (2008).
- 45 Tibshirani, R. The lasso method for variable selection in the Cox model. Stat Med
46 16, 385-395, (1997).
- 47 Morrison, D. F. Multivariate Statistical methods. (Belmont, 2004).
- 48 Olson, C. L. Comparative robustness of six tests in multivariate analysis of
49 variance. Journal of the American Statistical Association 69, 894- 908 (1974).
- 50 Storey, J. D. A direct approach to false discovery rates. J. R. Statist. Soc. B 63,
51 479-498, (2002).
- 52 Box, G. E. P. Non-normality and tests on variances. Biometrika 40, 318-335,
53 (1953).
- 54 Nath, R. & Pavur, R. A new statistic in the one-way multivariate analysis of
55 variance. Computational Statistics & Data Analysis 2, 297-315, (1985).
- 56 Tian, L. et al. Discovering statistically significant pathways in expression profiling
57 studies. Proc Natl Acad Sci U S A 102, 13544-13549, (2005).
- 58 Irizarry, R. A., Wang, C., Zhou, Y. & Speed, T. P. in Working Paper 185 (ed
59 Dept. of Biostatistics Working Papers Johns Hopkins University) (2009).
- 60 Rosenbaum, P. R. & Rubin, D. B. The central role of the propensity score in
61 observational studies for causal effects. Biometrika 70, 41-55, (1983).
- 62 Rosenbaum, P. R. Model-based direct adjustment. Journal of the American
63 Statistical Association 82, 387-394, (1987).
- 64 van Elteren, P. On the combination of independent two sample tests of Wilcoxon.
65 Bulletin of the International Statistical Institute 37, 351-261, (1960).

List of contributors to the Cardiogenics Transcriptomic Study

Department of Cardiovascular Sciences, University of Leicester, Glenfield Hospital, Leicester, LE3 9QP, UK; Peter Braund, Jay Gracey, Unni Krishnan , Jasbir S Moore, Chris P Nelson, Helen Pollard

Department of Haematology, University of Cambridge, Long Road, Cambridge, and National Health Service Blood and Transplant, Cambridge Centre, Long Road, Cambridge, CB2 2PT, UK; Tony Attwood, Abi Crisp-Hihn, Nicola Foad, Jennifer Jolley, Heather Lloyd-Jones, David Muir, Elizabeth Murray, Karen O'Leary, Angela Rankin, Jennifer Sambrook

INSERM UMRS 937, Pierre and Marie Curie University (UPMC, Paris 6) and Medical School, 91 Bd de l'Hôpital 75013, Paris, France; Tiphaine Godfroy, Jessy Brocheton, Carole Proust

Institut für Klinische Chemie und Laboratoriumsmedizin, Universität, Regensburg, D-93053 Regensburg, Germany; Gerd Schmitz

Klinik und Poliklinik für Innere Medizin II, Universität Regensburg, Germany; Susanne Heimerl , Ingrid Lugauer

Medizinische Klinik 2, Universität zu Lübeck, Lübeck Germany; Stephanie Belz, Stefanie Gulde, Patrick Linsel-Nitschke, Hendrik Sager, Laura Schroeder

Molecular Medicine, Department of Medical Sciences, Uppsala University, Uppsala, Sweden; Per Lundmark, Ann-Christine Syvannen

Trium, Analysis Online GmbH, Hohenlindenerstr. 1, 81677, München, Germany; Jessica Neudert, Michael Scholz

Wellcome Trust Sanger Institute, Wellcome Trust Genome Campus, Hinxton, Cambridge CB10 1SA, UK; Panos Deloukas, Emma Gray, Rhian Gwilliams, David Niblett

Supplementary Table 1: Genome-wide analysis of TF eQTL downstream effects. The table contains results of the PASTAA analysis: Gene symbol and Affymetrix rat230 2.0 probeset id of the TF, transfac matrix identifier of the TF, eQTL marker of the TF, tissue in which expression was measured: (aorta = aorta, adr = adrenal, fat = peritoneal fat, kdn = kidney, lv = left ventricle, liver = liver, skm = skeletal muscle). Optimized P is the most significant *P*-value in the iterated hypergeometric test (see Methods) which results from an intersection of the given size when using the first “cutoff eQTL” transcripts and the first “cutoff TF” predicted transcription factor targets from a universe of genes of size “total” (see Supplementary Information). Set size denotes the total number of genes used as potentially differentially expressed genes. The corrected *P*-value was obtained using permutation testing. The FDR accounts for the total number of 587 TF eQTLs tested.

TF symbol	TF Probeset	Matrix	Marker	Tissue	Optimized <i>P</i>	Intersect	Cutoff eQTL	Cutoff TF	Total	Set size	Corrected <i>P</i>	FDR
IrF7	1383564_at	V\$IRF7_01	J666808	adr	1.25E-09	4	17	25	27544	893	<1,0E-06	<5,10E-05
IrF7	1383564_at	V\$IRF7_01	J666808	kdn	1.37E-08	12	150	250	27544	883	<1,0E-06	<5,10E-05
IrF7	1383564_at	V\$IRF7_01	J666808	liver	6.06E-12	12	110	175	27544	893	<1,0E-06	<5,10E-05
IrF7	1383564_at	V\$IRF7_01	J666808	lv	2.60E-13	12	85	175	27544	871	<1,0E-06	<5,10E-05
Atf4	1367624_at	V\$ATF4_Q2	J5383383	adr	8.30E-11	17	300	200	27544	868	<1,0E-06	<5,10E-05
Atf4	1367624_at	V\$ATF4_Q2	J540732	adr	8.30E-11	17	300	200	27544	863	<1,0E-06	<5,10E-05
Tcf4	1368841_at	V\$EBOX_Q6_01	J1268931	kdn	2.11E-07	21	600	254	27544	862	2.10E-05	8.81E-04
Stat1	1387354_at	V\$STAT_Q6	gko-88g11_rp2_b1_418	lv	3.73E-07	13	78	801	27544	873	3.20E-05	1.22E-03
E2f1	1382511_at	V\$E2F1_Q4	WKY-G-i-07e07_r1_602	aorta	1.37E-06	7	600	27	27544	902	1.20E-04	3.81E-03
Atf1	1389623_at	V\$CREBATF_Q6	J519566	adr	1.81E-06	35	400	1002	27544	873	1.51E-04	4.53E-03
Atf1	1389623_at	V\$CREBATF_Q6	J557374	adr	2.62E-06	56	800	1002	27544	867	2.04E-04	5.58E-03
Srebf2	1371979_at	V\$SREBP_Q3	J489757	fat	3.23E-06	2	2	50	27544	901	2.61E-04	6.52E-03
E2f1	1382511_at	V\$E2F1_Q4	WKYc86h09_s1_364	aorta	3.79E-06	7	700	27	27544	901	3.02E-04	7.10E-03

Supplementary Table 2: Genes of the rat *Irf7* driven inflammatory network (iDIN) (n=305 Ensembl genes). Probeset identifiers are for the Affymetrix rat230 2.0 array. Type denotes whether a gene was a confirmed *Irf7* target, a predicted *Irf7* target in adrenal, kidney, left ventricle or liver, or whether it was included in the network expansion using all gene pairs from the Affymetrix rae230a array (expanded 15k) or all available pairs (expanded 30k). NA indicates that the Affymetrix probe did not have an Ensembl gene identifier and/or a gene symbol annotation.

Probeset	Symbol	Ensembl	Type	Description
1371152_a_at	<i>Oas1</i>	ENSRNOG00000001369	confirmed target	2',5'-oligoadenylate synthetase 1, 40/46kDa
1387946_at	<i>Lgals3bp</i>	ENSRNOG00000003217	confirmed target	lectin, galactoside-binding, soluble, 3 binding protein
1387770_at	<i>Ifl27l</i>	ENSRNOG00000009263	confirmed target	interferon, alpha-inducible protein 27-like
1376496_at	<i>LOC503164</i>	ENSRNOG00000023410	predicted target	hypothetical protein LOC503164
1383564_at	<i>Irf7</i>	ENSRNOG00000017414	confirmed target	interferon regulatory factor 7
1373523_at	<i>Fcgr3a</i>	ENSRNOG00000024382	predicted target	Fc fragment of IgG, low affinity IIIa, receptor
1367696_at	<i>Ifitm2</i>	ENSRNOG00000014936	predicted target	interferon induced transmembrane protein 2 (1-8D)
1372930_at	<i>Sp110</i>	ENSRNOG00000017273	predicted target	SP110 nuclear body protein
1387605_at	<i>Casp12</i>	ENSRNOG00000033434	predicted target	caspase 12
1370913_at	<i>Best5</i>	ENSRNOG00000007539	predicted target	Best5 protein
1390507_at	<i>Isg20</i>	ENSRNOG00000018151	predicted target	interferon stimulated exonuclease 20
1399161_a_at	<i>Arts1</i>	ENSRNOG00000009997	predicted target	type 1 tumor necrosis factor receptor shedding aminopeptidase regulator similar to interferon-inducible GTPase
1373992_at	<i>MGC108823</i>	ENSRNOG00000019542	predicted target	
1394819_at	<i>Sp110</i>	ENSRNOG00000017273	confirmed target	SP110 nuclear body protein
1391399_at	NA	NA	predicted target	NA
1379285_at	<i>Rtp4_predicted</i>	ENSRNOG00000028895	predicted target	receptor transporter protein 4 (predicted)
1391754_at	<i>Oas1i</i>	ENSRNOG00000001369	predicted target	2 '-5 ' oligoadenylate synthetase 1I
1396268_at	<i>Sp110</i>	ENSRNOG00000017273	predicted target	SP110 nuclear body protein
1396163_at	<i>Igtp</i>	ENSRNOG00000027008	predicted target	interferon gamma induced GTPase
1374033_at	<i>Psmb10</i>	ENSRNOG00000019494	predicted target	proteasome (prosome, macropain) subunit, beta type 10
1388056_at	<i>Oas1b</i>	ENSRNOG00000001372	predicted target	2-5 oligoadenylate synthetase 1B
1387897_at	<i>Cnp1</i>	ENSRNOG00000017496	predicted target	cyclic nucleotide phosphodiesterase 1
1389873_at	<i>Pycard</i>	ENSRNOG00000019675	predicted target	PYD and CARD domain containing
1373932_at	NA	NA	predicted target	NA
1367595_s_at	<i>B2m</i>	ENSRNOG00000000414	expanded 15k	beta-2 microglobulin
1367663_at	<i>Psme1</i>	ENSRNOG00000019041	expanded 15k	proteasome (prosome, macropain) 28 subunit, alpha
1367679_at	<i>Cd74</i>	ENSRNOG00000018735	expanded 30k	CD74 antigen (invariant polypeptide of major histocompatibility complex, class II antigen-associated)
1367710_at	<i>Psme2</i>	ENSRNOG00000019246	expanded 15k	proteasome (prosome, macropain) 28 subunit, beta
1367786_at	<i>Psmb8</i>	ENSRNOG00000000456	expanded 15k	proteasome (prosome, macropain) subunit, beta type 8
1367850_at	<i>Fcgr3</i>	NA	expanded 15k	Fc receptor, IgG, low affinity III
1367861_at	<i>Evl</i>	ENSRNOG00000014476	expanded 15k	Ena-vasodilator stimulated phosphoprotein

1367925_at	<i>Mvp</i>	ENSRNOG00000020182	expanded 15k	major vault protein
1367973_at	<i>Ccl2</i>	ENSRNOG00000007159	expanded 15k	chemokine (C-C motif) ligand 2
1368006_at	<i>Laptm5</i>	ENSRNOG00000011054	expanded 15k	lysosomal-associated protein transmembrane 5
1368073_at	<i>Irf1</i>	ENSRNOG00000008144	expanded 15k	interferon regulatory factor 1
1368187_at	<i>Gpnmb</i>	ENSRNOG00000008816	expanded 15k	glycoprotein (transmembrane) nmb
1368227_at	<i>Slc28a2</i>	ENSRNOG00000018204	expanded 15k	solute carrier family 28 (sodium-coupled nucleoside transporter), member 2
1368332_at	<i>Gbp2</i>	ENSRNOG00000031743	expanded 15k	guanylate nucleotide binding protein 2
1368356_a_at	<i>Arts1</i>	ENSRNOG00000009997	expanded 15k	type 1 tumor necrosis factor receptor shedding aminopeptidase regulator
1368482_at	<i>Bcl2a1</i>	ENSRNOG00000013001	expanded 15k	B-cell leukemia/lymphoma 2 related protein A1
1368515_at	<i>Epb4.1l3</i>	ENSRNOG00000016724	expanded 15k	erythrocyte protein band 4.1-like 3
1368518_at	<i>Cd53</i>	ENSRNOG00000017874	expanded 15k	CD53 antigen
1368521_at	<i>Napsa</i>	ENSRNOG00000019854	expanded 15k	napsin A aspartic peptidase
1368555_at	<i>Cd37</i>	ENSRNOG00000020699	expanded 30k	CD37 antigen
1368558_s_at	<i>Aif1</i>	ENSRNOG00000000151/ ENSRNOG00000000165	expanded 15k	allograft inflammatory factor 1
1368693_at	<i>Fgr</i>	ENSRNOG00000009912	expanded 15k	Gardner-Rasheed feline sarcoma viral (Fgr) oncogene homolog
1368732_at	<i>Tap2</i>	ENSRNOG0000000455	expanded 30k	transporter 2, ATP-binding cassette, sub-family B (MDR/TAP)
1368742_at	<i>C5r1</i>	NA	expanded 15k	complement component 5, receptor 1
1368835_at	<i>Stat1</i>	ENSRNOG00000014079	expanded 15k	signal transducer and activator of transcription 1
1368973_at	<i>Adar</i>	ENSRNOG00000020744	expanded 15k	adenosine deaminase, RNA-specific
1369029_at	<i>Plscr1</i>	ENSRNOG00000008048	expanded 15k	phospholipid scramblase 1
1369181_at	<i>Cybb</i>	ENSRNOG00000003622	expanded 15k	cytochrome b-245, beta polypeptide
1369186_at	<i>Casp1</i>	ENSRNOG00000007372	expanded 15k	caspase 1
1369204_at	<i>Hck</i>	ENSRNOG00000009331	expanded 15k	hemopoietic cell kinase
1369290_at	<i>Ccr5</i>	ENSRNOG00000006774	expanded 15k	chemokine (C-C motif) receptor 5
1369393_at	<i>Map3k8</i>	ENSRNOG00000016378	expanded 30k	mitogen-activated protein kinase kinase kinase 8
1369549_at	<i>Klrk1</i>	ENSRNOG00000009638	expanded 30k	killer cell lectin-like receptor subfamily K, member 1
1369557_at	<i>Casp7</i>	ENSRNOG00000016836	expanded 30k	caspase 7
1369559_a_at	<i>Cd47</i>	ENSRNOG00000001964	expanded 15k	CD47 antigen (Rh-related antigen, integrin-associated signal transducer)
1369716_s_at	<i>Lgals5</i>	ENSRNOG00000012557	expanded 15k	lectin, galactose binding, soluble 5
1369815_at	<i>Ccl3</i>	ENSRNOG00000011205	expanded 30k	chemokine (C-C motif) ligand 3
1369964_at	<i>Coro1a</i>	ENSRNOG00000019430	expanded 15k	coronin, actin binding protein 1A
1369973_at	<i>Xdh</i>	ENSRNOG00000007081/ ENSRNOG00000027042	expanded 30k	xanthine dehydrogenase
1370056_at	<i>Ly6c</i>	ENSRNOG00000023397	expanded 15k	Ly6-C antigen
1370090_at	<i>Lcp2</i>	ENSRNOG00000005620	expanded 15k	lymphocyte cytosolic protein 2
1370154_at	<i>Lyz</i>	ENSRNOG00000005825	expanded 15k	lysozyme
1370186_at	<i>Psmb9</i>	ENSRNOG00000000459	expanded 15k	proteosome (prosome, macropain) subunit, beta type 9
1370215_at	<i>C1qb</i>	ENSRNOG00000012749	expanded 15k	complement component 1, q subcomponent, beta polypeptide
1370219_at	<i>Cyba</i>	ENSRNOG00000013014	expanded	cytochrome b-245, alpha polypeptide

1370265_at	<i>Arrb2</i>	ENSRNOG00000000373	15k expanded 15k	arrestin, beta 2
1370307_at	<i>Agrn</i>	ENSRNOG00000020205	expanded 15k	agrin
1370351_at	<i>Tdrd7</i>	ENSRNOG00000009985	expanded 15k	tudor domain containing 7
1370400_at	<i>RT1-N3</i>	ENSRNOG00000000795	expanded 15k	RT1 class Ib gene, H2-TL-like, grc region (N3)
1370422_at	<i>Ripk3</i>	ENSRNOG00000020465	expanded 15k	receptor-interacting serine-threonine kinase 3
1370449_at	<i>P2ry14</i>	ENSRNOG00000013872	expanded 15k	purinergic receptor P2Y, G-protein coupled, 14
1370463_x_at	<i>RT1-CE16</i>	NA	expanded 15k	RT1 class I, CE16
1370493_a_at	<i>Lilrb3</i>	ENSRNOG00000025095	expanded 15k	leukocyte immunoglobulin-like receptor, subfamily B (with TM and ITIM domains), member 3
1370516_at	<i>Slc15a3</i>	ENSRNOG00000021644	expanded 15k	solute carrier family 15, member 3
1370628_at	<i>Gzmb</i>	ENSRNOG00000032868	expanded 15k	granzyme B
1370682_at	<i>Lilrb3</i>	ENSRNOG00000025095	expanded 15k	leukocyte immunoglobulin-like receptor, subfamily B (with TM and ITIM domains), member 3
1370693_a_at	<i>Cnp1</i>	ENSRNOG00000017496	expanded 15k	cyclic nucleotide phosphodiesterase 1
1370832_at	<i>Ccl4</i>	ENSRNOG00000011406	expanded 15k	chemokine (C-C motif) ligand 4
1370883_at	<i>RT1-Da</i>	ENSRNOG00000032844	expanded 30k	RT1 class II, locus Da
1370885_at	<i>Ctsz</i>	NA	expanded 15k	cathepsin Z
1370972_x_at	<i>RT1-Aw2</i>	ENSRNOG00000000724	expanded 15k	RT1 class Ib, locus Aw2
1370987_at	<i>Spn</i>	ENSRNOG00000036711	expanded 15k	sialophorin
1371015_at	<i>Mx1</i>	ENSRNOG00000001959	expanded 15k	myxovirus (influenza virus) resistance 1
1371070_at	<i>Zbp1</i>	ENSRNOG00000006314	expanded 15k	Z-DNA binding protein 1
1371079_at	<i>Fcgr2b</i>	ENSRNOG00000003138	expanded 30k	Fc receptor, IgG, low affinity IIb
1371123_x_at	<i>RT1-S3</i>	ENSRNOG00000000777/ ENSRNOG00000026051	expanded 15k	RT1 class Ib, locus S3
1371209_at	<i>RT1-Aw2</i>	ENSRNOG00000000724	expanded 15k	RT1 class Ib, locus Aw2
1371210_s_at	<i>RT1-Aw2</i>	ENSRNOG00000000724	expanded 15k	RT1 class Ib, locus Aw2
1371267_at	<i>RT1-Aw2</i>	ENSRNOG00000000724	expanded 30k	RT1 class Ib, locus Aw2
1371440_at	<i>B2m</i>	ENSRNOG00000000414	expanded 15k	beta-2 microglobulin
1371447_at	<i>Plac8_predicted</i>	ENSRNOG00000002217	expanded 15k	placenta-specific 8 (predicted)
1371925_at	<i>Atp13a1_predicted</i>	ENSRNOG00000010776	expanded 15k	ATPase type 13A1 (predicted)
1371987_at	<i>Pols_predicted</i>	ENSRNOG00000017613	expanded 15k	polymerase (DNA directed) sigma (predicted)
1372034_at	<i>RGD1310490_predict ed</i>	ENSRNOG00000023334	expanded 15k	similar to hypothetical protein MGC29390 (predicted)
1372070_at	<i>Ifi30</i>	ENSRNOG00000019387	expanded 15k	interferon gamma inducible protein 30
1372097_at	<i>Irf8</i>	ENSRNOG00000017869	expanded 30k	interferon regulatory factor 8
1372112_at	<i>RGD1304579</i>	ENSRNOG00000017191	expanded 15k	similar to 9230105E10Rik protein
1372200_at	<i>Gpsm3</i>	ENSRNOG00000000441	expanded 30k	G-protein signalling modulator 3 (AGS3-like, C. elegans)
1372254_at	<i>Serpingle1</i>	ENSRNOG00000007457	expanded 30k	serine (or cysteine) peptidase inhibitor, clade G, member 1
1372256_at	<i>LOC691657</i>	ENSRNOG00000027990	expanded 15k	similar to Cysteine-rich protein 1 (Cysteine-rich intestinal protein) (CRIP)
1372404_at	<i>Rac2</i>	ENSRNOG00000007350	expanded 15k	RAS-related C3 botulinum substrate 2

1372585_at	<i>RGD1566254_predicted</i>	NA	expanded 15k	RGD1566254 (predicted)
1372604_at	<i>RGD1309808_predicted</i>	ENSRNOG00000004849	expanded 15k	similar to apolipoprotein L2; apolipoprotein L-II (predicted)
1372691_at	<i>Upp1</i>	ENSRNOG00000004972	expanded 15k	uridine phosphorylase 1
1372757_at	<i>Stat1</i>	ENSRNOG00000014079	expanded 15k	signal transducer and activator of transcription 1
1372868_at	<i>Tor3a</i>	ENSRNOG00000004307	expanded 15k	torsin family 3, member A
1373025_at	<i>C1qg</i>	ENSRNOG00000012804	expanded 15k	complement component 1, q subcomponent, gamma polypeptide
1373037_at	<i>Ube2l6</i>	ENSRNOG00000007494	expanded 15k	ubiquitin-conjugating enzyme E2L 6
1373065_at	<i>Ptpn18</i>	ENSRNOG00000013415	expanded 15k	protein tyrosine phosphatase, non-receptor type 18
1373164_at	NA	NA	expanded 30k	NA
1373197_at	<i>LOC686701</i>	NA	expanded 15k	similar to Protein KIAA1404
1373490_at	<i>Gmfg</i>	ENSRNOG00000019838	expanded 15k	glia maturation factor, gamma
1373514_at	<i>LOC688296</i>	ENSRNOG00000003636	expanded 15k	similar to chromosome 17 open reading frame 27
1373575_at	<i>LOC498279</i>	NA	expanded 15k	similar to NADH dehydrogenase (ubiquinone) Fe-S protein 2
1373592_at	<i>MGC94010</i>	ENSRNOG00000033772	expanded 30k	similar to SPI6
1373670_at	<i>Stat2</i>	ENSRNOG00000031081	expanded 15k	signal transducer and activator of transcription 2
1373703_at	NA	NA	expanded 15k	NA
1373757_at	<i>Fln29</i>	ENSRNOG00000001351	expanded 15k	FLN29 gene product
1373785_at	<i>LOC362792</i>	ENSRNOG00000028566	expanded 15k	similar to phospholipase D family, member 4
1373912_at	<i>Enpp4_predicted</i>	ENSRNOG00000010174	expanded 30k	ectonucleotide pyrophosphatase/phosphodiesterase 4 (predicted)
1373913_at	<i>Pnpt1</i>	ENSRNOG00000003600	expanded 15k	polyribonucleotide nucleotidyltransferase 1
1374284_at	<i>Rassf4</i>	ENSRNOG00000013526	expanded 15k	Ras association (RalGDS/AF-6) domain family 4
1374337_at	NA	NA	expanded 15k	NA
1374469_at	<i>RGD1561343_predicted</i>	NA	expanded 15k	similar to C20orf118 (predicted)
1374499_at	<i>LOC682999</i>	ENSRNOG00000003730	expanded 15k	hypothetical protein LOC682999
1374526_at	<i>Ankfy1_predicted</i>	ENSRNOG00000016212	expanded 15k	ankyrin repeat and FYVE domain containing 1 (predicted)
1374551_at	<i>Ifi35</i>	ENSRNOG00000020678	expanded 15k	interferon-induced protein 35
1374627_at	NA	NA	expanded 15k	NA
1374718_at	<i>RGD1565144_predicted</i>	ENSRNOG00000023400	expanded 15k	similar to deltex 3-like (predicted)
1374725_at	<i>LOC310756</i>	ENSRNOG00000012946	expanded 15k	similar to Moloney leukemia virus 10
1374730_at	<i>Tyrobp</i>	ENSRNOG00000020845	expanded 15k	Tyro protein tyrosine kinase binding protein
1374731_at	<i>Coil</i>	ENSRNOG00000000244	expanded 15k	coillin
1374838_at	<i>Sp140</i>	ENSRNOG00000022800	expanded 30k	SP140 nuclear body protein
1374948_at	<i>Tmem106a</i>	ENSRNOG00000023628	expanded 15k	transmembrane protein 106A
1375006_at	NA	NA	expanded 15k	NA
1375010_at	<i>Cd68</i>	ENSRNOG00000037563	expanded 15k	CD68 antigen
1375211_at	<i>Rnaset2_predicted</i>	ENSRNOG00000013190	expanded 15k	ribonuclease T2 (predicted)
1375635_at	NA	NA	expanded 15k	NA

1375796_at	<i>Igtp</i>	ENSRNOG00000027008	expanded 15k	interferon gamma induced GTPase
1375917_at	<i>Gp49b</i>	ENSRNOG00000027811	expanded 30k	glycoprotein 49b
1375955_at	<i>Zfp313</i>	ENSRNOG00000009525	expanded 15k	zinc finger protein 313
1376022_at	<i>NA</i>	NA	expanded 15k	NA
1376029_at	<i>Rab2l</i>	ENSRNOG00000000474	expanded 15k	RAB2, member RAS oncogene family-like
1376056_at	<i>NA</i>	NA	expanded 15k	NA
1376130_a_at	<i>Dtnb</i>	ENSRNOG00000011914	expanded 15k	dystrobrevin, beta
1376144_at	<i>Parp9_predicted</i>	ENSRNOG00000023463	expanded 15k	poly (ADP-ribose) polymerase family, member 9 (predicted)
1376151_a_at	<i>RGD1564081_predicted</i>	ENSRNOG00000026821	expanded 15k	similar to novel protein similar to human oligophrenin 1 (OPHN1) (predicted)
1376390_at	<i>Ms4a11_predicted</i>	ENSRNOG00000020991	expanded 15k	membrane-spanning 4-domains, subfamily A, member 11 (predicted)
1376652_at	<i>C1qa</i>	ENSRNOG00000012807	expanded 15k	complement component 1, q subcomponent, alpha polypeptide similar to CD300A antigen
1376675_at	<i>LOC501736</i>	ENSRNOG00000024399	expanded 15k	
1376693_at	<i>RGD1563091_predicted</i>	ENSRNOG00000039801	expanded 15k	similar to OEF2 (predicted)
1376835_at	<i>Slc35b2</i>	ENSRNOG00000019907	expanded 15k	solute carrier family 35, member B2
1376845_at	<i>isg12(b)</i>	ENSRNOG00000026605	expanded 15k	putative ISG12(b) protein
1376908_at	<i>Ifit3</i>	ENSRNOG00000022839	expanded 15k	interferon-induced protein with tetratricopeptide repeats 3
1376920_at	<i>LOC500013</i>	NA	expanded 15k	similar to sterile alpha motif domain containing 9-like
1376943_at	<i>NA</i>	NA	expanded 15k	NA
1376960_at	<i>RGD1310039</i>	ENSRNOG00000015137	expanded 15k	similar to hypothetical protein FLJ10058
1377116_at	<i>Rnasel</i>	ENSRNOG00000027017	expanded 15k	ribonuclease L (2',5'-oligoisoadenylate synthetase-dependent)
1377117_at	<i>NA</i>	NA	expanded 30k	NA
1377239_at	<i>Apbb1ip</i>	ENSRNOG00000017803	expanded 15k	amyloid beta (A4) precursor protein-binding, family B, member 1 interacting protein
1377497_at	<i>Oasl1</i>	ENSRNOG0000001187	expanded 15k	2'-5' oligoadenylate synthetase-like 1
1377626_at	<i>LOC690768</i>	NA	expanded 30k	hypothetical protein LOC690768
1377671_at	<i>NA</i>	NA	expanded 30k	NA
1377755_at	<i>Ascc3_predicted</i>	ENSRNOG00000024531	expanded 30k	activating signal cointegrator 1 complex subunit 3 (predicted)
1377826_at	<i>NA</i>	NA	expanded 30k	NA
1377893_at	<i>LOC690000</i>	ENSRNOG00000014966	expanded 30k	similar to CG3740-PA
1377908_at	<i>NA</i>	NA	expanded 30k	NA
1377916_at	<i>Sifn2_predicted</i>	ENSRNOG00000009553	expanded 30k	schlafen 2 (predicted)
1377918_at	<i>RGD1559463_predicted</i>	ENSRNOG00000008530	expanded 30k	similar to Stomatin-like 1 (predicted)
1377943_at	<i>Cd86</i>	ENSRNOG0000002289	expanded 30k	cd86 antigen
1377950_at	<i>RGD1309362</i>	ENSRNOG00000019542	expanded 30k	similar to interferon-inducible GTPase
1378043_at	<i>RGD1563091_predicted</i>	ENSRNOG00000039801	expanded 30k	similar to OEF2 (predicted)
1378140_at	<i>Arl11</i>	ENSRNOG00000014653	expanded 30k	ADP-ribosylation factor-like 11
1378184_at	<i>RGD1563387_predicted</i>	ENSRNOG0000002046	expanded 30k	similar to antigen identified by monoclonal antibody MRC OX-2 receptor (predicted)
1378193_at	<i>Ms4a7_predicted</i>	ENSRNOG00000020953	expanded 30k	membrane-spanning 4-domains, subfamily A, member 7 (predicted)

1378257_at	<i>Trex1</i>	ENSRNOG00000020670/ ENSRNOG00000022540	expanded 30k	three prime repair exonuclease 1
1378321_at	<i>Rassf4</i>	ENSRNOG00000013526	expanded 30k	Ras association (RalGDS/AF-6) domain family 4
1378418_at	<i>RGD1311681</i>	ENSRNOG00000011947	expanded 30k	similar to MGC37193 protein
1378428_at	<i>NA</i>	NA	expanded 30k	NA
1378443_at	<i>Slamf9_predicted</i>	ENSRNOG00000008045	expanded 30k	SLAM family member 9 (predicted)
1378633_at	<i>Lpxn</i>	ENSRNOG00000012611	expanded 30k	leupaxin
1379223_x_at	<i>NA</i>	NA	expanded 30k	NA
1379293_at	<i>Gzma</i>	ENSRNOG00000010603	expanded 30k	granzyme A
1379316_at	<i>NA</i>	NA	expanded 30k	NA
1379344_at	<i>Cybb</i>	ENSRNOG00000003622	expanded 30k	cytochrome b-245, beta polypeptide
1379387_at	<i>Rgs18</i>	ENSRNOG00000003959	expanded 15k	regulator of G-protein signaling 18
1379482_at	<i>Tm6sf1_predicted</i>	ENSRNOG00000019662	expanded 30k	transmembrane 6 superfamily member 1 (predicted)
1379496_at	<i>RT1-Aw2</i>	ENSRNOG00000000724	expanded 30k	RT1 class Ib, locus Aw2
1379538_at	<i>Cenpj_predicted</i>	ENSRNOG00000022597	expanded 30k	centromere protein J (predicted)
1379568_at	<i>Ifit2</i>	ENSRNOG00000036604	expanded 30k	interferon-induced protein with tetratricopeptide repeats 2
1379613_at	<i>RGD1310490_predicted</i>	ENSRNOG00000023334	expanded 30k	similar to hypothetical protein MGC29390 (predicted)
1379631_at	<i>Csf1</i>	ENSRNOG00000018659	expanded 30k	colony stimulating factor 1 (macrophage)
1379633_a_at	<i>Ube1l_predicted</i>	ENSRNOG00000029195	expanded 30k	ubiquitin-activating enzyme E1-like (predicted)
1379634_at	<i>Ube1l_predicted</i>	ENSRNOG00000029195	expanded 30k	ubiquitin-activating enzyme E1-like (predicted)
1379698_at	<i>NA</i>	NA	expanded 30k	NA
1379742_at	<i>LOC363269</i>	ENSRNOG00000022769	expanded 30k	similar to Nuclear autoantigen Sp-100 (Speckled 100 kDa) (Nuclear dot-associated Sp100 protein)
1379748_at	<i>LOC310968</i>	NA	expanded 30k	similar to histocompatibility 28
1379760_at	<i>Tnfaip8l2</i>	ENSRNOG00000021100	expanded 30k	tumor necrosis factor, alpha-induced protein 8-like 2
1379766_at	<i>Sla</i>	ENSRNOG00000005797	expanded 15k	src-like adaptor
1379794_at	<i>Gzmb</i>	ENSRNOG00000032868	expanded 30k	granzyme B
1379891_at	<i>MGC94600</i>	ENSRNOG00000020667	expanded 30k	scotin
1379957_at	<i>Slfn8</i>	ENSRNOG00000021412	expanded 30k	schlafen 8
1380019_at	<i>Tcigr1</i>	ENSRNOG00000017220	expanded 30k	T-cell, immune regulator 1
1380071_at	<i>Parp12_predicted</i>	ENSRNOG00000008196	expanded 30k	poly (ADP-ribose) polymerase family, member 12 (predicted)
1380077_at	<i>RGD1561123_predicted</i>	ENSRNOG00000036703	expanded 30k	similar to mFLJ00114 protein (predicted)
1380079_at	<i>RGD1561472_predicted</i>	NA	expanded 30k	similar to mKIAA2005 protein (predicted)
1380110_at	<i>Jak2</i>	ENSRNOG00000015547	expanded 30k	Janus kinase 2
1380129_at	<i>NA</i>	NA	expanded 15k	NA
1380162_at	<i>LOC246120</i>	ENSRNOG00000001385	expanded 30k	RDCR-0918-3 protein
1380297_at	<i>NA</i>	NA	expanded 30k	NA
1380377_at	<i>Btk</i>	ENSRNOG00000011331	expanded 30k	Bruton agammaglobulinemia tyrosine kinase
1380425_at	<i>Rnasel</i>	ENSRNOG00000027017	expanded 30k	ribonuclease L (2',5'-oligoisoadenylate synthetase-dependent)

1380474_at	<i>Loxl2_predicted</i>	ENSRNOG00000016758	expanded 30k	lysyl oxidase-like 2 (predicted)
1380521_at	<i>Hcls1</i>	ENSRNOG00000038881	expanded 30k	hematopoietic cell specific Lyn substrate 1
1380537_at	<i>Nckap1l_predicted</i>	ENSRNOG00000017989	expanded 30k	NCK associated protein 1 like (predicted)
1380621_at	<i>RGD1564385_predicted</i>	ENSRNOG00000011683	expanded 30k	similar to tyrosine kinase Fps/Fes (predicted)
1380728_at	NA	NA	expanded 30k	NA
1380894_at	<i>Lilrc1</i>	NA	expanded 30k	leukocyte immunoglobulin-like receptor
1381014_at	<i>Ifi44</i>	ENSRNOG00000022218	expanded 30k	interferon-induced protein 44
1381129_at	NA	NA	expanded 30k	NA
1381228_at	NA	NA	expanded 30k	NA
1381311_at	<i>Emr1</i>	NA	expanded 30k	EGF-like module containing, mucin-like, hormone receptor-like sequence 1
1381525_at	<i>Enah</i>	ENSRNOG00000003156	expanded 30k	enabled homolog (Drosophila)
1381556_at	<i>RGD1560014_predicted</i>	ENSRNOG00000014541	expanded 30k	similar to hypothetical protein FLJ20035 (predicted)
1381875_at	<i>Nmi</i>	ENSRNOG00000027502	expanded 30k	N-myc (and STAT) interactor
1382026_at	<i>Arhgap9</i>	ENSRNOG00000006946	expanded 30k	Rho GTPase activating protein 9
1382033_at	<i>Klf1_predicted</i>	ENSRNOG00000003443	expanded 30k	Kruppel-like factor 1 (erythroid) (predicted)
1382043_at	<i>Unc93b1</i>	ENSRNOG00000017703	expanded 30k	unc-93 homolog B1 (C. elegans)
1382074_at	<i>Ibrdc3_predicted</i>	ENSRNOG0000000123	expanded 30k	IBR domain containing 3 (predicted)
1382078_at	NA	NA	expanded 30k	NA
1382106_at	<i>Ccl6</i>	ENSRNOG00000030021	expanded 30k	chemokine (C-C motif) ligand 6
1382153_at	<i>Clecsf6</i>	ENSRNOG00000010045	expanded 30k	C-type (calcium dependent, carbohydrate recognition domain) lectin, superfamily member 6
1382177_at	NA	NA	expanded 30k	NA
1382274_at	<i>Rarres1</i>	ENSRNOG00000021339	expanded 30k	retinoic acid receptor responder (tazarotene induced) 1
1382277_at	<i>Ly96</i>	ENSRNOG00000040315	expanded 30k	lymphocyte antigen 96
1382314_at	<i>G1p2_predicted</i>	ENSRNOG00000021802	expanded 30k	interferon, alpha-inducible protein (clone IFI-15K) (predicted)
1382454_at	<i>Cxcl9</i>	ENSRNOG00000022242	expanded 30k	chemokine (C-X-C motif) ligand 9
1382531_at	<i>Tlr7_predicted</i>	ENSRNOG0000004249	expanded 15k	toll-like receptor 7 (predicted)
1382546_at	<i>Phf11</i>	ENSRNOG00000011580	expanded 30k	PHD finger protein 11
1382601_at	<i>RGD1564316_predicted</i>	ENSRNOG00000012779	expanded 30k	similar to scavenger receptor type A SR-A (predicted)
1382902_at	<i>Herc6</i>	ENSRNOG00000023969	expanded 30k	potential ubiquitin ligase
1382926_s_at	<i>Pum2</i>	ENSRNOG00000006180	expanded 30k	pumilio 2 (Drosophila)
1382950_at	NA	NA	expanded 30k	NA
1383131_at	<i>Itgb2</i>	ENSRNOG0000001224	expanded 30k	integrin beta 2
1383189_at	NA	NA	expanded 30k	NA
1383369_at	<i>Trim26</i>	ENSRNOG00000000782	expanded 30k	tripartite motif protein 26
1383372_at	<i>Ptafr</i>	ENSRNOG00000013231	expanded 30k	platelet-activating factor receptor
1383391_a_at	<i>C2</i>	NA	expanded 30k	complement component 2
1383392_at	<i>C2</i>	NA	expanded 30k	complement component 2

1383424_at	<i>Tyki_predicted</i>	ENSRNOG00000007690	expanded 30k	thymidylate kinase family LPS-inducible member (predicted)
1383435_at	<i>Scn3b</i>	ENSRNOG00000006937	expanded 30k	sodium channel, voltage-gated, type III, beta
1383448_at	<i>lsgf3g</i>	ENSRNOG00000019478	expanded 30k	interferon dependent positive acting transcription factor 3 gamma
1383658_at	<i>Laptm5</i>	ENSRNOG00000011054	expanded 30k	lysosomal-associated protein transmembrane 5
1383662_at	<i>LOC500956</i>	ENSRNOG00000020580	expanded 30k	hypothetical protein LOC500956
1383679_at	<i>Rnf31_predicted</i>	ENSRNOG00000019438	expanded 30k	ring finger protein 31 (predicted)
1383786_at	<i>RGD155997_predicted</i>	ENSRNOG00000014258	expanded 30k	similar to RAB32 (predicted)
1383863_at	<i>Lmo2</i>	ENSRNOG00000009401	expanded 30k	LIM domain only 2
1384070_at	<i>Gmip_predicted</i>	ENSRNOG00000027257	expanded 30k	Gem-interacting protein (predicted)
1384180_at	<i>Ifit2</i>	ENSRNOG00000036604	expanded 30k	interferon-induced protein with tetratricopeptide repeats 2
1384298_at	<i>Myo1f_predicted</i>	ENSRNOG00000008409	expanded 30k	myosin IF (predicted)
1384457_at	<i>RGD1566133_predicted</i>	ENSRNOG00000030027	expanded 30k	similar to Fbxw17 protein (predicted)
1384483_at	<i>RGD1561157_predicted</i>	NA	expanded 30k	RGD1561157 (predicted)
1384765_at	<i>Rhbd16_predicted</i>	ENSRNOG00000011459	expanded 30k	rhomboid, veinlet-like 6 (Drosophila) (predicted)
1384946_at	NA	NA	expanded 30k	NA
1385001_at	<i>Gsdmdc1_predicted</i>	ENSRNOG00000007728	expanded 30k	gasdermin domain containing 1 (predicted)
1385029_at	NA	NA	expanded 30k	NA
1385051_at	<i>Gbp4_predicted</i>	ENSRNOG00000028768	expanded 30k	guanylate nucleotide binding protein 4 (predicted)
1385213_at	<i>RGD1563207_predicted</i>	ENSRNOG00000009471	expanded 30k	similar to epithelial stromal interaction 1 isoform a (predicted)
1385252_at	<i>Trim34_predicted</i>	ENSRNOG00000017147	expanded 30k	tripartite motif protein 34 (predicted)
1385276_a_at	<i>RGD1310093_predicted</i>	ENSRNOG00000018247	expanded 30k	similar to hypothetical protein FLJ11354 (predicted)
1385277_x_at	<i>RGD1310093_predicted</i>	ENSRNOG00000018247	expanded 30k	similar to hypothetical protein FLJ11354 (predicted)
1385439_x_at	<i>RGD1310093_predicted</i>	ENSRNOG00000018247	expanded 30k	similar to hypothetical protein FLJ11354 (predicted)
1385440_at	<i>Hcst</i>	ENSRNOG00000020849	expanded 30k	hematopoietic cell signal transducer
1385502_at	<i>Trim21_predicted</i>	ENSRNOG00000018517	expanded 30k	tripartite motif protein 21 (predicted)
1385557_at	NA	NA	expanded 30k	NA
1385571_at	<i>LOC679623</i>	NA	expanded 30k	similar to Nuclear autoantigen Sp-100 (Speckled 100 kDa) (Nuclear dot-associated Sp100 protein)
1385572_at	NA	NA	expanded 30k	NA
1385658_at	<i>Zfp313</i>	ENSRNOG00000009525	expanded 30k	zinc finger protein 313
1385696_at	<i>RGD1561016_predicted</i>	ENSRNOG00000012965	expanded 30k	similar to BC013712 protein (predicted)
1385702_at	<i>Mnda</i>	ENSRNOG00000003486	expanded 30k	myeloid cell nuclear differentiation antigen
1385832_s_at	<i>RGD1560293_predicted</i>	ENSRNOG00000004409	expanded 30k	similar to RIKEN cDNA 1200013B08 (predicted)
1386023_at	<i>Lgi1</i>	ENSRNOG00000014758	expanded 30k	leucine-rich repeat LGI family, member 1
1386252_at	NA	NA	expanded 30k	NA
1386277_at	<i>Ube1l_predicted</i>	ENSRNOG00000029195	expanded 30k	ubiquitin-activating enzyme E1-like (predicted)
1386893_at	<i>Grn</i>	ENSRNOG00000021031	expanded 15k	granulin
1386925_at	<i>Arpc1b</i>	ENSRNOG0000000991	expanded 15k	actin related protein 2/3 complex, subunit 1B

1386986_at	<i>Ogfr</i>	ENSRNOG00000009355	expanded 15k	opioid growth factor receptor
1387005_at	<i>Ctss</i>	ENSRNOG00000021157	expanded 15k	cathepsin S
1387027_a_at	<i>Lgals9</i>	ENSRNOG00000012681	expanded 15k	lectin, galactose binding, soluble 9
1387134_at	<i>Slfn3</i>	ENSRNOG00000021357	expanded 15k	schlafen 3
1387242_at	<i>Prkr</i>	NA	expanded 15k	Protein kinase, interferon-inducible double stranded RNA dependent
1387256_at	<i>Adam1a</i>	ENSRNOG00000001347	expanded 15k	a disintegrin and metallopeptidase domain 1a
1387283_at	<i>Mx2</i>	ENSRNOG00000001963	expanded 15k	myxovirus (influenza virus) resistance 2
1387354_at	<i>Stat1</i>	ENSRNOG000000014079	expanded 15k	signal transducer and activator of transcription 1
1387687_at	<i>Igsf6</i>	ENSRNOG000000017277	expanded 15k	immunoglobulin superfamily, member 6
1387800_at	<i>Daxx</i>	ENSRNOG00000000477	expanded 15k	Fas death domain-associated protein
1387818_at	<i>Casp4</i>	ENSRNOG000000007372	expanded 30k	caspase 4, apoptosis-related cysteine peptidase
1387831_at	<i>Xcl1</i>	ENSRNOG00000002964	expanded 30k	chemokine (C motif) ligand 1
1387839_at	<i>RT1-N1</i>	ENSRNOG00000000777/ ENSRNOG00000026051	expanded 15k	RT1 class Ib gene, H2-TL-like, grc region (N1)
1387956_s_at	<i>Ckif</i>	ENSRNOG00000000576	expanded 30k	chemokine-like factor
1387969_at	<i>Cxcl10</i>	ENSRNOG000000022256	expanded 15k	chemokine (C-X-C motif) ligand 10
1387984_at	<i>Ckif</i>	ENSRNOG00000000576	expanded 15k	chemokine-like factor
1387995_a_at	<i>Ifitm3</i>	NA	expanded 15k	interferon induced transmembrane protein 3
1388071_x_at	<i>RT1-Aw2</i>	ENSRNOG00000000724	expanded 15k	RT1 class Ib, locus Aw2
1388149_at	<i>Tap1</i>	ENSRNOG00000000457	expanded 15k	transporter 1, ATP-binding cassette, sub-family B (MDR/TAP)
1388164_at	<i>RT1-S3</i>	ENSRNOG00000000777/ ENSRNOG00000026051	expanded 15k	RT1 class Ib, locus S3
1388203_x_at	<i>RT1-Aw2</i>	ENSRNOG00000000724	expanded 15k	RT1 class Ib, locus Aw2
1388212_a_at	<i>RT1-S3</i>	ENSRNOG00000000777/ ENSRNOG00000026051	expanded 15k	RT1 class Ib, locus S3
1388213_a_at	<i>RT1-S3</i>	ENSRNOG00000000777/ ENSRNOG00000026051	expanded 15k	RT1 class Ib, locus S3
1388255_x_at	<i>RT1-Aw2</i>	ENSRNOG00000000724	expanded 15k	RT1 class Ib, locus Aw2
1388347_at	<i>LOC362934</i>	ENSRNOG00000007091	expanded 15k	similar to lymphocyte antigen 6 complex, locus E
1388460_at	<i>Capg</i>	ENSRNOG00000013668	expanded 15k	capping protein (actin filament), gelsolin-like
1388574_at	<i>Wars</i>	ENSRNOG00000004359	expanded 30k	tryptophanyl-tRNA synthetase
1388596_at	<i>Cotl1_predicted</i>	ENSRNOG00000016257	expanded 15k	coactosin-like 1 (<i>Dictyostelium</i>) (predicted)
1388600_at	NA	NA	expanded 15k	NA
1388673_at	<i>Lsp1</i>	ENSRNOG00000020300	expanded 15k	lymphocyte specific 1
1388740_at	<i>Trpt1_predicted</i>	ENSRNOG00000023023	expanded 15k	tRNA phosphotransferase 1 (predicted)
1388754_at	<i>Nudt7_predicted</i>	ENSRNOG00000011976	expanded 15k	nudix (nucleoside diphosphate linked moiety X)-type motif 7 (predicted)
1388776_at	<i>MGC94600</i>	ENSRNOG00000020667	expanded 15k	scotin
1388784_at	<i>Csf1r</i>	ENSRNOG00000018414	expanded 15k	colony stimulating factor 1 receptor
1388791_at	<i>RGD1309930</i>	ENSRNOG00000016012	expanded 15k	similar to 2810022L02Rik protein
1388880_at	NA	NA	expanded 15k	NA
1389006_at	NA	NA	expanded 15k	NA
1389034_at	<i>Usp18</i>	ENSRNOG00000037198	expanded	ubiquitin specific peptidase 18

1389123_at	<i>Ccl6</i>	ENSRNOG00000030021	15k expanded 15k	chemokine (C-C motif) ligand 6
1389170_at	<i>Casp7</i>	ENSRNOG00000016836	expanded 15k	caspase 7
1389210_at	<i>Lcp1</i>	ENSRNOG00000010319	expanded 15k	lymphocyte cytosolic protein 1
1389347_at	<i>Pitpnm1</i>	ENSRNOG00000018553	expanded 30k	phosphatidylinositol transfer protein, membrane-associated 1
1389365_at	<i>LOC690000</i>	ENSRNOG00000014966	expanded 15k	similar to CG3740-PA
1389387_at	<i>LOC682071</i>	ENSRNOG00000009640	expanded 15k	similar to Proteasome inhibitor PI31 subunit
1389413_at	<i>LOC685433</i>	ENSRNOG00000022764	expanded 15k	similar to ecotropic viral integration site 2A
1389553_at	<i>Dcir3</i>	ENSRNOG00000010018	expanded 15k	dendritic cell inhibitory receptor 3
1389571_at	<i>Stat2</i>	ENSRNOG00000031081	expanded 15k	signal transducer and activator of transcription 2
1389659_at	<i>RGD1565540_predicted</i>	ENSRNOG00000039971	expanded 30k	similar to ctna-2-beta protein (141 AA) (predicted)
1389696_at	NA	NA	expanded 15k	NA
1389732_at	<i>LOC679937</i>	ENSRNOG00000038916	expanded 15k	similar to CG4025-PA
1390022_at	<i>Arpc5</i>	ENSRNOG00000028062	expanded 30k	actin related protein 2/3 complex, subunit 5
1390226_at	<i>RGD1562552_predicted</i>	NA	expanded 15k	similar to hypothetical protein LOC340061 (predicted)
1390312_at	<i>RGD1561472_predicted</i>	NA	expanded 15k	similar to mKIAA2005 protein (predicted)
1390348_at	<i>Folr2_predicted</i>	ENSRNOG00000019890	expanded 15k	folate receptor 2 (fetal) (predicted)
1390472_at	<i>Asahl_predicted</i>	ENSRNOG00000002273	expanded 30k	N-acylsphingosine amidohydrolase (acid ceramidase)-like (predicted)
1390510_at	<i>Ms4a6b</i>	ENSRNOG00000030689	expanded 15k	membrane-spanning 4-domains, subfamily A, member 6B
1390529_at	<i>Cd83_predicted</i>	ENSRNOG00000018092	expanded 15k	CD83 antigen (predicted)
1390531_at	<i>RGD1306056_predicted</i>	ENSRNOG00000013267	expanded 15k	similar to Peroxisomal proliferator-activated receptor A interacting complex 285 kDa protein (PPAR-alpha interacting complex protein 285) (predicted)
1390738_at	<i>Bst2</i>	ENSRNOG00000023370	expanded 15k	bone marrow stromal cell antigen 2
1390798_at	<i>Ptprc</i>	ENSRNOG00000000655	expanded 15k	protein tyrosine phosphatase, receptor type, C
1390866_at	NA	NA	expanded 30k	NA
1390909_at	NA	NA	expanded 30k	NA
1391266_at	<i>RT1-Aw2</i>	ENSRNOG00000000724	expanded 30k	RT1 class Ib, locus Aw2
1391463_at	<i>Ddx58_predicted</i>	ENSRNOG00000006384	expanded 30k	DEAD (Asp-Glu-Ala-Asp) box polypeptide 58 (predicted)
1391489_at	<i>Irgm</i>	ENSRNOG00000031138	expanded 30k	immunity-related GTPase family, M
1391593_at	<i>Rassf4</i>	ENSRNOG00000013526	expanded 30k	Ras association (RalGDS/AF-6) domain family 4
1391737_at	<i>LOC500904</i>	ENSRNOG00000006940	expanded 30k	similar to neutrophil cytosolic factor 4
1391979_at	NA	NA	expanded 30k	NA
1392280_at	<i>Tlr2</i>	ENSRNOG00000009822	expanded 30k	toll-like receptor 2
1392308_at	<i>Pla2g2d</i>	ENSRNOG00000016826	expanded 30k	phospholipase A2, group IID
1392407_at	<i>RGD1561419_predicted</i>	ENSRNOG00000004192	expanded 15k	similar to RIKEN cDNA 6030405P05 gene (predicted)
1392515_at	<i>LOC690097</i>	NA	expanded 30k	similar to immunoreceptor Ly49si3
1392528_at	<i>Csf2ra</i>	NA	expanded 30k	granulocyte-macrophage colony stimulating receptor alpha
1392547_at	<i>MGC105649</i>	ENSRNOG00000029643	expanded 30k	hypothetical LOC302884

1392628_at	NA	NA	expanded 30k	NA
1392637_at	NA	NA	expanded 30k	NA
1392648_at	<i>Mrc1_predicted</i>	ENSRNOG00000018251	expanded 30k	mannose receptor, C type 1 (predicted)
1392655_at	NA	NA	expanded 30k	NA
1392737_at	<i>Ccr5</i>	ENSRNOG00000006774	expanded 30k	chemokine (C-C motif) receptor 5
1392777_at	NA	NA	expanded 15k	NA
1392819_at	<i>Ms4a11_predicted</i>	ENSRNOG00000020991	expanded 15k	membrane-spanning 4-domains, subfamily A, member 11 (predicted)
1392840_at	NA	NA	expanded 30k	NA
1392842_at	NA	NA	expanded 30k	NA
1392905_at	<i>Gng2</i>	NA	expanded 30k	guanine nucleotide binding protein, gamma 2
1392922_at	<i>Rap2b</i>	ENSRNOG00000014420	expanded 30k	RAP2B, member of RAS oncogene family
1392978_at	<i>LOC688811</i>	ENSRNOG00000016751	expanded 30k	similar to solute carrier family 25, member 28
1393038_at	<i>Fcgr1</i>	ENSRNOG00000021199	expanded 30k	Fc receptor, IgG, high affinity I
1393044_at	<i>Tyki_predicted</i>	ENSRNOG00000007690	expanded 30k	thymidylate kinase family LPS-inducible member (predicted)
1393085_at	<i>RGD1307700</i>	ENSRNOG00000018467	expanded 30k	similar to hypothetical protein BC018453
1393144_at	<i>Nmi</i>	ENSRNOG00000027502	expanded 30k	N-myc (and STAT) interactor
1393187_at	NA	NA	expanded 30k	NA
1393219_at	<i>C2</i>	NA	expanded 30k	complement component 2
1393280_at	<i>Ly86_predicted</i>	ENSRNOG00000000137	expanded 15k	lymphocyte antigen 86 (predicted)
1393401_at	NA	NA	expanded 30k	NA
1393682_at	<i>GPR34_predicted</i>	ENSRNOG00000039759	expanded 30k	G-protein-coupled receptor GPR34 (predicted)
1393776_at	<i>LOC362934</i>	ENSRNOG00000007091	expanded 30k	similar to lymphocyte antigen 6 complex, locus E
1393832_at	<i>RGD1306676</i>	ENSRNOG00000004673	expanded 30k	similar to RIKEN cDNA 0610033I05
1393863_at	<i>Cd180_predicted</i>	ENSRNOG00000010266	expanded 30k	CD180 antigen (predicted)
1393885_at	<i>LOC688900</i>	NA	expanded 30k	similar to schlafen 1
1393957_at	NA	NA	expanded 30k	NA
1394340_at	<i>Inpp1</i>	ENSRNOG00000012375	expanded 30k	inositol polyphosphate-1-phosphatase
1394352_at	<i>Ifih1</i>	ENSRNOG00000006227	expanded 30k	similar to HELICARD (predicted)
1394528_at	<i>Adar</i>	ENSRNOG00000020744	expanded 30k	adenosine deaminase, RNA-specific
1394673_at	<i>LOC687856</i>	ENSRNOG00000037331	expanded 30k	similar to Myeloid cell surface antigen CD33 precursor (Siglec-3)
1394678_at	<i>Fgd2_predicted</i>	ENSRNOG00000000528	expanded 30k	FYVE, RhoGEF and PH domain containing 2 (predicted)
1394743_at	NA	NA	expanded 30k	NA
1395003_at	<i>Clec4a1</i>	NA	expanded 30k	C-type lectin domain family 4, member a1
1395034_at	<i>RGD1311481_predicted</i>	ENSRNOG00000021018	expanded 30k	similar to RIKEN cDNA 4933430F08 (predicted)
1395124_at	<i>Wars</i>	ENSRNOG00000004359	expanded 30k	tryptophanyl-tRNA synthetase
1395184_at	NA	NA	expanded 30k	NA
1395336_at	<i>RGD1309930</i>	ENSRNOG00000016012	expanded 30k	similar to 2810022L02Rik protein
1395665_at	NA	NA	expanded	NA

1395788_at	NA	NA	30k expanded 30k	NA
1396671_at	NA	NA	30k expanded 30k	NA
1396993_at	NA	NA	30k expanded 30k	NA
1397304_at	NA	NA	30k expanded 30k	NA
1397457_at	NA	NA	30k expanded 30k	NA
1398027_at	RT1-Aw2	ENSRNOG000000000724	expanded 30k	RT1 class Ib, locus Aw2
1398246_s_at	Fcgr3	NA	expanded 15k	Fc receptor, IgG, low affinity III
1398591_at	Ccrl2_predicted	ENSRNOG00000033234	expanded 30k	chemokine (C-C motif) receptor-like 2 (predicted)
1398765_at	Ap2m1	ENSRNOG00000001709	expanded 15k	adaptor-related protein complex 2, mu 1 subunit
1398925_at	RGD1307801	ENSRNOG00000000532	expanded 15k	similar to RIKEN cDNA 1300018I05
1367918_at	Fez1	ENSRNOG00000006075	expanded 15k	fasciculation and elongation protein zeta 1 (zygin I)
1368412_a_at	Ptpro	ENSRNOG00000006231	expanded 15k	protein tyrosine phosphatase, receptor type, O
1369173_at	C3ar1	ENSRNOG00000009211	expanded 15k	complement component 3a receptor 1
1369213_at	L1cam	ENSRNOG00000024683	expanded 15k	L1 cell adhesion molecule
1369427_at	Mpeg1	NA	expanded 15k	macrophage expressed gene 1
1369743_a_at	P2rx4	ENSRNOG00000001300	expanded 15k	purinergic receptor P2X, ligand-gated ion channel 4
1370161_at	Ssg1	ENSRNOG00000002052	expanded 15k	steroid sensitive gene 1
1370229_at	Ndrg4	ENSRNOG00000012482	expanded 15k	N-myc downstream regulated gene 4
1370248_at	Fxyd6	ENSRNOG00000016412	expanded 15k	FXYD domain-containing ion transport regulator 6
1370389_at	Gpm6b	ENSRNOG00000004613	expanded 15k	glycoprotein m6b
1370442_at	Tmsbl1	NA	expanded 15k	thymosin beta-like protein 1
1370450_at	Tpm3	ENSRNOG00000017441	expanded 15k	tropomyosin 3, gamma
1370483_at	Cd244	ENSRNOG00000000045	expanded 15k	CD244 natural killer cell receptor 2B4
1370503_s_at	Epb4.1l3	ENSRNOG00000016724	expanded 15k	erythrocyte protein band 4.1-like 3
1370892_at	C4a	ENSRNOG00000000443	expanded 15k	complement component 4a
1371694_at	Dpysl2	ENSRNOG00000009625	expanded 15k	dihydropyrimidinase-like 2
1372006_at	Loxl2_predicted	ENSRNOG00000016758	expanded 15k	lysyl oxidase-like 2 (predicted)
1372013_at	Ifitm1_predicted	ENSRNOG00000004273	expanded 15k	interferon induced transmembrane protein 1 (predicted)
1373028_at	Ryk	ENSRNOG00000008593	expanded 15k	receptor-like tyrosine kinase
1373136_at	RGD1307672	ENSRNOG00000000398	expanded 15k	hypothetical LOC294390
1373406_at	Tor1b	ENSRNOG00000006435	expanded 15k	torsin family 1, member B
1373513_at	NA	NA	expanded 15k	NA
1374103_at	Freq	ENSRNOG00000008761	expanded 15k	frequenin homolog (Drosophila)
1374106_at	NA	NA	expanded 15k	NA
1374457_at	Pomt2	ENSRNOG00000012210	expanded 15k	protein-O-mannosyltransferase 2
1374544_at	MGC112715	ENSRNOG00000000569	expanded 15k	hypothetical protein LOC690899
1375853_at	RGD1309995_predicted	ENSRNOG00000008331	expanded 15k	similar to CG13957-PA (predicted)

1376869_at	NA	NA	expanded 15k	NA
1377185_at	<i>RGD1562622_predicted</i>	ENSRNOG00000010646	expanded 15k	similar to RIKEN cDNA 6330442E10 gene (predicted)
1380822_at	NA	NA	expanded 15k	NA
1383906_at	<i>LOC316326</i>	ENSRNOG00000015366	expanded 15k	similar to lung inducible neuralized-related C3HC4 RING finger protein
1387131_at	<i>Serpini1</i>	ENSRNOG00000010248	expanded 15k	serine (or cysteine) peptidase inhibitor, clade I, member 1
1387799_at	<i>Fxyd2</i>	ENSRNOG00000016469	expanded 15k	FXYD domain-containing ion transport regulator 2
1387883_a_at	<i>Tmsb4x</i>	NA	expanded 15k	thymosin, beta 4
1387884_at	<i>Psma5</i>	ENSRNOG00000019868	expanded 15k	proteasome (prosome, macropain) subunit, alpha type 5
1387893_at	<i>C1s</i>	ENSRNOG00000011971	expanded 15k	complement component 1, s subcomponent
1388131_at	<i>Tubb2b</i>	ENSRNOG00000017558	expanded 15k	tubulin, beta 2b
1388408_at	<i>RGD1307129</i>	NA	expanded 15k	similar to RIKEN cDNA 1110020C13
1388774_at	<i>Mbd2_predicted</i>	NA	expanded 15k	methyl-CpG binding domain protein 2 (predicted)
1388915_at	NA	NA	expanded 15k	NA
1389477_at	NA	NA	expanded 15k	NA
1389734_x_at	<i>RT1-Aw2</i>	ENSRNOG00000000724	expanded 15k	RT1 class Ib, locus Aw2
1390024_at	NA	NA	expanded 15k	NA
1390659_at	NA	NA	expanded 15k	NA
1390722_at	NA	NA	expanded 15k	NA
1392794_at	NA	NA	expanded 15k	NA
1398365_at	<i>RGD1305061</i>	ENSRNOG00000016890	expanded 15k	similar to RIKEN cDNA 2700055K07
1398380_at	<i>Vwa1</i>	ENSRNOG00000018338	expanded 15k	von Willebrand factor A domain containing 1
1398386_at	<i>LOC501515</i>	ENSRNOG00000016629	expanded 15k	similar to Zinc finger CCHC domain-containing protein 6

Supplementary Table 3: Gene ontology enrichment of the rat iDIN. ID refers to the Gene Ontology term id, *P*-values have been computed using the standard hypergeometric test using all genes on the Affymetrix rat230 2.0 chip that are annotated to Entrez genes. Odds ratio is the observed count of genes from this GO term in the iDIN divided by the expected counts, which are also given in the table (Count, ExpCount). Size gives the total number of genes annotated to this GO term.

GO term ID	<i>P</i> -value	OddsRatio	ExpCount	Count	Size	Term
GO:0002376	6.49E-34	9.62	11.05	65	524	immune system process
GO:0006955	7.47E-29	10.43	7.28	50	345	immune response
GO:0019882	1.65E-21	42.64	0.89	19	42	antigen processing and presentation
GO:0006952	1.03E-16	6.70	7.30	37	346	defense response
GO:0050896	8.75E-15	3.38	37.02	83	1755	response to stimulus
GO:0048002	2.10E-12	49.02	0.42	10	20	antigen processing and presentation of peptide antigen
GO:0006935	5.55E-10	9.88	1.92	15	91	chemotaxis
GO:0042330	5.55E-10	9.88	1.92	15	91	taxis
GO:0006954	5.60E-10	5.67	4.91	23	233	inflammatory response
GO:0019884	2.56E-09	56.25	0.27	7	13	antigen processing and presentation of exogenous antigen
GO:0002443	3.83E-09	12.09	1.29	12	61	leukocyte mediated immunity
GO:0002449	9.61E-09	12.87	1.12	11	53	lymphocyte mediated immunity
GO:0050776	1.15E-08	9.47	1.71	13	81	regulation of immune response
GO:0002252	4.26E-08	8.36	1.90	13	90	immune effector process
GO:0050778	6.46E-08	10.38	1.33	11	63	positive regulation of immune response
GO:0007626	8.45E-08	6.02	3.14	16	149	locomotory behavior
GO:0051707	1.04E-07	6.95	2.40	14	114	response to other organism
GO:0048584	1.06E-07	7.65	2.05	13	97	positive regulation of response to stimulus
GO:0002684	1.36E-07	7.47	2.09	13	99	positive regulation of immune system process
GO:0016064	1.66E-07	13.26	0.89	9	42	immunoglobulin mediated immune response
GO:0032020	1.92E-07	Inf	0.08	4	4	ISG15-protein conjugation
GO:0048583	1.92E-07	5.63	3.33	16	158	regulation of response to stimulus
GO:0019724	2.06E-07	12.87	0.91	9	43	B cell mediated immunity
GO:0002460	2.10E-07	10.61	1.18	10	56	adaptive immune response based on somatic recombination of immune receptors built from immunoglobulin superfamily domains
GO:0002250	2.10E-07	10.61	1.18	10	56	adaptive immune response
GO:0002478	2.10E-07	79.49	0.17	5	8	antigen processing and presentation of exogenous peptide antigen
GO:0009607	2.96E-07	5.44	3.44	16	163	response to biotic stimulus
GO:0002682	3.01E-07	6.31	2.62	14	124	regulation of immune system process
GO:0002526	3.11E-07	8.69	1.54	11	73	acute inflammatory response
GO:0006959	5.61E-07	11.21	1.01	9	48	humoral immune response
GO:0001775	6.17E-07	5.12	3.63	16	172	cell activation
GO:0045087	6.74E-07	10.93	1.03	9	49	innate immune response
GO:0002253	6.74E-07	10.93	1.03	9	49	activation of immune response
GO:0045321	7.17E-07	5.40	3.23	15	153	leukocyte activation
GO:0009615	9.57E-07	12.89	0.80	8	38	response to virus

GO:0031347	1.14E-06	10.16	1.10	9	52	regulation of defense response
GO:0009605	1.38E-06	2.88	12.93	32	613	response to external stimulus
GO:0042379	2.22E-06	14.57	0.63	7	31	chemokine receptor binding
GO:0008009	2.22E-06	14.57	0.63	7	31	chemokine activity
GO:0002673	2.78E-06	34.05	0.25	5	12	regulation of acute inflammatory response
GO:0002474	2.78E-06	34.05	0.25	5	12	antigen processing and presentation of peptide antigen via MHC class I
GO:0002883	2.78E-06	94.87	0.13	4	6	regulation of hypersensitivity
GO:0002864	2.78E-06	94.87	0.13	4	6	regulation of acute inflammatory response to antigenic stimulus
GO:0002861	2.78E-06	94.87	0.13	4	6	regulation of inflammatory response to antigenic stimulus
GO:0002703	4.44E-06	29.79	0.27	5	13	regulation of leukocyte mediated immunity
GO:0002706	4.44E-06	29.79	0.27	5	13	regulation of lymphocyte mediated immunity
GO:0051240	4.53E-06	4.91	3.27	14	155	positive regulation of multicellular organismal process
GO:0002697	4.57E-06	17.96	0.46	6	22	regulation of immune effector process
GO:0009611	6.76E-06	3.19	8.20	23	389	response to wounding
GO:0002437	6.78E-06	26.48	0.30	5	14	inflammatory response to antigenic stimulus
GO:0002524	1.26E-05	47.42	0.17	4	8	hypersensitivity
GO:0002438	1.26E-05	47.42	0.17	4	8	acute inflammatory response to antigenic stimulus
GO:0002274	1.31E-05	14.36	0.55	6	26	myeloid leukocyte activation
GO:0051704	1.92E-05	3.82	4.72	16	224	multi-organism process
GO:0006958	1.99E-05	19.85	0.36	5	17	complement activation, classical pathway
GO:0002455	1.99E-05	19.85	0.36	5	17	humoral immune response mediated by circulating immunoglobulin
GO:0031349	2.08E-05	13.05	0.59	6	28	positive regulation of defense response
GO:0002822	2.22E-05	37.93	0.19	4	9	regulation of adaptive immune response based on somatic recombination of immune receptors built from immunoglobulin superfamily domains
GO:0002819	2.22E-05	37.93	0.19	4	9	regulation of adaptive immune response
GO:0001816	3.19E-05	6.41	1.62	9	77	cytokine production
GO:0002758	3.64E-05	141.53	0.08	3	4	innate immune response-activating signal transduction
GO:0042535	3.64E-05	141.53	0.08	3	4	positive regulation of tumor necrosis factor biosynthetic process
GO:0002218	3.64E-05	141.53	0.08	3	4	activation of innate immune response
GO:0050766	3.64E-05	31.61	0.21	4	10	positive regulation of phagocytosis
GO:0019864	7.99E-05	73.52	0.10	3	5	IgG binding
GO:0050764	8.30E-05	23.70	0.25	4	12	regulation of phagocytosis
GO:0002712	8.95E-05	70.76	0.11	3	5	regulation of B cell mediated immunity

GO:0002889	8.95E-05	70.76	0.11	3	5	regulation of immunoglobulin mediated immune response
GO:0005057	1.19E-04	4.75	2.35	10	116	receptor signaling protein activity
GO:0007259	1.48E-04	8.69	0.82	6	39	JAK-STAT cascade
GO:0015198	1.57E-04	49.01	0.12	3	6	oligopeptide transporter activity
GO:0019763	1.57E-04	49.01	0.12	3	6	immunoglobulin receptor activity
GO:0050727	1.72E-04	8.43	0.84	6	40	regulation of inflammatory response
GO:0019886	1.76E-04	47.17	0.13	3	6	antigen processing and presentation of exogenous peptide antigen via MHC class II
GO:0042116	1.76E-04	47.17	0.13	3	6	macrophage activation
GO:0002495	1.76E-04	47.17	0.13	3	6	antigen processing and presentation of peptide antigen via MHC class II
GO:0004871	1.82E-04	1.99	24.05	42	1185	signal transducer activity
GO:0060089	1.82E-04	1.99	24.05	42	1185	molecular transducer activity
GO:0042221	2.19E-04	2.25	14.45	29	685	response to chemical stimulus
GO:0031328	2.24E-04	6.46	1.24	7	59	positive regulation of cellular biosynthetic process
GO:0009891	2.49E-04	6.33	1.27	7	60	positive regulation of biosynthetic process
GO:0042742	2.62E-04	10.34	0.59	5	28	defense response to bacterium
GO:0002541	2.62E-04	10.34	0.59	5	28	activation of plasma proteins during acute inflammatory response
GO:0006956	2.62E-04	10.34	0.59	5	28	complement activation
GO:0030593	2.86E-04	15.79	0.34	4	16	neutrophil chemotaxis
GO:0042534	3.04E-04	35.37	0.15	3	7	regulation of tumor necrosis factor biosynthetic process
GO:0042533	3.04E-04	35.37	0.15	3	7	tumor necrosis factor biosynthetic process
GO:0032640	3.04E-04	35.37	0.15	3	7	tumor necrosis factor production
GO:0006857	3.04E-04	35.37	0.15	3	7	oligopeptide transport
GO:0032101	3.38E-04	5.99	1.33	7	63	regulation of response to external stimulus
GO:0045807	3.68E-04	14.58	0.36	4	17	positive regulation of endocytosis
GO:0001664	4.00E-04	4.99	1.79	8	88	G-protein-coupled receptor binding
GO:0015197	4.28E-04	29.40	0.16	3	8	peptide transporter activity
GO:0006911	4.78E-04	28.29	0.17	3	8	phagocytosis, engulfment
GO:0002708	4.78E-04	28.29	0.17	3	8	positive regulation of lymphocyte mediated immunity
GO:0002705	4.78E-04	28.29	0.17	3	8	positive regulation of leukocyte mediated immunity
GO:0002504	4.78E-04	28.29	0.17	3	8	antigen processing and presentation of peptide or polysaccharide antigen via MHC class II
GO:0006917	4.97E-04	3.63	3.33	11	158	induction of apoptosis
GO:0012502	5.24E-04	3.61	3.35	11	159	induction of programmed cell death
GO:0045429	7.06E-04	23.57	0.19	3	9	positive regulation of nitric oxide biosynthetic process
GO:0002698	7.06E-04	23.57	0.19	3	9	negative regulation of immune effector process
GO:0030097	7.15E-04	3.46	3.48	11	165	hemopoiesis
GO:0002757	8.65E-04	11.14	0.44	4	21	immune response-activating signal transduction

GO:0002764	8.65E-04	11.14	0.44	4	21	immune response-regulating signal transduction
GO:0051239	9.04E-04	2.56	7.23	17	343	regulation of multicellular organismal process
GO:0051173	9.93E-04	20.20	0.21	3	10	positive regulation of nitrogen compound metabolic process
GO:0045089	9.93E-04	20.20	0.21	3	10	positive regulation of innate immune response
GO:0002699	9.93E-04	20.20	0.21	3	10	positive regulation of immune effector process
GO:0001909	9.93E-04	20.20	0.21	3	10	leukocyte mediated cytotoxicity
GO:0050900	9.96E-04	7.43	0.78	5	37	leukocyte migration
GO:0007610	1.09E-03	2.60	6.71	16	318	behavior
GO:0019865	1.20E-03	18.37	0.22	3	11	immunoglobulin binding
GO:0030693	1.20E-03	18.37	0.22	3	11	caspase activity
GO:0048534	1.22E-03	3.23	3.71	11	176	hemopoietic or lymphoid organ development
GO:0042108	1.24E-03	9.97	0.49	4	23	positive regulation of cytokine biosynthetic process
GO:0006968	1.27E-03	6.99	0.82	5	39	cellular defense response
GO:0003779	1.30E-03	3.19	3.73	11	184	actin binding
GO:0002444	1.34E-03	17.68	0.23	3	11	myeloid leukocyte mediated immunity
GO:0046649	1.50E-03	3.64	2.70	9	128	lymphocyte activation
GO:0006508	1.53E-03	2.21	10.36	21	491	proteolysis
GO:0016787	1.59E-03	1.73	29.19	45	1438	hydrolase activity
GO:0002520	1.67E-03	3.09	3.86	11	183	immune system development
GO:0006909	1.71E-03	9.01	0.53	4	25	phagocytosis
GO:0045088	1.76E-03	15.71	0.25	3	12	regulation of innate immune response
GO:0030217	1.99E-03	6.25	0.91	5	43	T cell differentiation
GO:0030595	1.99E-03	8.60	0.55	4	26	leukocyte chemotaxis
GO:0005125	2.11E-03	3.19	3.39	10	167	cytokine activity
GO:0007260	2.26E-03	14.14	0.27	3	13	tyrosine phosphorylation of STAT protein
GO:0045576	2.26E-03	14.14	0.27	3	13	mast cell activation
GO:0050777	2.26E-03	14.14	0.27	3	13	negative regulation of immune response
GO:0045428	2.26E-03	14.14	0.27	3	13	regulation of nitric oxide biosynthetic process
GO:0042110	2.50E-03	4.13	1.86	7	88	T cell activation
GO:0001906	2.83E-03	12.85	0.30	3	14	cell killing
GO:0048518	3.00E-03	1.80	20.23	33	959	positive regulation of biological process
GO:0002521	3.41E-03	3.89	1.96	7	93	leukocyte differentiation
GO:0042107	3.56E-03	5.39	1.03	5	49	cytokine metabolic process
GO:0042089	3.56E-03	5.39	1.03	5	49	cytokine biosynthetic process
GO:0002683	3.86E-03	7.01	0.65	4	31	negative regulation of immune system process
GO:0009617	4.29E-03	4.26	1.54	6	73	response to bacterium
GO:0007165	4.82E-03	1.54	45.14	61	2140	signal transduction
GO:0008283	4.83E-03	1.90	13.69	24	649	cell proliferation
GO:0032103	4.86E-03	6.52	0.70	4	33	positive regulation of response to external stimulus
GO:0051250	5.05E-03	10.09	0.36	3	17	negative regulation of lymphocyte activation
GO:0030100	5.42E-03	6.30	0.72	4	34	regulation of endocytosis
GO:0046651	5.42E-03	4.84	1.14	5	54	lymphocyte proliferation

GO:0051050	5.42E-03	4.84	1.14	5	54	positive regulation of transport
GO:0032943	5.42E-03	4.84	1.14	5	54	mononuclear cell proliferation
GO:0051094	5.58E-03	2.24	7.19	15	341	positive regulation of developmental process
GO:0043065	5.95E-03	2.59	4.56	11	216	positive regulation of apoptosis
GO:0050866	5.96E-03	9.42	0.38	3	18	negative regulation of cell activation
GO:0002695	5.96E-03	9.42	0.38	3	18	negative regulation of leukocyte activation
GO:0043068	6.16E-03	2.57	4.58	11	217	positive regulation of programmed cell death
GO:0018108	6.33E-03	4.65	1.18	5	56	peptidyl-tyrosine phosphorylation
GO:0045727	6.66E-03	5.91	0.76	4	36	positive regulation of translation
GO:0050729	6.97E-03	8.83	0.40	3	19	positive regulation of inflammatory response
GO:0018212	7.34E-03	4.47	1.22	5	58	peptidyl-tyrosine modification
GO:0004175	7.88E-03	2.28	6.07	13	299	endopeptidase activity
GO:0030099	8.00E-03	3.70	1.75	6	83	myeloid cell differentiation
GO:0015833	8.86E-03	5.40	0.82	4	39	peptide transport
GO:0051171	9.28E-03	7.85	0.44	3	21	regulation of nitrogen compound metabolic process
GO:0008154	9.68E-03	5.25	0.84	4	40	actin polymerization and/or depolymerization
GO:0042035	9.68E-03	5.25	0.84	4	40	regulation of cytokine biosynthetic process

Supplementary Table 4: Characterization of candidate genes at the rat locus controlling the iDIN.

Location (Mb)	Gene Symbol	Gene name	Expression [†]	Differential expression*	CDNA sequence variation**	Cell type enrichment [‡]
106.550 - 106.592	S15A1	Solute carrier family 15 member 1	0	n/a	no	NS
106.629 - 106.804	Dock9	Dedicator of cytokinesis	7.0	NS	S SNP (A/G) at 106631154	NS
107.005 - 107.125	Phgdh1	Phosphoglycerate dehydrogenase like 1	7.1	NS	no	NK, $P = 5.5 \times 10^{-8}$
107.014 - 107.018	Gpr18	N-arachidonyl glycine receptor	0	n/a	no	NS
107.056 - 107.067	Gpr183 (Ebi2)	Orphan GPCR	2.4	-1.7 fold, $P < 10^{-2}$	SNP (A/G) at 107067871 in 5'UTR	DC, $P = 4.9 \times 10^{-11}$
107.145 - 107.148	Timm8a2	Translocase of inner mitochondrial membrane 8 homolog a2	0	n/a	no	NS
107.228 - 107.277	Tm9sf2	Transmembrane 9 superfamily member 2	8.2	NS	S SNP (A/G) at 107253621; N.S. SNP (G/T; amino acid L/F; non-pathogenic [#]) at 107246348; S SNP (T/A) at 107228867	NS

[†] Log₂ of mean RNA-Seq exon coverage in the heart of the BN reference strain. Expression = 0 when <1x coverage per exon base.

* between SHR and BN parental strains, fold change relative to BN strain

** SNP alleles given as (BN/SHR), S = synonymous, N.S. = non synonymous. Sequence data from SHR sequence (TJA, personal communication) and the BN reference strain

[‡] Bonferroni corrected P-value for enrichment in both human and mouse gene expression across cell types and tissues (<http://biogps.gnf.org>). NK, natural killer cells of lymphoid origin; DC, dendritic cells of myeloid origin

[#] non-pathogenic – PolyPhen (<http://genetics.bwh.harvard.edu/pph/>). NS, not significant ($P > 0.05$)

Supplementary Table 5: Genes of the human immune response network (n=496 unique Ensembl genes). The network was constructed from the GHS sample using TFBS enrichment analysis, analogous to that performed in the rat, and expanded the by co-expression analysis (see Supplementary Information) and the same analysis was applied in the Cardiogenics sample (not shown). Probeset denotes the identifier of the probe set on the microarray Illumina v3. Type denotes whether a gene was a predicted target in GHS (target ghs), Cardiogenics (target cardio) or both (target both), or it was included by expansion of the network by correlation in GHS (expanded ghs) or GHS and Cardiogenics (expanded both). For each Illumina probe we report the assigned quality grade: “Perfect” if it perfectly and uniquely matches the target transcript; “Good” if the probe, although imperfectly matching the target transcript, is still likely to provide considerably sensitive signal; “Bad” if the probe matches repeat sequences, intergenic or intronic regions, or is unlikely to provide specific signal for any transcript; “No match” if it does not match any genomic region or transcript. We found that 92.3% of all probesets were classified as “Good” or “Perfect”. The probe quality assignments were retrieved from <http://www.compbio.group.cam.ac.uk/Resources/Annotation/> and are described in detail in Barbosa-Moraes N. L., et al. A re-annotation pipeline for Illumina BeadArrays: improving the interpretation of gene expression data. *Nucleic Acids Res.* 2010, 38(3):e17. NA indicates that the Illumina probe did not have an Ensembl gene identifier (Ensembl release 54) and/or a gene symbol annotation.

Probeset	Ensembl ID	Symbol	Type	Probe quality
ILMN_2388547	ENSG00000133106	<i>EPSTI1</i>	target both	Perfect
ILMN_1760062	ENSG00000137965	<i>IFI44</i>	target both	Perfect
ILMN_2347798	ENSG00000126709	<i>IFI6</i>	target both	Perfect
ILMN_1707695	ENSG00000185745	<i>IFIT1</i>	target both	Perfect
ILMN_1699331	ENSG00000185745	<i>IFIT1</i>	target both	Bad
ILMN_1739428	ENSG00000119922	<i>IFIT2</i>	target both	Perfect
ILMN_2239754	ENSG00000119917	<i>IFIT3</i>	target both	Perfect
ILMN_1701789	ENSG00000119917	<i>IFIT3</i>	target both	Perfect
ILMN_1664543	ENSG00000119917	<i>IFIT3</i>	target both	Perfect
ILMN_2054019	ENSG00000187608	<i>ISG15</i>	target both	Perfect
ILMN_1736729	ENSG00000111335	<i>OAS2</i>	target both	Perfect
ILMN_1709333	ENSG00000111335	<i>OAS2</i>	target both	Perfect
ILMN_1674063	ENSG00000111335	<i>OAS2</i>	target both	Bad
ILMN_1681721	ENSG00000135114	<i>OASL</i>	target cardio	Perfect
ILMN_1674811	ENSG00000135114	<i>OASL</i>	target cardio	Perfect
ILMN_1708672	ENSG00000120437	<i>ACAT2</i>	expanded ghs	Perfect
ILMN_1749014	ENSG00000131473	<i>ACLY</i>	expanded ghs	Perfect
ILMN_2344956	ENSG00000143727	<i>ACP1</i>	expanded ghs	Perfect
ILMN_2370882	ENSG00000197142	<i>ACSL5</i>	expanded ghs	Perfect
ILMN_2388605	ENSG00000138071	<i>ACTR2</i>	expanded ghs	Perfect
ILMN_2320964	ENSG00000160710	<i>ADAR</i>	expanded both	Perfect
ILMN_1655935	ENSG00000121281	<i>ADCY7</i>	expanded ghs	Perfect
ILMN_2129015	ENSG00000172493	<i>AFF1</i>	expanded ghs	Perfect
ILMN_1767722	ENSG00000119844	<i>AFTP</i>	expanded ghs	Perfect
ILMN_1662049	ENSG00000155189	<i>AGPAT5</i>	expanded both	Perfect
ILMN_1770454	ENSG00000188157	<i>AGRN</i>	expanded ghs	Perfect
ILMN_1703538	ENSG00000204472/// ENSG00000206319/// ENSG00000206428	<i>AIF1</i>	expanded ghs	Perfect

ILMN_1792473	ENSG00000204472/// ENSG00000206319/// ENSG00000206428	AIF1	expanded ghs	Perfect
ILMN_1797974	ENSG00000146416	AIG1	expanded ghs	Perfect
ILMN_1681301	ENSG00000163568	AIM2	expanded ghs	Perfect
ILMN_1709348	ENSG00000165092	ALDH1A1	expanded ghs	Perfect
ILMN_2078697	NA	NA	expanded ghs	Bad
ILMN_1799848	ENSG00000152766	ANKRD22	expanded ghs	Perfect
ILMN_2132599	ENSG00000152766	ANKRD22	expanded both	Perfect
ILMN_1711899	ENSG00000182718	ANXA2	expanded both	Perfect
ILMN_2399627	ENSG00000166747	AP1G1	expanded ghs	Perfect
ILMN_2362122	ENSG00000185009	AP3M1	expanded ghs	Perfect
ILMN_2412172	ENSG00000128394	APOBEC3F	expanded both	Perfect
ILMN_1702706	ENSG00000128394	APOBEC3F	expanded ghs	Perfect
ILMN_1802106	ENSG00000128394/// ENSG00000221877	APOBEC3G	expanded ghs	Perfect
ILMN_2232478	ENSG00000128394/// ENSG00000221877	APOBEC3G	expanded both	Perfect
ILMN_1756862	NA	NA	expanded both	Bad
ILMN_1717154	ENSG00000021776	AQR	expanded ghs	Perfect
ILMN_1723884	ENSG00000168374	ARF4	expanded both	Perfect
ILMN_1777998	ENSG00000163219	ARHGAP25	expanded ghs	Perfect
ILMN_2408851	ENSG00000186517	ARHGAP30	expanded ghs	Perfect
ILMN_1795247	ENSG00000189079	ARID2	expanded ghs	Perfect
ILMN_1781151	ENSG00000114098	ARMC8	expanded both	Perfect
ILMN_1716026	ENSG00000198960	ARMCX6	expanded ghs	Perfect
ILMN_1655561	ENSG00000111229	ARPC3	expanded ghs	Perfect
ILMN_1712587	ENSG00000113273	ARSB	expanded ghs	Perfect
ILMN_2221673	ENSG00000138381	ASNSD1	expanded ghs	Perfect
ILMN_2374865	ENSG00000162772	ATF3	expanded ghs	Perfect
ILMN_1772540	ENSG00000166454	ATMIN	expanded ghs	Perfect
ILMN_2367753	ENSG00000058668	ATP2B4	expanded ghs	Perfect
ILMN_2340565	ENSG00000017260	ATP2C1	expanded both	Perfect
ILMN_1672191	ENSG00000116459	ATP5F1	expanded ghs	Perfect
ILMN_1794912	ENSG00000167863	ATP5H	expanded ghs	Perfect
ILMN_1666372	ENSG00000167863	ATP5H	expanded ghs	Perfect
ILMN_1652806	ENSG00000154723	ATP5J	expanded ghs	Perfect
ILMN_1772929	ENSG00000154723	ATP5J	expanded ghs	Perfect
ILMN_2348093	ENSG00000154723	ATP5J	expanded ghs	Perfect
ILMN_1711102	ENSG00000170340	B3GNT2	expanded both	Perfect
ILMN_1690241	ENSG00000168062	BATF2	expanded both	Perfect
ILMN_1658327	ENSG00000198604	BAZ1A	expanded ghs	Perfect
ILMN_2372413	ENSG00000015475	BID	expanded ghs	Perfect
ILMN_2147920	NA	BRD7P2	expanded ghs	Perfect
ILMN_1696420	ENSG00000166164	BRD7	expanded ghs	Perfect
ILMN_2349600	ENSG00000112983	BRD8	expanded ghs	Perfect
ILMN_1701711	ENSG00000112983	BRD8	expanded ghs	Perfect
ILMN_1770085	ENSG00000159388	BTG2	expanded ghs	Perfect
ILMN_2373831	ENSG00000111801	BTN3A3	expanded ghs	Perfect
ILMN_1749210	ENSG00000137656	BUD13	expanded ghs	Perfect
ILMN_1792270	ENSG00000151893	C10orf46	expanded both	Perfect
ILMN_1671905	ENSG00000156384	C10orf78	expanded ghs	Perfect
ILMN_1786759	ENSG00000134825	C11orf10	expanded both	Perfect

ILMN_1773148	ENSG00000120458	C11orf61	expanded ghs	Perfect
ILMN_1779163	ENSG00000087884	C11orf67	expanded ghs	Perfect
ILMN_1758093	ENSG00000070269	C14orf101	expanded ghs	Perfect
ILMN_1706305	ENSG00000133983	COX16	expanded ghs	Perfect
ILMN_1734440	ENSG00000151445	C14orf133	expanded ghs	Perfect
ILMN_1661945	ENSG00000119705	C14orf156	expanded ghs	Perfect
ILMN_1652722	ENSG00000156411	C14orf2	expanded ghs	Perfect
ILMN_1702526	ENSG00000170222	C17orf48	expanded ghs	Perfect
ILMN_1710740	ENSG00000166278/// ENSG00000204364/// ENSG00000206372	C2	expanded ghs	Perfect
ILMN_2049727	ENSG00000132823	C20orf111	expanded ghs	Perfect
ILMN_1728168	ENSG00000101166	SLMO2	expanded both	Perfect
ILMN_1787370	ENSG00000003509	C2orf56	expanded both	Perfect
ILMN_1697742	ENSG00000179021	C3orf38	expanded ghs	Perfect
ILMN_1666827	ENSG00000168538	C4orf41	expanded ghs	Perfect
ILMN_1752086	ENSG00000168538	C4orf41	expanded ghs	Perfect
ILMN_1798108	ENSG00000146476	C6orf211	expanded ghs	Perfect
ILMN_1680867	NA	NA	expanded ghs	Bad
ILMN_1659524	ENSG00000123545	C6orf66	expanded ghs	Perfect
ILMN_1695485	NA	C9orf109	expanded ghs	Perfect
ILMN_1665004	ENSG00000108349	CASC3	expanded ghs	Perfect
ILMN_2325574	ENSG00000166734	CASC4	expanded ghs	Perfect
ILMN_2373763	NA	NA	expanded ghs	Bad
ILMN_2150352	ENSG00000172785	CBWD5	expanded ghs	Perfect
ILMN_1745946	ENSG00000152240	CCDC5	expanded ghs	Perfect
ILMN_1707783	NA	LOC100130394	expanded ghs	Perfect
ILMN_1720048	ENSG00000108691	CCL2	expanded both	Perfect
ILMN_1772964	ENSG00000108700	CCL8	expanded both	Perfect
ILMN_2276996	ENSG00000121807/// ENSG00000215782	FLJ78302	expanded ghs	Perfect
ILMN_1777461	ENSG00000121807/// ENSG00000215782	FLJ78302	expanded ghs	Perfect
ILMN_1669062	ENSG00000121807/// ENSG00000215782	CCR2	expanded ghs	Bad
ILMN_1679382	ENSG00000166226	CCT2	expanded ghs	Perfect
ILMN_1722622	ENSG00000177575	CD163	expanded ghs	Perfect
ILMN_2413808	ENSG00000143119	CD53	expanded ghs	Perfect
ILMN_1662843	ENSG00000143119	CD53	expanded ghs	Perfect
ILMN_1675156	ENSG00000070831	CDC42	expanded ghs	Perfect
ILMN_1736327	ENSG00000163171	CDC42EP3	expanded both	Perfect
ILMN_1790973	ENSG00000101290	CDS2	expanded ghs	Perfect
ILMN_1810977	ENSG00000091527	CDV3	expanded both	Perfect
ILMN_1673788	ENSG00000091527	CDV3	expanded ghs	Perfect
ILMN_1686283	ENSG00000093072	CECR1	expanded both	Perfect
ILMN_1766798	ENSG00000114331	ACAP2	expanded ghs	Bad
ILMN_1758778	ENSG00000119397	CEP110	expanded ghs	Perfect
ILMN_1774287	ENSG00000166285/// ENSG00000204359	CFB	expanded both	Perfect
ILMN_2324375	ENSG00000170791	CHCHD7	expanded ghs	Perfect
ILMN_2094166	ENSG00000086065	CHMP5	expanded both	Perfect
ILMN_1774110	ENSG00000106069	CHN2	expanded ghs	Perfect
ILMN_1790471	NA	NA	expanded ghs	Bad

ILMN_1671516	ENSG00000138433	CIR	expanded ghs	Perfect
ILMN_1716336	ENSG00000175216	CKAP5	expanded ghs	Perfect
ILMN_1719256	ENSG00000173207	CKS1B	expanded ghs	Perfect
ILMN_2292178	ENSG00000172322	CLEC12A	expanded both	Perfect
ILMN_1711702	NA	NA	expanded ghs	Bad
ILMN_1709204	ENSG00000111729	CLEC4A	expanded ghs	Perfect
ILMN_1704084	NA	CMAH	expanded ghs	Perfect
ILMN_1714082	ENSG00000111726	CMAS	expanded ghs	Perfect
ILMN_1783621	ENSG00000134326	CMPK2	expanded both	Perfect
ILMN_1786532	ENSG00000100528	CNIH	expanded both	Perfect
ILMN_1772651	ENSG00000111596	CNOT2	expanded ghs	Perfect
ILMN_1776154	ENSG00000136152	COG3	expanded ghs	Perfect
ILMN_1698621	ENSG00000164597	COG5	expanded ghs	Perfect
ILMN_1726591	ENSG00000204397	CARD16	expanded ghs	Perfect
ILMN_1701293	ENSG00000112695	COX7A2	expanded ghs	Good
ILMN_1668582	ENSG00000113851	CRBN	expanded ghs	Perfect
ILMN_1760593	ENSG00000008405	CRY1	expanded ghs	Perfect
ILMN_1665797	ENSG00000124207	CSE1L	expanded ghs	Perfect
ILMN_1706238	ENSG00000124207	CSE1L	expanded ghs	Perfect
ILMN_1799208	ENSG00000169826	CSGALNACT2	expanded both	Perfect
ILMN_1785988	ENSG00000113712	CSNK1A1	expanded both	Perfect
ILMN_1762002	ENSG00000176102	CSTF3	expanded ghs	Perfect
ILMN_2242463	ENSG00000109861	CTSC	expanded ghs	Perfect
ILMN_1696347	ENSG00000109861	CTSC	expanded ghs	Perfect
ILMN_1791759	ENSG00000169245	CXCL10	expanded both	Perfect
ILMN_1801584	ENSG00000121966	CXCR4	expanded both	Perfect
ILMN_1663751	ENSG00000172115	CYCS	expanded ghs	Perfect
ILMN_2305544	ENSG00000155368	DBI	expanded ghs	Perfect
ILMN_1755926	ENSG00000155368	DBI	expanded ghs	Perfect
ILMN_1776005	ENSG00000198856	OSTC	expanded ghs	Perfect
ILMN_1666192	NA	NA	expanded ghs	Bad
ILMN_1744059	ENSG00000104671	DCTN6	expanded ghs	Good
ILMN_1700628	ENSG00000089737	DDX24	expanded ghs	Perfect
ILMN_1747162	ENSG00000213782	DDX47	expanded both	Perfect
ILMN_1797001	ENSG00000107201	DDX58	expanded both	Perfect
ILMN_1795181	ENSG00000137628	DDX60	expanded both	Perfect
ILMN_1699711	ENSG00000158796	DEDD	expanded ghs	Perfect
ILMN_2384181	ENSG00000073737	DHRS9	expanded ghs	Perfect
ILMN_1744308	ENSG00000005100	DHX33	expanded ghs	Perfect
ILMN_2325008	NA	DHX40P	expanded ghs	Perfect
ILMN_1678422	ENSG00000108771	DHX58	expanded both	Perfect
ILMN_1656016	ENSG00000135829	DHX9	expanded both	Perfect
ILMN_1755589	ENSG00000066084	DIP2B	expanded ghs	Perfect
ILMN_1799796	ENSG00000083520	DIS3	expanded ghs	Perfect
ILMN_1742276	ENSG00000127993	C7orf64	expanded both	Perfect
ILMN_1705663	ENSG00000104093	DMXL2	expanded both	Perfect
ILMN_1752455	ENSG00000147459	DOCK5	expanded ghs	Perfect
ILMN_1770048	ENSG00000117543	DPH5	expanded ghs	Perfect
ILMN_1658259	ENSG00000185721	DRG1	expanded ghs	Perfect
ILMN_1784380	NA	NA	expanded both	Bad
ILMN_2137464	ENSG00000161202	DVL3	expanded ghs	Perfect
ILMN_1773847	ENSG00000077380	DYNC1I2	expanded both	Perfect
ILMN_1678766	ENSG00000146425	DYNLT1	expanded ghs	Perfect

ILMN_2374293	ENSG00000157540	DYRK1A	expanded ghs	Perfect
ILMN_1660663	ENSG00000157540	DYRK1A	expanded both	Perfect
ILMN_1664560	ENSG00000157540	DYRK1A	expanded ghs	Perfect
ILMN_1653143	ENSG00000122882	ECD	expanded ghs	Perfect
ILMN_1690939	ENSG0000025708	TYMP	expanded ghs	Perfect
ILMN_1729167	ENSG00000140598	EFTUD1	expanded ghs	Perfect
ILMN_2404629	ENSG00000140598	EFTUD1	expanded ghs	Perfect
ILMN_1706502	ENSG00000055332	EIF2AK2	expanded both	Perfect
ILMN_1655497	ENSG00000063046	EIF4B	expanded ghs	Perfect
ILMN_1738326	ENSG00000135930	EIF4E2	expanded both	Perfect
ILMN_1796146	ENSG00000163412	EIF4E3	expanded ghs	Bad
ILMN_2279635	ENSG00000110321	EIF4G2	expanded both	Perfect
ILMN_1709747	ENSG00000157036	EXOG	expanded ghs	Perfect
ILMN_1746276	ENSG00000120616	EPC1	expanded ghs	Perfect
ILMN_1795495	ENSG00000134899	ERCC5	expanded ghs	Perfect
ILMN_1781795	ENSG00000100632	ERH	expanded ghs	Perfect
ILMN_1700671	ENSG00000010030	ETV7	expanded ghs	Perfect
ILMN_2394750	ENSG00000131558	EXOC4	expanded both	Perfect
ILMN_1660840	ENSG00000121644	PPPDE1	expanded ghs	Perfect
ILMN_1669555	ENSG00000102710	FAM48A	expanded ghs	Perfect
ILMN_2378100	ENSG00000118564	FBXL5	expanded ghs	Perfect
ILMN_2123743	ENSG00000158869	FCER1G	expanded ghs	Perfect
ILMN_2261600	ENSG00000150337	FCGR1C	expanded both	Perfect
ILMN_1706523	ENSG00000143226	FCGR2A	expanded both	Perfect
ILMN_2370976	ENSG00000138119	MYOF	expanded both	Perfect
ILMN_1797895	ENSG00000126262	FFAR2	expanded both	Perfect
ILMN_1693009	ENSG00000127951	FGL2	expanded ghs	Perfect
ILMN_1768743	ENSG00000145216	FIP1L1	expanded ghs	Perfect
ILMN_1683658	ENSG00000088832	FKBP1A	expanded both	Perfect
ILMN_1726930	ENSG00000113597	C5orf44	expanded ghs	Perfect
ILMN_1680644	ENSG00000164654	MIOS	expanded ghs	Perfect
ILMN_2392569	ENSG00000171049	FPR2	expanded both	Perfect
ILMN_1740875	ENSG00000171049	FPR2	expanded ghs	Perfect
ILMN_2154052	ENSG00000119537	KDSR	expanded ghs	Perfect
ILMN_2151281	ENSG00000139112	GABARPL1	expanded ghs	Perfect
ILMN_1659682	ENSG00000156958	GALK2	expanded both	Perfect
ILMN_1681984	ENSG00000164574	GALNT10	expanded ghs	Perfect
ILMN_1793220	ENSG00000159131	GART	expanded both	Perfect
ILMN_2148785	ENSG00000117228	GBP1	expanded both	Perfect
ILMN_1701114	ENSG00000117228	GBP1	expanded ghs	Perfect
ILMN_1774077	ENSG00000162645	GBP2	expanded both	Perfect
ILMN_1771385	ENSG00000162654	GBP4	expanded both	Perfect
ILMN_2114568	ENSG00000154451	GBP5	expanded both	Perfect
ILMN_1812759	ENSG00000131979	GCH1	expanded both	Perfect
ILMN_2335813	ENSG00000131979	GCH1	expanded both	Perfect
ILMN_1769383	ENSG00000196329	GIMAP5	expanded ghs	Perfect
ILMN_1776678	ENSG00000179144	GIMAP7	expanded ghs	Perfect
ILMN_1760922	ENSG00000139436	GIT2	expanded both	Perfect
ILMN_2355776	ENSG00000139436	GIT2	expanded ghs	Perfect
ILMN_1694323	ENSG00000119392	GLE1	expanded both	Perfect
ILMN_1737308	ENSG00000173221	GLRX	expanded ghs	Perfect
ILMN_1713756	ENSG00000148672	GLUD1	expanded ghs	Perfect
ILMN_1757074	ENSG00000059769	GNG10	expanded ghs	Perfect

ILMN_1671237	ENSG00000167083	GNGT2	expanded ghs	Perfect
ILMN_2324056	ENSG00000163938	GNL3	expanded both	Perfect
ILMN_1716821	ENSG00000114745	GORASP1	expanded both	Perfect
ILMN_1656818	ENSG00000187037	GPR141	expanded ghs	Perfect
ILMN_1780368	ENSG00000125245	GPR18	expanded both	Perfect
ILMN_1737857	ENSG00000137947	GTF2B	expanded both	Perfect
ILMN_2208158	NA	GTF2IP1	expanded ghs	Perfect
ILMN_1750658	ENSG00000143575	HAX1	expanded ghs	Perfect
ILMN_2398903	ENSG00000143575	HAX1	expanded ghs	Perfect
ILMN_1707236	ENSG00000004961	HCCS	expanded ghs	Perfect
ILMN_1729749	NA	NA	expanded both	Bad
ILMN_1654639	ENSG00000138642	HERC6	expanded both	Perfect
ILMN_2374159	ENSG00000051108	HERPUD1	expanded ghs	Perfect
ILMN_2374164	ENSG00000051108	HERPUD1	expanded ghs	Perfect
ILMN_1785158	ENSG00000122557	HERPUD2	expanded ghs	Perfect
ILMN_1742929	ENSG00000163666	HESX1	expanded both	Perfect
ILMN_1763007	ENSG00000156875	HIAT1	expanded ghs	Perfect
ILMN_1689655	ENSG00000204287///	HLA-DRA	expanded ghs	Perfect
	ENSG00000206243			
ILMN_1790881	ENSG00000150540	HNMT	expanded ghs	Perfect
ILMN_2362245	ENSG00000126945	HNRNPH2	expanded both	Perfect
ILMN_1807633	ENSG00000132541	HRSP12	expanded ghs	Perfect
ILMN_1838310	NA	NA	expanded ghs	Perfect
ILMN_1835092	ENSG00000137959	IFI44L	expanded ghs	Perfect
ILMN_1913060	NA	NA	expanded ghs	Bad
ILMN_1847965	NA	NA	expanded ghs	Perfect
ILMN_1840920	NA	NA	expanded ghs	Perfect
ILMN_1848843	NA	NA	expanded ghs	Bad
ILMN_1856861	ENSG00000114933	INO80D	expanded ghs	Perfect
ILMN_1845037	NA	NA	expanded ghs	Bad
ILMN_1860051	NA	NA	expanded ghs	Bad
ILMN_1822495	NA	NA	expanded ghs	Perfect
ILMN_1908488	NA	NA	expanded ghs	Perfect
ILMN_1913537	NA	NA	expanded ghs	Perfect
ILMN_1841620	NA	NA	expanded ghs	Perfect
ILMN_1910908	NA	NA	expanded ghs	Perfect
ILMN_1788017	NA	NA	expanded both	Bad
ILMN_1733956	ENSG00000196305	IARS	expanded ghs	Perfect
ILMN_1696432	ENSG00000138413	IDH1	expanded ghs	Perfect
ILMN_1698533	NA	NA	expanded ghs	Bad
ILMN_1710937	ENSG00000163565	IFI16	expanded ghs	Perfect
ILMN_2058782	ENSG00000165949	IFI27	expanded both	Perfect
ILMN_1745374	ENSG00000068079	IFI35	expanded both	Perfect
ILMN_1723912	ENSG00000137959	IFI44L	expanded both	Perfect
ILMN_1687384	NA	NA	expanded ghs	Bad
ILMN_1696654	NA	NA	expanded both	Bad
ILMN_1801246	ENSG00000185885	IFITM1	expanded both	Perfect
ILMN_1673352	ENSG00000185201	IFITM2	expanded both	Perfect
ILMN_1805750	ENSG00000142089	IFITM3	expanded both	Perfect
ILMN_2369221	ENSG00000164136	IL15	expanded both	Perfect
ILMN_1697710	ENSG00000125571	IL1F7	expanded both	Perfect
ILMN_1689734	ENSG00000136689	IL1RN	expanded both	Perfect
ILMN_1782579	ENSG00000132305	IMMT	expanded ghs	Perfect

ILMN_2381603	ENSG00000071243	<i>ING3</i>	expanded both	Perfect
ILMN_2394561	ENSG00000168264	<i>IRF2BP2</i>	expanded ghs	Perfect
ILMN_2349061	ENSG00000185507	<i>IRF7</i>	expanded both	Perfect
ILMN_1798181	ENSG00000185507	<i>IRF7</i>	expanded both	Perfect
ILMN_1659913	ENSG00000172183	<i>ISG20</i>	expanded both	Perfect
ILMN_1662128	ENSG00000172780///	<i>ISY1</i>	expanded both	Perfect
		ENSG00000221812	expanded both	Perfect
ILMN_1714820	ENSG00000150093	<i>ITGB1</i>	expanded both	Perfect
ILMN_1793384	ENSG00000162434	<i>JAK1</i>	expanded both	Perfect
ILMN_1683178	ENSG00000096968	<i>JAK2</i>	expanded ghs	Perfect
ILMN_1697597	ENSG00000159658	<i>KIAA0494</i>	expanded ghs	Perfect
ILMN_1733115	ENSG00000170471	<i>KIAA1219</i>	expanded ghs	Perfect
ILMN_1674891	ENSG00000180843	<i>KIAA1618</i>	expanded ghs	Perfect
ILMN_2289093	NA	NA	expanded both	Bad
ILMN_1838885	ENSG00000152223	<i>KIAA1632</i>	expanded ghs	Perfect
ILMN_1769140	ENSG00000165185	<i>KIAA1958</i>	expanded ghs	Perfect
ILMN_1803254	ENSG00000100796	<i>SMEK1</i>	expanded ghs	Perfect
ILMN_1811472	ENSG00000137807	<i>KIF23</i>	expanded ghs	Perfect
ILMN_1683792	ENSG00000002549	<i>LAP3</i>	expanded both	Perfect
ILMN_1750321	NA	<i>LBA1</i>	expanded ghs	Perfect
ILMN_1768969	ENSG00000143815	<i>LBR</i>	expanded both	Perfect
ILMN_1658962	ENSG00000043462	<i>LCP2</i>	expanded ghs	Perfect
ILMN_1801553	ENSG00000166477	<i>LEO1</i>	expanded ghs	Perfect
ILMN_1782743	ENSG00000050426	<i>LETMD1</i>	expanded ghs	Perfect
ILMN_1659688	ENSG00000108679	<i>LOC100133842</i>	expanded both	Perfect
ILMN_1715760	ENSG00000168961	<i>LGALS9</i>	expanded both	Perfect
ILMN_1747744	ENSG00000145685	<i>LHFPL2</i>	expanded ghs	Perfect
ILMN_1683678	ENSG00000196141	<i>LOC26010</i>	expanded both	Perfect
ILMN_1729269	NA	<i>LOC285074</i>	expanded ghs	Perfect
ILMN_1690911	ENSG00000155330	<i>C16orf87</i>	expanded ghs	Perfect
ILMN_1782487	ENSG00000117228	<i>GBP1</i>	expanded ghs	Perfect
ILMN_1792528	ENSG00000118181	<i>RPS25</i>	expanded ghs	Good
ILMN_1761281	NA	NA	expanded ghs	Bad
ILMN_1757072	NA	NA	expanded ghs	Bad
ILMN_1695034	NA	<i>LOC100132528</i>	expanded ghs	Good
ILMN_1813801	NA	<i>LOC643668</i>	expanded ghs	Perfect
ILMN_1721659	ENSG00000100764	<i>PSMC1</i>	expanded ghs	Perfect
ILMN_1701753	NA	<i>LOC644063</i>	expanded ghs	Perfect
ILMN_1801999	ENSG00000162825	<i>LOC727908</i>	expanded ghs	Good
ILMN_1779258	NA	NA	expanded ghs	Bad
ILMN_1742887	ENSG00000134248	<i>HBXIP</i>	expanded ghs	Perfect
ILMN_1720745	NA	<i>LOC644037</i>	expanded ghs	Good
ILMN_1732328	ENSG00000116251	<i>RPL22</i>	expanded ghs	Perfect
ILMN_1700950	ENSG00000198856	<i>LOC646567</i>	expanded ghs	Perfect
ILMN_1702585	ENSG00000119335	<i>LOC646817</i>	expanded ghs	Perfect
ILMN_1761922	NA	NA	expanded ghs	Bad
ILMN_1732313	NA	<i>LOC647195</i>	expanded ghs	Perfect
ILMN_1665736	NA	<i>LOC642784</i>	expanded ghs	Perfect
ILMN_1732074	NA	<i>LOC644037</i>	expanded ghs	Perfect
ILMN_1737574	ENSG00000185973	<i>LOC648605</i>	expanded ghs	Perfect
ILMN_1726667	NA	<i>hCG_1789710</i>	expanded ghs	Good
ILMN_1651680	NA	<i>LOC644604</i>	expanded ghs	Perfect
ILMN_1690063	NA	NA	expanded ghs	Bad

ILMN_1718353	NA	LOC652455	expanded ghs	Good
ILMN_1666564	NA	LOC100133788	expanded ghs	Perfect
ILMN_1708627	ENSG00000143742///	<i>hCG_1781062</i>	expanded ghs	Perfect
	ENSG00000180581			
ILMN_1790819	ENSG00000162959	<i>MEMO1</i>	expanded ghs	Perfect
ILMN_1719344	ENSG00000148572	<i>NRBF2</i>	expanded ghs	Perfect
ILMN_1757336	ENSG00000186001	<i>LRCH3</i>	expanded both	Perfect
ILMN_2094396	ENSG00000171488	<i>LRRC8C</i>	expanded ghs	Perfect
ILMN_1695404	ENSG00000160932	<i>LY6E</i>	expanded both	Perfect
ILMN_1703132	ENSG00000083099	<i>LYRM2</i>	expanded ghs	Perfect
ILMN_2084353	ENSG00000003056	<i>M6PR</i>	expanded both	Perfect
ILMN_1798454	ENSG00000124688	<i>MAD2L1BP</i>	expanded both	Perfect
ILMN_1661577	ENSG00000182759	<i>MAFA</i>	expanded ghs	Perfect
ILMN_2215656	ENSG00000162385	<i>MAGOH</i>	expanded ghs	Good
ILMN_2379326	ENSG00000135341	<i>MAP3K7</i>	expanded both	Perfect
ILMN_1681101	ENSG00000145416	38776	expanded ghs	Perfect
ILMN_1673960	ENSG00000038274	<i>MAT2B</i>	expanded both	Perfect
ILMN_1806818	ENSG00000112118	<i>MCM3</i>	expanded ghs	Perfect
ILMN_1736460	ENSG00000111554	<i>MDM1</i>	expanded both	Perfect
ILMN_1674506	ENSG00000112282	<i>MED23</i>	expanded ghs	Perfect
ILMN_1659537	NA	NA	expanded ghs	Bad
ILMN_1655635	ENSG00000165819	<i>METTL3</i>	expanded ghs	Perfect
ILMN_1715863	ENSG00000168404	<i>MLKL</i>	expanded ghs	Perfect
ILMN_1737498	NA	NA	expanded both	Bad
ILMN_1736165	ENSG00000055609	<i>MLL3</i>	expanded ghs	Perfect
ILMN_2408877	ENSG00000055609	<i>MLL3</i>	expanded ghs	Perfect
ILMN_1694596	ENSG00000064763	<i>FAR2</i>	expanded ghs	Good
ILMN_1738992	ENSG00000163563	<i>MNDA</i>	expanded ghs	Perfect
ILMN_2274923	ENSG00000164172	<i>MOCS2</i>	expanded ghs	Perfect
ILMN_1666156	ENSG00000123562	<i>MORF4L2</i>	expanded ghs	Perfect
ILMN_1725700	ENSG00000155363	<i>MOV10</i>	expanded both	Perfect
ILMN_1752355	ENSG00000197629	<i>MPEG1</i>	expanded ghs	Perfect
ILMN_1709483	ENSG00000020922	<i>MRE11A</i>	expanded ghs	Perfect
ILMN_1663220	ENSG00000082515	<i>MRPL22</i>	expanded ghs	Perfect
ILMN_1753016	ENSG00000132313	<i>MRPL35</i>	expanded ghs	Perfect
ILMN_1658416	ENSG00000163319	<i>MRPS18C</i>	expanded ghs	Perfect
ILMN_1701306	NA	NA	expanded ghs	Bad
ILMN_1721035	ENSG00000110077	<i>MS4A6A</i>	expanded ghs	Perfect
ILMN_2359800	ENSG00000110077	<i>MS4A6A</i>	expanded ghs	Perfect
ILMN_1691156	ENSG00000205362	<i>MT1A</i>	expanded ghs	Perfect
ILMN_1686664	ENSG00000125148	<i>MT2A</i>	expanded both	Good
ILMN_2405521	ENSG00000065911	<i>MTHFD2</i>	expanded both	Perfect
ILMN_1686985	ENSG00000171100	<i>MTM1</i>	expanded ghs	Perfect
ILMN_1662358	ENSG00000157601	<i>MX1</i>	expanded both	Perfect
ILMN_2231928	ENSG00000183486	<i>MX2</i>	expanded both	Perfect
ILMN_1688071	ENSG00000171428	<i>NAT1</i>	expanded ghs	Perfect
ILMN_1674250	ENSG00000123338	<i>NCKAP1L</i>	expanded both	Perfect
ILMN_1784286	ENSG00000125356	<i>NDUFA1</i>	expanded ghs	Perfect
ILMN_1760741	ENSG00000139180	<i>NDUFA9</i>	expanded ghs	Perfect
ILMN_1776104	ENSG00000168653	<i>NDUFS5</i>	expanded ghs	Perfect
ILMN_1785711	ENSG00000129559	<i>NEDD8</i>	expanded ghs	Perfect
ILMN_1690325	ENSG00000001167	<i>NFYA</i>	expanded ghs	Perfect
ILMN_1690049	ENSG00000129460	<i>NGDN</i>	expanded ghs	Perfect

ILMN_2324998	ENSG00000129460	NGDN	expanded ghs	Perfect
ILMN_2330994	NA	NA	expanded ghs	Bad
ILMN_1716704	ENSG00000140853	NLRC5	expanded both	Perfect
ILMN_1703153	ENSG00000140632	N-PAC	expanded ghs	Good
ILMN_1812384	ENSG00000113580	NR3C1	expanded ghs	Perfect
ILMN_1800897	ENSG00000078618	NRD1	expanded ghs	Perfect
ILMN_1680687	ENSG00000073969	NSF	expanded ghs	Perfect
ILMN_1815723	ENSG00000163002	NUP35	expanded ghs	Perfect
ILMN_1732776	ENSG00000110713	NUP98	expanded ghs	Perfect
ILMN_2410826	ENSG00000089127	OAS1	expanded both	Perfect
ILMN_1675640	ENSG00000089127	OAS1	expanded both	Perfect
ILMN_2248970	NA	NA	expanded both	Bad
ILMN_2184262	NA	NA	expanded both	Bad
ILMN_1745397	NA	NA	expanded ghs	Bad
ILMN_1715809	ENSG00000119900	OGFRL1	expanded ghs	Perfect
ILMN_1670079	ENSG00000162600	OMA1	expanded ghs	Perfect
ILMN_1784946	ENSG00000135336	ORC3L	expanded ghs	Perfect
ILMN_2328378	ENSG00000070882	OSBPL3	expanded ghs	Perfect
ILMN_1663347	ENSG00000115155	OTOF	expanded both	Perfect
ILMN_1664525	ENSG00000181631	P2RY13	expanded ghs	Perfect
ILMN_1786429	ENSG00000139679	P2RY5	expanded ghs	Perfect
ILMN_1652753	ENSG00000175575	PAAF1	expanded ghs	Perfect
ILMN_1736806	ENSG00000076641	PAG1	expanded ghs	Perfect
ILMN_1767365	ENSG00000149269	PAK1	expanded ghs	Perfect
ILMN_1781819	ENSG00000138801	PAPSS1	expanded ghs	Perfect
ILMN_1710844	ENSG00000178685	PARP10	expanded ghs	Perfect
ILMN_1718558	ENSG00000059378	PARP12	expanded both	Perfect
ILMN_2053527	ENSG00000138496	PARP9	expanded both	Perfect
ILMN_1731224	ENSG00000138496	PARP9	expanded ghs	Perfect
ILMN_1667925	ENSG00000115539	PDCL3	expanded ghs	Perfect
ILMN_2278819	ENSG00000205268	PDE7A	expanded ghs	Perfect
ILMN_1689518	ENSG00000198802	PECAM1	expanded ghs	Perfect
ILMN_2384536	ENSG00000198721	PECI	expanded ghs	Perfect
ILMN_1679268	ENSG00000197329	PELI1	expanded ghs	Perfect
ILMN_1755536	ENSG00000123349	PFDN5	expanded ghs	Perfect
ILMN_2356284	ENSG00000123349	PFDN5	expanded ghs	Good
ILMN_1713031	ENSG00000104324	PGCP	expanded ghs	Perfect
ILMN_1755749	NA	LOC100132888	expanded ghs	Perfect
ILMN_2401769	ENSG00000106443	PHF14	expanded ghs	Perfect
ILMN_1775901	ENSG00000100410	PHF5A	expanded ghs	Perfect
ILMN_1652412	ENSG00000102893	PHKB	expanded both	Perfect
ILMN_2083567	ENSG00000040199	PHLPPL	expanded ghs	Perfect
ILMN_1815134	ENSG00000038210	PI4K2B	expanded ghs	Perfect
ILMN_1780598	ENSG00000033800	PIAS1	expanded ghs	Perfect
ILMN_1778709	ENSG00000073921	PICALM	expanded ghs	Perfect
ILMN_2397571	ENSG00000135845	PIGC	expanded ghs	Perfect
ILMN_1808938	ENSG00000151665	PIGF	expanded ghs	Perfect
ILMN_1774949	ENSG00000185808	PIGP	expanded ghs	Perfect
ILMN_1769606	ENSG00000134627	PIWIL4	expanded ghs	Perfect
ILMN_2093343	ENSG00000145287	PLAC8	expanded ghs	Perfect
ILMN_1653026	ENSG00000145287	PLAC8	expanded ghs	Perfect
ILMN_1733666	NA	NA	expanded ghs	Bad
ILMN_1749634	ENSG00000171566	PLRG1	expanded ghs	Perfect

ILMN_1745242	ENSG00000188313	<i>PLSCR1</i>	expanded both	Perfect
ILMN_2088172	ENSG00000047315	<i>POLR2B</i>	expanded ghs	Perfect
ILMN_1791093	ENSG00000134283	<i>PPHLN1</i>	expanded ghs	Perfect
ILMN_2322842	ENSG00000134283	<i>PPHLN1</i>	expanded both	Perfect
ILMN_1801913	ENSG00000171960	<i>PPIH</i>	expanded both	Perfect
ILMN_2070044	ENSG00000163644	<i>PPM1K</i>	expanded ghs	Perfect
ILMN_1738784	ENSG00000066027	<i>PPP2R5A</i>	expanded ghs	Perfect
ILMN_1789283	ENSG00000078304	<i>PPP2R5C</i>	expanded ghs	Good
ILMN_2364971	ENSG00000078304	<i>PPP2R5C</i>	expanded both	Perfect
ILMN_1796962	ENSG00000115953	<i>PPP3R1</i>	expanded ghs	Perfect
ILMN_2366391	ENSG00000117450	<i>PRDX1</i>	expanded both	Good
ILMN_2395969	ENSG00000165672	<i>PRDX3</i>	expanded ghs	Good
ILMN_2395974	ENSG00000165672	<i>PRDX3</i>	expanded ghs	Perfect
ILMN_1787509	ENSG00000130589	<i>PRIC285</i>	expanded both	Perfect
ILMN_1695868	ENSG00000124593	<i>PRICKLE4</i>	expanded ghs	Good
ILMN_1751984	ENSG00000181929	<i>PRKAG1</i>	expanded ghs	Perfect
ILMN_2360415	ENSG00000171867	<i>PRNP</i>	expanded ghs	Perfect
ILMN_1715392	ENSG00000117360	<i>PRPF3</i>	expanded ghs	Perfect
ILMN_2387553	ENSG00000100567	<i>PSMA3</i>	expanded ghs	Perfect
ILMN_2318011	ENSG00000100567	<i>PSMA3</i>	expanded ghs	Perfect
ILMN_1704094	ENSG00000100902	<i>PSMA6</i>	expanded ghs	Perfect
ILMN_2376108	ENSG00000204261///	<i>PSMB9</i>	expanded both	Perfect
	ENSG00000206232///			
	ENSG00000206296			
ILMN_1687887	ENSG0000013275	<i>PSMC4</i>	expanded ghs	Perfect
ILMN_1702837	ENSG00000173692	<i>PSMD1</i>	expanded ghs	Perfect
ILMN_1776102	ENSG00000101843	<i>PSMD10</i>	expanded ghs	Perfect
ILMN_2281128	ENSG00000101843	<i>PSMD10</i>	expanded ghs	Perfect
ILMN_2383435	ENSG00000101843	<i>PSMD10</i>	expanded both	Perfect
ILMN_1786612	ENSG00000100911	<i>PSME2</i>	expanded both	Perfect
ILMN_1760575	ENSG00000112245	<i>PTP4A1</i>	expanded ghs	Perfect
ILMN_2311548	ENSG00000141378	<i>PTRH2</i>	expanded ghs	Perfect
ILMN_1753196	ENSG00000164611	<i>PTTG1</i>	expanded ghs	Perfect
ILMN_1752582	ENSG00000111540	<i>RAB5B</i>	expanded ghs	Perfect
ILMN_1790354	ENSG00000137955	<i>RABGGTB</i>	expanded ghs	Perfect
ILMN_1687782	ENSG00000152942	<i>RAD17</i>	expanded ghs	Perfect
ILMN_2321634	ENSG00000152942	<i>RAD17</i>	expanded ghs	Perfect
ILMN_1806266	ENSG00000138698	<i>RAP1GDS1</i>	expanded ghs	Perfect
ILMN_1725992	ENSG00000158987	<i>RAPGEF6</i>	expanded ghs	Perfect
ILMN_1701613	ENSG00000133321	<i>RARRES3</i>	expanded both	Perfect
ILMN_1756999	ENSG00000103479	<i>RBL2</i>	expanded ghs	Perfect
ILMN_1673024	ENSG00000179837	<i>RBM15B</i>	expanded ghs	Perfect
ILMN_1695717	ENSG00000089682	<i>RBM41</i>	expanded ghs	Perfect
ILMN_2338480	ENSG00000126858	<i>RHOT1</i>	expanded ghs	Perfect
ILMN_1754051	ENSG00000178966	<i>RMI1</i>	expanded ghs	Bad
ILMN_1697529	ENSG00000022840	<i>RNF10</i>	expanded ghs	Perfect
ILMN_1752526	ENSG00000137393	<i>RNF144B</i>	expanded ghs	Perfect
ILMN_1685679	ENSG00000118518	<i>RNF146</i>	expanded ghs	Perfect
ILMN_2353327	ENSG00000137075	<i>RNF38</i>	expanded both	Perfect
ILMN_1688606	ENSG00000189050	<i>RNFT1</i>	expanded both	Perfect
ILMN_1659255	NA	NA	expanded ghs	Bad
ILMN_2160388	ENSG00000114391	<i>RPL24</i>	expanded ghs	Good
ILMN_1731546	ENSG00000161970	<i>RPL26</i>	expanded ghs	Good

ILMN_1754303	ENSG00000156482	RPL30	expanded ghs	Perfect
ILMN_1754195	ENSG00000071082	RPL31	expanded ghs	Good
ILMN_1774823	ENSG00000109475	RPL34	expanded ghs	Perfect
ILMN_1756360	ENSG00000182899	RPL35A	expanded ghs	Good
ILMN_2189936	ENSG00000165502	RPL36AL	expanded ghs	Perfect
ILMN_2189933	ENSG00000165502	RPL36AL	expanded ghs	Perfect
ILMN_1717490	NA	RPL6P27	expanded both	Perfect
ILMN_1787949	ENSG00000134419	RPS15A	expanded ghs	Perfect
ILMN_2255310	ENSG00000134419	RPS15A	expanded ghs	Perfect
ILMN_2399893	ENSG00000138326	RPS24	expanded ghs	Perfect
ILMN_1746516	ENSG00000118181	RPS25	expanded ghs	Good
ILMN_2166831	ENSG00000198034	RPS4X	expanded ghs	Perfect
ILMN_1810577	ENSG00000198034	RPS4X	expanded ghs	Perfect
ILMN_1808939	ENSG00000137154	RPS6	expanded both	Perfect
ILMN_1656791	ENSG00000137154	RPS6	expanded ghs	Good
ILMN_1806294	ENSG00000177189	RPS6KA3	expanded both	Perfect
ILMN_1661000	ENSG00000136643	RPS6KC1	expanded ghs	Perfect
ILMN_1657871	ENSG00000134321	RSAD2	expanded both	Perfect
ILMN_2173975	ENSG00000136514	RTP4	expanded both	Perfect
ILMN_2119297	ENSG00000020577	SAMD4A	expanded both	Perfect
ILMN_1814305	NA	NA	expanded both	Bad
ILMN_1799467	NA	NA	expanded both	Bad
ILMN_1700044	ENSG00000136715	SAP130	expanded ghs	Perfect
ILMN_1689842	ENSG00000052802	SC4MOL	expanded ghs	Perfect
ILMN_1701621	ENSG00000130489	SCO2	expanded both	Perfect
ILMN_2363591	ENSG00000137575	SDCBP	expanded ghs	Perfect
ILMN_1772489	ENSG00000165525	SDCCAG1	expanded ghs	Perfect
ILMN_1732575	ENSG00000129657	SEC14L1	expanded ghs	Perfect
ILMN_1708619	ENSG00000085415	SEH1L	expanded ghs	Perfect
ILMN_2134110	ENSG00000113811	SELK	expanded ghs	Good
ILMN_1724422	ENSG00000188404	SELL	expanded ghs	Perfect
ILMN_1801121	ENSG00000163904	SENP2	expanded ghs	Perfect
ILMN_2123567	ENSG00000163904	SENP2	expanded ghs	Perfect
ILMN_2338452	ENSG00000197249	SERPINA1	expanded ghs	Perfect
ILMN_1670305	ENSG00000149131	SERPING1	expanded both	Perfect
ILMN_1724495	ENSG00000187231	SESTD1	expanded ghs	Perfect
ILMN_1703720	ENSG00000115128	SF3B14	expanded ghs	Perfect
ILMN_2391750	ENSG00000163935	SFMBT1	expanded ghs	Perfect
ILMN_2069593	ENSG00000139218	SFRS2IP	expanded ghs	Perfect
ILMN_2128128	ENSG00000127922	SHFM1	expanded ghs	Good
ILMN_1794505	ENSG00000127922	SHFM1	expanded ghs	Perfect
ILMN_1725320	ENSG00000088827	SIGLEC1	expanded both	Perfect
ILMN_2344007	ENSG00000092208	SIP1	expanded ghs	Good
ILMN_1672662	ENSG00000144136	SLC20A1	expanded ghs	Perfect
ILMN_1752639	ENSG00000085491	SLC25A24	expanded both	Perfect
ILMN_1742705	ENSG00000133195	SLC39A11	expanded ghs	Perfect
ILMN_1682738	ENSG00000166949	SMAD3	expanded ghs	Perfect
ILMN_1768271	ENSG00000112305	SMAP1	expanded ghs	Perfect
ILMN_1808148	NA	NA	expanded ghs	Bad
ILMN_1687519	ENSG00000092531	SNAP23	expanded both	Perfect
ILMN_2365479	ENSG00000028528	SNX1	expanded ghs	Perfect
ILMN_2365484	ENSG00000028528	SNX1	expanded ghs	Bad
ILMN_1738491	ENSG00000148158	SNX30	expanded ghs	Perfect

ILMN_1709772	ENSG00000089006	SNX5	expanded ghs	Perfect
ILMN_1685327	ENSG00000159140	SON	expanded ghs	Perfect
ILMN_1703427	ENSG00000159140	SON	expanded both	Perfect
ILMN_1767135	ENSG00000115904	SOS1	expanded ghs	Perfect
ILMN_1764414	ENSG00000100485	SOS2	expanded ghs	Perfect
ILMN_1813455	ENSG00000135899	SP110	expanded both	Perfect
ILMN_1703263	ENSG00000079263	SP140	expanded both	Perfect
ILMN_1778599	NA	NA	expanded both	Bad
ILMN_2246882	ENSG00000079263	SP140	expanded both	Perfect
ILMN_1657423	ENSG00000090487	SPG21	expanded both	Perfect
ILMN_1704290	ENSG00000100596	SPTLC2	expanded both	Perfect
ILMN_2286334	ENSG00000163714	SR140	expanded ghs	Perfect
ILMN_2169152	ENSG00000122862	SRGN	expanded ghs	Perfect
ILMN_1760347	ENSG00000122862	SRGN	expanded ghs	Perfect
ILMN_1759883	ENSG00000143742//	SRP9	expanded ghs	Good
	ENSG00000180581			
ILMN_1783226	ENSG00000163479	SSR2	expanded ghs	Perfect
ILMN_1690105	ENSG00000115415	STAT1	expanded both	Perfect
ILMN_1691364	ENSG00000115415	STAT1	expanded both	Perfect
ILMN_1777325	ENSG00000115415	STAT1	expanded both	Perfect
ILMN_2152581	ENSG00000112079	STK38	expanded ghs	Perfect
ILMN_1696419	ENSG00000148175	STOM	expanded both	Perfect
ILMN_1746090	ENSG00000134910	STT3A	expanded ghs	Perfect
ILMN_1752895	ENSG00000170310	STX8	expanded ghs	Perfect
ILMN_2333594	ENSG00000184900	SUMO2	expanded both	Perfect
ILMN_1781516	ENSG00000092201	SUPT16H	expanded ghs	Perfect
ILMN_1756590	NA	NA	expanded ghs	Bad
ILMN_1653367	ENSG00000120656	TAF12	expanded ghs	Perfect
ILMN_1694888	ENSG00000064313	TAF2	expanded ghs	Perfect
ILMN_1777565	NA	NA	expanded ghs	Bad
ILMN_1734138	ENSG00000157014	TATDN2	expanded ghs	Perfect
ILMN_1744316	ENSG00000203705	TATDN3	expanded both	Perfect
ILMN_2374770	ENSG00000106052	TAX1BP1	expanded ghs	Perfect
ILMN_2402272	ENSG00000180964	TCEAL8	expanded ghs	Perfect
ILMN_1726245	ENSG00000163513	TGFBR2	expanded ghs	Perfect
ILMN_1740345	ENSG00000151500	THYN1	expanded ghs	Perfect
ILMN_2334042	ENSG00000151500	THYN1	expanded ghs	Perfect
ILMN_1712634	ENSG00000116001	TIA1	expanded ghs	Perfect
ILMN_1717745	ENSG00000151923	TIAL1	expanded ghs	Perfect
ILMN_1796855	ENSG00000151923	TIAL1	expanded ghs	Perfect
ILMN_1654560	ENSG00000174125	TLR1	expanded ghs	Perfect
ILMN_1705047	ENSG00000101916	TLR8	expanded ghs	Perfect
ILMN_1724139	ENSG00000152558	TMEM123	expanded both	Perfect
ILMN_1683575	ENSG00000185973	LOC648605	expanded ghs	Perfect
ILMN_1768816	ENSG00000120802	TMPO	expanded both	Perfect
ILMN_1801307	ENSG00000121858	TNFSF10	expanded both	Perfect
ILMN_1768181	ENSG00000186283	TOR3A	expanded ghs	Perfect
ILMN_1764851	NA	NA	expanded ghs	Bad
ILMN_2392143	ENSG00000175104	TRAF6	expanded ghs	Perfect
ILMN_1758250	ENSG00000135148	TRAFD1	expanded ghs	Perfect
ILMN_1779252	NA	NA	expanded both	Bad

ILMN_1738704	ENSG00000137313///	<i>TRIM26</i>	expanded ghs	Perfect
	ENSG00000206421///			
	ENSG00000206499			
ILMN_1704383	ENSG00000108395	<i>TRIM37</i>	expanded ghs	Perfect
ILMN_2413517	ENSG00000204599///	<i>TRIM39</i>	expanded ghs	Perfect
	ENSG00000206419///			
	ENSG00000206495			
ILMN_1796063	ENSG00000166326	<i>TRIM44</i>	expanded ghs	Perfect
ILMN_1704972	ENSG00000132256	<i>TRIM5</i>	expanded both	Perfect
ILMN_1737599	ENSG00000132256	<i>TRIM5</i>	expanded ghs	Perfect
ILMN_2404665	ENSG00000132256	<i>TRIM5</i>	expanded both	Perfect
ILMN_1805481	ENSG00000066651	<i>TRMT11</i>	expanded ghs	Perfect
ILMN_1713668	ENSG00000116918	<i>TSNAX</i>	expanded ghs	Perfect
ILMN_2038776	ENSG00000136810	<i>TXN</i>	expanded ghs	Perfect
ILMN_1680314	ENSG00000136810	<i>TXN</i>	expanded ghs	Perfect
ILMN_1783753	ENSG00000117862	<i>TXNDC12</i>	expanded both	Perfect
ILMN_1772156	ENSG0000023318	<i>ERP44</i>	expanded ghs	Perfect
ILMN_2324157	ENSG00000144744	<i>UBA3</i>	expanded both	Perfect
ILMN_1703108	ENSG00000156587	<i>UBE2L6</i>	expanded both	Perfect
ILMN_1692168	ENSG00000159202	<i>UBE2Z</i>	expanded ghs	Perfect
ILMN_1798380	ENSG00000135018	<i>UBQLN1</i>	expanded ghs	Perfect
ILMN_1795964	ENSG00000159459	<i>UBR1</i>	expanded both	Perfect
ILMN_2110281	ENSG00000143222	<i>UFC1</i>	expanded ghs	Perfect
ILMN_1737705	ENSG00000111647	<i>UHRF1BP1L</i>	expanded ghs	Perfect
ILMN_2232936	ENSG00000173660	<i>UQCRRH</i>	expanded ghs	Perfect
ILMN_1739454	ENSG00000115464	<i>USP34</i>	expanded ghs	Perfect
ILMN_1773505	ENSG00000114316	<i>USP4</i>	expanded both	Perfect
ILMN_1809467	ENSG00000168899	<i>VAMP5</i>	expanded ghs	Perfect
ILMN_1692546	ENSG00000112303	<i>VNN2</i>	expanded ghs	Perfect
ILMN_1758864	ENSG00000112303	<i>VNN2</i>	expanded ghs	Perfect
ILMN_2181089	ENSG00000145041	<i>VPRBP</i>	expanded ghs	Perfect
ILMN_1809582	ENSG00000129003	<i>VPS13C</i>	expanded both	Perfect
ILMN_2280911	ENSG00000006715	<i>VPS41</i>	expanded both	Perfect
ILMN_1683243	ENSG00000136631	<i>VPS45</i>	expanded ghs	Perfect
ILMN_1727271	ENSG00000140105	<i>WARS</i>	expanded ghs	Perfect
ILMN_1716086	ENSG00000136709	<i>WDR33</i>	expanded ghs	Perfect
ILMN_1741869	ENSG00000085433	<i>WDR47</i>	expanded ghs	Perfect
ILMN_1799814	ENSG00000060688	<i>SNRNP40</i>	expanded ghs	Perfect
ILMN_1747759	ENSG00000109046	<i>WSB1</i>	expanded ghs	Perfect
ILMN_1742618	ENSG00000132530	<i>XAF1</i>	expanded both	Perfect
ILMN_2174884	ENSG00000130227	<i>XPO7</i>	expanded both	Good
ILMN_2188374	ENSG00000184575	<i>XBOT</i>	expanded both	Perfect
ILMN_1677098	ENSG00000175155	<i>YPEL2</i>	expanded ghs	Perfect
ILMN_1765994	NA	NA	expanded both	Bad
ILMN_1655206	ENSG00000177125	<i>ZBTB34</i>	expanded ghs	Perfect
ILMN_1795905	ENSG00000174282	<i>ZBTB4</i>	expanded ghs	Perfect
ILMN_1693227	ENSG00000122299	<i>ZC3H7A</i>	expanded ghs	Perfect
ILMN_1729973	ENSG00000105939	<i>ZC3HAV1</i>	expanded both	Bad
ILMN_1724837	ENSG00000105939	<i>ZC3HAV1</i>	expanded both	Perfect
ILMN_1684663	ENSG00000177054	<i>ZDHHC13</i>	expanded ghs	Perfect
ILMN_1785831	ENSG00000177054	<i>ZDHHC13</i>	expanded ghs	Perfect
ILMN_1741288	ENSG00000196646	<i>ZNF136</i>	expanded ghs	Perfect
ILMN_1669516	ENSG00000137185	<i>ZNF193</i>	expanded ghs	Perfect

ILMN_2376833	ENSG00000010539	ZNF200	expanded ghs	Perfect
ILMN_1661293	ENSG00000186019	ZNF224	expanded ghs	Perfect
ILMN_1710873	ENSG00000109445	ZNF330	expanded ghs	Perfect
ILMN_1773247	ENSG00000119725	ZNF410	expanded ghs	Perfect
ILMN_1764415	ENSG00000196967	ZNF585A	expanded ghs	Perfect
ILMN_1654819	ENSG00000164048	ZNF589	expanded ghs	Perfect
ILMN_1764854	ENSG00000160336	ZNF761	expanded ghs	Perfect
ILMN_1750044	ENSG00000108278	ZNHIT3	expanded ghs	Perfect

Supplementary Table 6: Gene ontology enrichment of the human iDIN. *P*-values have been computed using the standard hypergeometric test using all genes on the Illumina human ht12 chip annotated in David (<http://david.abcc.ncifcrf.gov/>). Term refers to the Gene Ontology term id or terms defined in the David data base. Fold enrichment is the observed count (given in the table) of genes from this GO term in the iDIN divided by the expected counts.

Term	Count	Fold Enrichment	P-value	Benjamini FDR
GO:0009615~response to virus	22	9.16	1.88E-013	9.89E-10
GO:0003723~RNA binding	54	1.74	5.95E-011	1.71E-07
GO:0006955~immune response	60	2.33	1.28E-009	3.37E-06
GO:0051707~response to other organism	24	1.25	6.28E-009	1.10E-05
GO:0005515~protein binding	250	1.21	6.71E-009	9.66E-06
GO:0009607~response to biotic stimulus	30	1.26	9.01E-009	1.18E-05
alternative splicing	202	1.30	2.17E-008	2.32E-05
antiviral defense	11	1.30	7.62E-008	4.06E-05
GO:0002376~immune system process	64	2.42	1.09E-007	1.14E-04
GO:0044428~nuclear part	59	4.32	1.13E-007	2.45E-05
GO:0032991~macromolecular complex	110	2.32	4.04E-007	7.01E-05
Direct protein sequencing	106	4.18	4.22E-007	1.50E-04
GO:0044446~intracellular organelle part	136	5.95	9.82E-007	1.42E-04
GO:004422~organelle part	136	1.92	1.18E-006	1.46E-04
GO:0043231~intracellular membrane-bound organelle	240	1.95	1.24E-006	1.35E-04
GO:0043227~membrane-bound organelle	240	36.66	1.29E-006	1.25E-04
ribosome	12	1.95	1.44E-006	3.84E-04
rna-binding	32	22.00	2.68E-006	5.72E-04
GO:0006952~defense response	37	3.71	3.25E-006	2.85E-03
protein biosynthesis	19	2.11	3.51E-006	6.24E-04
acetylation	37	1.52	3.64E-006	5.53E-04
GO:0031974~membrane-enclosed lumen	50	2.37	3.87E-006	3.36E-04
GO:0043233~organelle lumen	50	1.69	3.87E-006	3.36E-04
GO:0044260~cellular macromolecule metabolic process	137	3.74	4.02E-006	3.01E-03
GO:0005829~cytosol	34	5.43	4.19E-006	3.03E-04
GO:0043229~intracellular organelle	266	24.44	4.82E-006	3.22E-04
GO:0005830~cytosolic ribosome (sensu Eukaryota)	12	2.68	4.92E-006	3.05E-04
GO:0043226~organelle	266	2.33	5.06E-006	2.92E-04
cytoplasm	101	3.71	5.86E-006	7.80E-04
GO:0019538~protein metabolic process	141	2.96	5.96E-006	3.91E-03
phosphoprotein	167	1.87	6.86E-006	8.12E-04
GO:0044445~cytosolic part	16	1.58	7.31E-006	3.97E-04
GO:0051704~multi-organism process	25	1.85	7.65E-006	4.45E-03
GO:0031981~nuclear lumen	39	7.85	8.08E-006	4.13E-04

GO:0044267~cellular protein metabolic process	134	19.35	8.18E-006	4.29E-03
GO:0043234~protein complex	88	15.48	1.60E-005	7.70E-04
ribosomal protein	18	1.25	4.66E-005	4.96E-03
GO:0005488~binding	377	1.87	6.29E-005	5.85E-02
GO:0044444~cytoplasmic part	134	3.95	6.61E-005	3.01E-03
IPR006117:2-5-oligoadenylate synthetase	4	3.73	6.68E-005	3.26E-01
GO:0003824~catalytic activity	197	4.87	7.05E-005	4.95E-02
GO:0000502~proteasome complex (sensu Eukaryota)	9	32.82	9.42E-005	4.08E-03
GO:0033279~ribosomal subunit	14	2.21	9.85E-005	4.06E-03
GO:0033036~macromolecule localization	43	1.35	1.04E-004	4.83E-02
GO:0044464~cell part	415	6.63	1.06E-004	4.17E-03
GO:0005623~cell protein transport	415	5.37	1.08E-004	4.07E-03
IPR006116:2-5 oligoadenylate synthetase, ubiquitin-like region	26	1.58	1.17E-004	1.13E-02
IPR006116:2-5 oligoadenylate synthetase, ubiquitin-like region	4	6.74	1.64E-004	3.84E-01
GO:0009058~biosynthetic process	66	3.20	1.95E-004	8.17E-02
GO:0006954~inflammatory response	21	1.84	2.28E-004	8.79E-02
proteasome	9	1.19	2.32E-004	2.04E-02
GO:0008104~protein localization	40	1.26	2.39E-004	8.59E-02
PIRSF005680:interferon-induced 56K protein	4	5.93	2.79E-004	5.80E-01
PIRSF005552:guanine nucleotide-binding protein 1	4	3.52	2.79E-004	5.80E-01
GO:0045184~establishment of protein localization	38	19.31	3.06E-004	1.02E-01
GO:0009059~macromolecule biosynthetic process	44	2.44	3.19E-004	9.94E-02
GO:0005654~nucleoplasm	28	1.58	3.58E-004	1.29E-02
splice variant	149	6.60	3.59E-004	9.99E-01
GO:0017111~nucleoside-triphosphatase activity	33	4.26	3.68E-004	1.91E-01
GO:0015031~protein transport	36	24.44	3.69E-004	1.08E-01
GO:0044238~primary metabolic process	260	1.77	5.02E-004	1.36E-01
GO:0006412~translation	33	8.46	5.22E-004	1.34E-01
GO:0005842~cytosolic large ribosomal subunit (sensu Eukaryota)	7	3.21	5.25E-004	1.81E-02
GO:0051607~defense response to virus	5	19.35	5.81E-004	1.42E-01
GO:0043170~macromolecule metabolic process	230	1.77	7.14E-004	1.64E-01
GO:0044249~cellular biosynthetic process	51	1.94	7.34E-004	1.61E-01
GO:0016462~pyrophosphatase activity	33	4.50	7.41E-004	2.99E-01
GO:0006886~intracellular protein transport	24	1.38	7.41E-004	1.56E-01
GO:0044237~cellular metabolic process	258	1.18	8.26E-004	1.65E-01
hsa03010:Ribosome	12	1.41	8.31E-004	1.54E-01

GO:0016818~hydrolase activity, acting on acid anhydrides, in phosphorus-containing anhydrides	33	1.43	8.39E-004	2.92E-01
GO:0016814~hydrolase activity, acting on carbon-nitrogen (but not peptide) bonds, in cyclic amidines	6	2.19	8.65E-004	2.67E-01
IPR003191:Guanylate-binding protein, C-terminal	4	3.75	8.65E-004	8.19E-01

Supplementary Table 7: Overview of the region of interest on human chromosome 13. The region is defined by syntheny to the rat chromosome 15 locus (Supplementary Figure 4). The boundaries for the region are determined by the human orthologous genes of the rat genes flanking the region. Gene annotation was obtained from Ensembl release 51. SNP ids refer to dbSNP significantly associated with *EBI2* expression in either GHS or Cardiogenics cohorts. The cohort where *Ebi2* eQTL in monocytes was identified is indicated (GHS, Gutenberg Heart Study; Card, Cardiogenics Study).

Ensembl Gene ID	HGNC symbol	SNP id	Chromosome Name	Gene Start (bp)	Gene End (bp)	Biotype	Comment	Cohort
ENSG00000088387	<i>DOCK9</i>		13	98243742	98536661	protein_coding		
ENSG00000207298			13	98475489	98475600	snRNA		
ENSG00000210366			13	98611288	98611438	scRNA_pseudogene		
ENSG00000210371			13	98611797	98611920	scRNA_pseudogene		
ENSG00000134882	<i>UBAC2</i>		13	98651109	98836682	protein_coding		
ENSG00000201793			13	98655963	98656302	misc_RNA		
ENSG00000125245	<i>GPR18</i>		13	98704973	98711999	protein_coding		
ENSG00000169508	<i>EBI2</i>		13	98744791	98757695	protein_coding		
ENSG00000207719			13	98806386	98806483	miRNA		
		rs9557217	13	98866518	98866518	SNP	<i>EBI2</i> eQTL	Card
		rs9585056	13	98879767	98879767	SNP	T1D SNP, <i>EBI2</i> eQTL	GHS/Card
		rs9517723	13	98882680	98882680	SNP	<i>EBI2</i> eQTL	GHS
		rs9517725	13	98883134	98883134	SNP	Imputed <i>EBI2</i> eQTL	GHS/Card
		rs7325697	13	98915794	98915794	SNP	<i>EBI2</i> eQTL	GHS
ENSG00000125304	<i>TM9SF2</i>		13	98951672	99013635	protein_coding		
ENSG00000212197			13	98986576	98986651	misc_RNA		
ENSG00000125246	<i>CLYBL</i>		13	99056924	99359714	protein_coding		
ENSG00000201245			13	99234112	99234238	snoRNA		
ENSG00000210404			13	99234310	99234412	snoRNA_pseudogene		

Supplementary Table 8: Association of iDIN genes with T1D. We considered the intersection (human and rat, n = 51) and the union (human or rat, n = 697, which comprises 496 human Ensembl genes from Supplementary Table 5 and 201 rat genes from Supplementary Table 2 that have orthologous human Ensembl genes) of the human and rat immune response network or their orthologous genes for the enrichment analysis. Ensembl genes were mapped to all SNPs in a 1 Mb region for the analysis. Since the HLA region is known to be highly associated to T1D, we also analyzed the sets without genes in the region in order to assess the impact of the HLA region on the gene set enrichment for T1D. Since many immune and viral response genes have been associated to T1D previously, we tested our sets against different backgrounds: the whole genome and genes annotated to the GO term “immune response”. Here we report the value of the Z statistic and the one-sided P-value (see Supplementary Information).

iDIN genes		rat and human		rat or human	
	background	Z	P-value	Z	P-value
with HLA	whole genome	2.45	7.05×10^{-3}	6.23	2.40×10^{-10}
		2.88	2.01×10^{-3}	5.03	2.41×10^{-7}
without HLA	immune response	-2.46	9.93×10^{-1}	4.29	8.85×10^{-6}
		-0.44	6.71×10^{-1}	3.14	8.57×10^{-4}

Supplementary Table 9: T1D association results. Association testing of rs9585056 T>C using observed genotypes in a subset of the T1D GWA samples, additional case control samples and family samples. N is the number of cases/controls, or number of informative transmissions. Fq is the frequency of the minor allele in controls or parents.

Cohort	N	Fq (C)	Odds ratio (C:T)	(95% CI)	P-value
GWAS	5678/5268	0.248	1.18	(1.11-1.25)	1.60×10^{-7}
Additional	2708/4816	0.253	1.11	(1.03-1.20)	0.00862
Families	3038	0.260	1.09	(1.01-1.17)	0.022
Case-control combined	8386/10084	0.25	1.15	(1.1-1.21)	5.20×10^{-9}
Families & case-control	(see above)	-	-	-	7.05×10^{-10}

Supplementary Table 10: Oligonucleotide primers and probes used for quantitative ChIP-PCR.

Gene	Forward primer (5'- 3')	Reverse primer (5'-3')	Taqman Probe (5'-3')
<i>lrf7</i>	CCAGGCCAGTGAAACGAAA	GCGCTTGTGAGCTGTTGG	TCCGTCTCGGAAAATGAAACCTAAACTG
<i>Ifi27l</i>	GCTGTCTTCAGTCACGAGGTGTA	AGATAGGTTTGGTGTCCCAGTTC	CTTCACCCAGAGTGGACTTCTAAGGCCTG
<i>Lgals3bp</i>	GCAGCTCGAAGCTTCTGTAGAC	GGAAGAGGCTGAGGAAAACCA	TCAGCTGAGAAAGGCCACCA
<i>Oas1</i>	GGCCTGGATAATTGCATATCC	TGGTTGAATTGGAACAAGATTTTC	CGCCCCCTCTCGGAAATGGAAA
<i>Sp110</i>	TGCCCGGAGTGGAGTGA	CCCCCTCCGTGTTTCC	AGGCAGGGAGGCTAAGGACCAGCA